

1072-11977

BUREAU OF MINES  
Pittsburgh Energy Research Center  
Pittsburgh, Pennsylvania 15213

DIELECTRIC PROPERTIES OF BATTERY ELECTROLYTES

CASE FILE  
COPY

A-1  
FINAL REPORT

Sabri Ergun, Research Supervisor, Solid State Physics  
Albert R. Plantz, Electrical Research Engineer  
8-412-892-2391

NASA Request No. WO 6085 PR 68 221  
National Aeronautics and Space Administration  
NASA Headquarters, Washington, D. C. 20546

## DIELECTRIC PROPERTIES OF BATTERY ELECTROLYTES

### 1. Introduction

This study is concerned with the relationship between electromagnetic radiation and the properties of electrochemical cells. There are many situations (such as in space vehicles) where batteries are used as a power source in close proximity to a high power source of electromagnetic radiation (a radio transmitter). The intent of the investigation is to obtain information that can be used to determine if the electromagnetic radiation can in any way affect the terminal properties of the battery.

One possible approach would be to set up a battery, subject it to electromagnetic radiation in some particular configuration, and measure the terminal properties of the battery as a function of frequency and intensity of radiation under various conditions of the battery. Unfortunately, this information would not be very useful in predicting how a battery would behave under a slightly different set of circumstances. It is much more desirable to obtain basic physical data on the battery, independent of geometry, which can be used to predict the behavior of the battery under a wide variety of conditions. The logical thing to do is measure the basic electromagnetic properties of the various constituents of the battery.

### 2. Objective

The objective was to characterize the parts of a battery in terms of their electromagnetic properties. These properties could be used to predict how much electromagnetic radiation would be absorbed by a battery in a particular field configuration. The frequency range to be covered was 0-40 GHz with the greatest emphasis on the microwave range from 2.6-40 GHz. The measurements were to be made on NiCd, AgZn, and lead acid cells.

Given this general objective, questions arise concerning components of the cell that should be analyzed and the manner in which they should be characterized. The logical answer seems to be that any part of the cell which can absorb appreciable amounts of energy from the electromagnetic field should be investigated. One obvious component which will strongly absorb microwave energy is the aqueous electrolyte in the cell. Another absorber of energy will be the metallic parts, i.e., the electrodes. Another area which may act as an energy absorber is the region of the electrolyte adjacent to the electrodes. Because of the polarization which takes place in the electrolyte in this region there is a possibility of some energy absorption different from the bulk of the electrolyte.

The physical property used to characterize the electrolyte will be the complex dielectric constant as a function of frequency. The electrodes can be characterized in terms of a conductivity. The electrodes are not just plain sheets of metal; they usually consist of a porous plaque which contains the metal or some compound of the metal. It is to be expected that the effective conductivity measured

will be significantly different from that of the metal itself. The polarized layer in the electrolyte will be more difficult to characterize in terms of a basic physical property. It may be characterized by a deviation in the effective conductivity of the electrode when it is surrounded by electrolyte.

More specifically then the objective of the study is to measure the dielectric constant of battery electrolytes as a function of frequency and the effective conductivity of the electrodes both dry and wet with electrolyte.

### 3. Methods of measurement of dielectric constant and conductivity

There are a number of ways of measuring dielectric constant. One is to fill or partially fill a closed microwave cavity with the material and measure the change in resonant frequency of the cavity. There are a number of ways which make use of the material as the propagating medium in a section of the waveguide. There are also the free space methods where the microwave signal is transmitted by an antenna and the material placed in a sheet or some other configuration in front of the antenna.

To choose a method for dielectric constant measurement we must consider the constraints placed by the sample. First of all, the sample is a liquid which is likely to be corrosive to a metal structure. Second, the loss tangent is probably very high.

Because of the wide frequency range to be covered it is probably best to use a broad band method which allows a whole frequency band to be covered without retuning the apparatus. This eliminates the cavity methods from consideration.

The free space methods generally require a large amount of material and suffer from geometrical effects which are hard to account for. The best choice seems to be a transmission line method. Some of these (the bridge methods) essentially involve a tuned structure like a cavity, so even with the transmission line methods we should restrict the choice to a broad band method.

The commonly used transmission line techniques involve filling a section of the waveguide and measuring the signal transmitted through the sample or the signal reflected from the sample or both. In one particular configuration the section filled with sample is adjacent to a short circuiting plate and the combined reflection from the short circuit and the sample is measured. This is the method of Roberts and von Hippel.<sup>1</sup> This method seems particularly attractive from the standpoint of convenient handling of the sample. By orienting the waveguide vertically the short circuiting plate across the end of the waveguide forms the bottom of a container for the liquid. Since nothing is required to contain the liquid on the top surface, the depth of the liquid can be adjusted easily. This configuration also lends itself easily to the measurement of the electrode conductivity by using the electrode as the short circuiting plate. For these reasons this configuration was chosen as the method to be used in this study. Later analysis of the data taken using this method shows that this was not the best possible choice of configuration. This will be discussed more fully along with the presentation of data.

4. Theory of dielectric constant measurement using a section of sample in front of a short circuit.

The physical property of the electrolyte, which we wish to obtain, is the complex dielectric constant. The quantity being measured for the chosen configuration is the magnitude of the reflection coefficient  $|\rho|$  of the sample and short circuit. It is necessary to relate this reflection coefficient to the basic physical property of the material, i.e. the dielectric constant.

From transmission line theory the reflection coefficient is given by

$$\rho = \frac{(z_f/z_o) - 1}{(z_f/z_o) + 1} \quad (1)$$

where  $z_f$  is the impedance presented by the material in front of the short circuit, and  $z_o$  is the characteristic impedance of the empty waveguide.  $z_f/z_o$  can then be expressed in terms of  $\gamma$ , the propagation constant in the material, as follows:

$$\frac{z_f}{z_o} = \frac{\tanh \gamma l_d}{C \gamma l_d} \quad (2)$$

where  $l_d$  is the length of the material along the waveguide and

$$C = -j \frac{\lambda_g}{2\pi l_d} \quad (3)$$

$\lambda_g$  is the empty waveguide wave length.  $\gamma$  can be expressed in terms of dielectric constant as

$$\gamma^2 = \omega^2 \epsilon \mu_o - \left(\frac{\pi}{a}\right)^2,$$

where

$a$  = the width of the waveguide

$\omega = 2\pi f$  where  $f$  is the frequency

$\mu_o$  = free space permeability.

Since  $\epsilon$  is complex ( $\epsilon' - j\epsilon''$ ),  $\gamma$  is complex. Thus equation (2) is a complex transcendental equation. In the case where the magnitude and phase of  $\rho$  are measured (complex  $\rho$ ),  $z_f/z_o$  can be calculated directly from  $\rho$ . Equation (2) must then be solved for  $\gamma$ . This can be done by separating the real and

imaginary parts of equation (2), giving two nonlinear equations in two unknowns. These can be solved for  $\gamma$  numerically by several different methods.

If the apparatus is capable only of measuring the amplitude of the reflection coefficient (as is the case with the reflectometer), then the amplitude of  $\rho$  must be measured for two or more lengths of sample. Then equations (1) and (2) must be combined, giving  $\rho$  as a function of  $\gamma$ . Two values of  $|\rho|$  give again two nonlinear equations in two unknowns to be solved for  $\gamma$ .

If more than two values of  $|\rho|$  are used, the equation for  $|\rho|$  can be fitted to the data by the method of least squares.

## 5. Equipment

Because of the wide frequency range over which information was desired, it was decided to make the measurements using a sweep reflectometer system. To increase the frequency accuracy of the signal source, it was obtained with a phase synchronization system which was capable of sweeping a complete frequency band while maintaining the frequency stability of the reference frequency standard to which the output signal was phase synchronized. This kind of a signal source is the basic component in a microwave spectrometer. In our equipment a special modification was made to allow pulse modulation of the signal. The signal was modulated with a 1000 Hz square wave so that detection of low level reflected signals could be accomplished. The signal source has outputs in the range of 10-100mW (depending on the band) in the following bands:

- 1 - 2 GHz
- 2 - 4 GHz
- 4 - 8 GHz
- 8 - 12.4 GHz
- 12.4 - 18 GHz
- 18 - 26.5 GHz
- 26.5 - 40 GHz.

To measure the signal reflected from the liquid electrolyte sample, a waveguide reflectometer was constructed for each of the seven waveguide bands. These bands covered the following frequency ranges:

- 2.6 - 3.95 GHz
- 3.95 - 5.85 GHz
- 5.85 - 8.2 GHz
- 8.2 - 12.4 GHz
- 12.4 - 18 GHz

18 - 26.5 GHz

26.5 - 40 GHz.

Each of these waveguide reflectometers was constructed principally of two waveguide directional couplers with detectors on their secondary arms. The two directional couplers are aimed in opposite directions so that one monitors the signal transmitted toward the sample and the other measures the signal reflected from the sample. The coupler monitoring the transmitted signal forms part of a closed loop servo used to stabilize the output of the signal source to a constant level. This maintains the accuracy of the reflection measurement over the long time required to analyze one sample.

In a conventional reflectometer the reflected signal as measured at the detector on the secondary arm of the directional coupler is a 1000 Hz square wave. This 1000 Hz square wave is amplified by a narrow band amplifier to reduce the noise on the signal. The amplified signal is then displayed on a meter or recorded in some way. To further reduce the noise in our system the detected 1000 Hz square wave is connected to the input of a lock-in amplifier. The modulating 1000 Hz square wave is used as the reference signal of the lock-in amplifier. This allows the effective band width to be made as narrow as required to reduce the noise to a very low level.

The amplified signal is recorded on the y-axis of an x-y recorder and a printing digital volt meter. The x axis of the recorder records a reference voltage proportional to the frequency supplied by the signal source. This forms a plot of reflected signal versus frequency.

The frequency is monitored by an eight digit counter which measures the frequency of the reference standard. The output of the signal source is an exact harmonic of this reference standard. A logic signal from this frequency counter commands the printing digital voltmeter to print at prescribed intervals of frequency.

Figure 1 is an overall schematic of the system.

#### 6. Construction of sample cell

The sample configuration chosen for this experiment was a vertical section of waveguide with a short circuiting plate across the end. The liquid sample was placed to a certain depth above the short circuit inside the waveguide. For convenience the waveguide reflectometers were assembled horizontally on a table and an E-plane bend was used to connect to the vertical sample sections.

The initial attempts at data taking were done with a sample cell to which a known volume of liquid was added to pouring it in the top. This sample cell was then bolted to the reflectometer and the data taken. To add more liquid the cell had to be unbolted from the reflectometer. This was unsatisfactory for

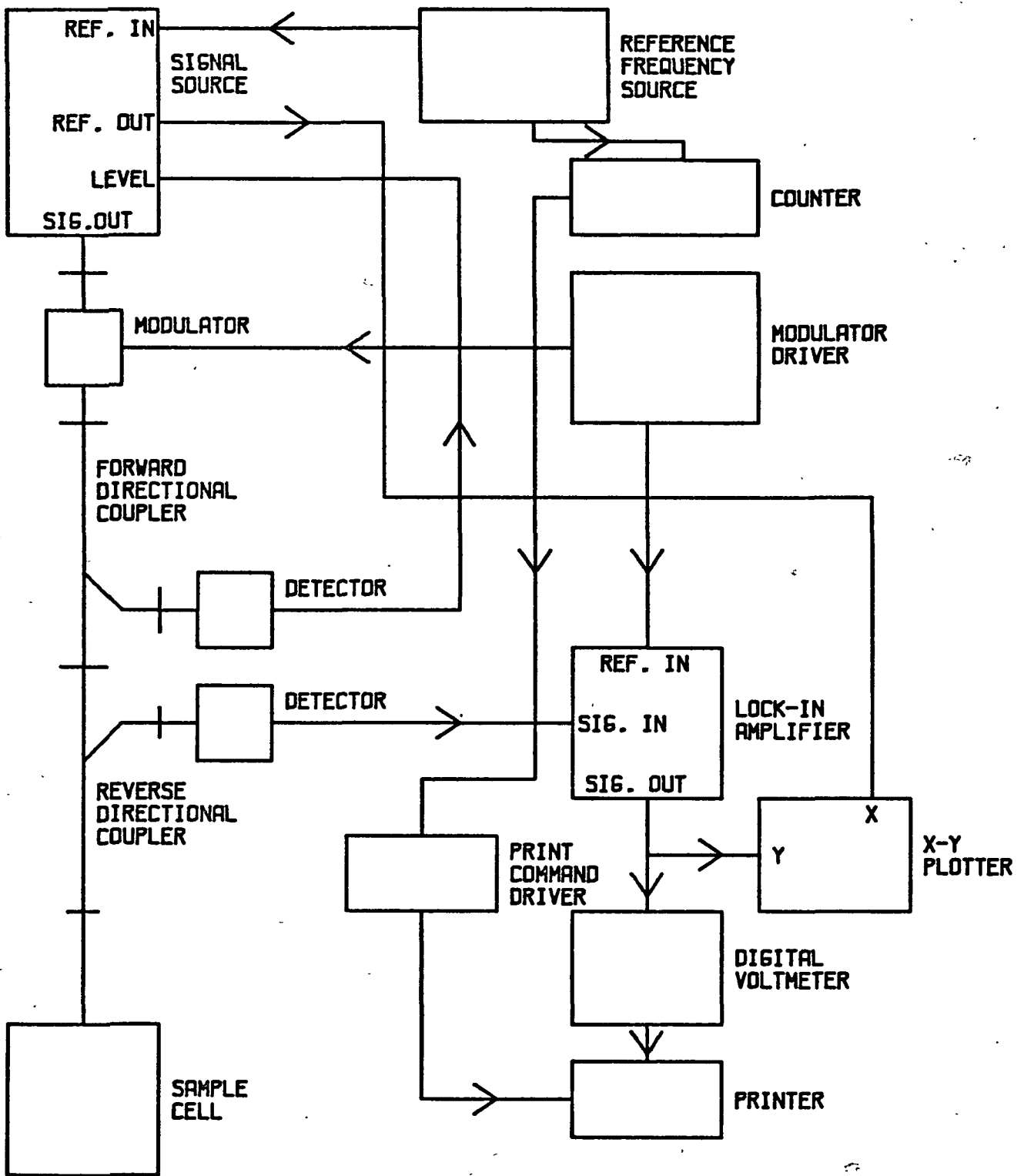


Figure 1.--System schematic.

several reasons. Removing the sample cell from the reflectometer to change the depth was much too time consuming. Preliminary data had shown that 20 to 30 different depths of the sample were necessary to obtain satisfactory results. Analysis of the preliminary data had also shown that accurate measurement of the depth was very important.

To measure the depth accurately a micrometer depth gauge was modified so that an electrical indication was given when the top of the gauge touched the surface of the liquid. With this an accurate measurement of the distance from the top of the cell to the surface of the liquid could be made. By subtracting that distance from the total depth of the cell (which could also be measured accurately) the depth of the liquid above the bottom of the cell could be obtained.

To reduce the time required to take the data for this experiment, a sample cell had to be designed which would allow adding liquid to the cell in such a way that the change in depth would be known accurately but which would not require the cell to be removed from the reflectometer. This objective was met by the sample cell design shown in figure 2. This cell design utilizes a precision micrometer syringe to inject a precise amount of liquid through a small hole in the short circuit plate into the waveguide. By calibration with a special depth gauge an amount of liquid injected by the syringe can be related to a certain depth increment inside the waveguide. A cell of this design was constructed for each of the seven waveguide frequency bands.

#### 7. Method of data collection

The first step in data collection is depth calibration of the sample cell. This is done by injecting equal increments of water with the precision syringe and measuring the depth of the liquid with the depth gauge after each increment. A straight line is then fitted to this data using the method of least squares. The slope of this line is used to obtain the increment in depth from the increment in volume during the taking of data.

Before data can be taken, it is necessary to obtain correction constants for the reflectometer. If the reflected signal from a perfect short circuit (reflectivity  $|\rho| = 1$ ) is measured as the short circuit is moved along the waveguide toward the reflectometer, the signal will be observed to have a sinusoidal variation. This is because of the presence of small spurious reflections within the reflectometer. The amplitude and phase of this sinusoidal variation can be used to correct the reflectivity measurement of the sample. The details of this correction will be covered in the discussion of the method of data analysis.

Before the sample cell is filled with liquid a scan of the frequency range is made with the cell empty. This measures the signal corresponding to a perfect short circuit ( $|\rho| = 1$ ). All the other signal measurements are divided by this empty cell measurement to normalize them to the range 0-1.0. After the empty cell scan is made, the cell and syringe are carefully filled with the liquid sample so that no air bubbles are trapped. The syringe is then turned in several turns to take up any back lash. Liquid is then pipetted out of the cell until a thin layer of liquid remains. An initial depth measurement is then made with the special micrometer depth gauge. A frequency scan is made, the liquid level is incremented by the micrometer syringe, and this process is repeated until 20 to 30 frequency scans have been made. The depth is then



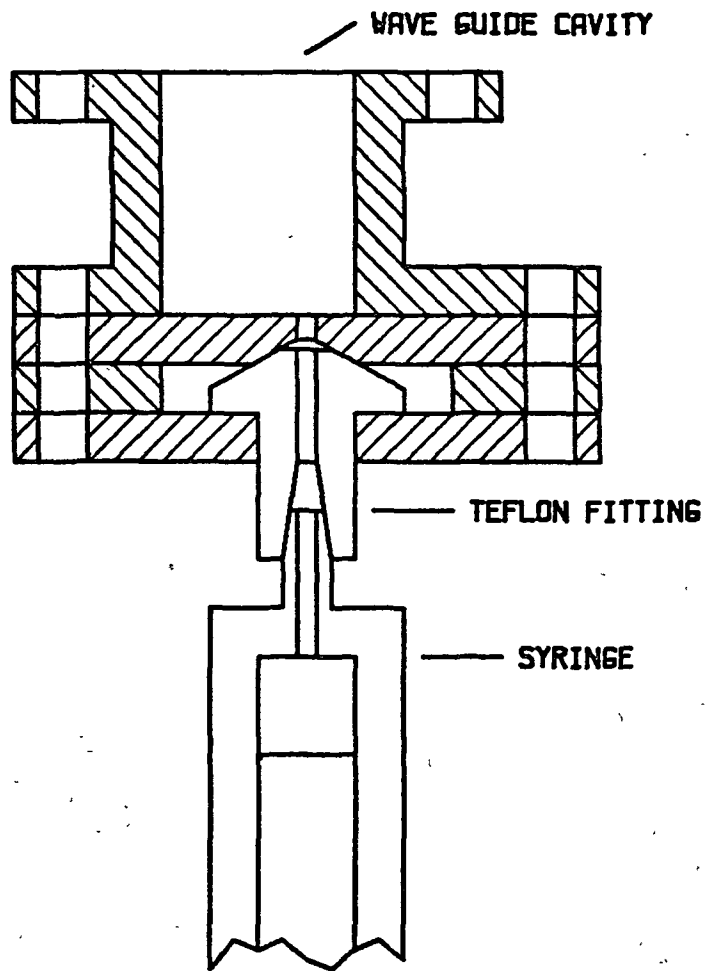


Figure 2.--Construction detail of waveguide electrolyte cell.

checked again with the micrometer depth gauge as a check of the accuracy of the depth increments as given by the syringe volume increments. After this, the cell is emptied and dried and a second empty frequency scan is made. This serves as a check on the amplitude stability of the signal source.

### 8. Method of Data Analysis

The initial attempt at analyzing the data showed that data taken at only two depths of liquid were not sufficient for proper analysis. The reason for this can be seen by examining the shape of a plot of the magnitude of the reflection coefficient  $|\rho|$  as a function of depth of sample. Figure 3 shows  $|\rho|$  versus depth for a sample with a dielectric constant of  $70.18 - j29.95$ . The curve has a series of minima; the depth and spacing of these minima depend on the value of the dielectric constant. Analysis of the data consists of finding a value of the dielectric constant for which the calculated  $|\rho|$  matches the measured  $|\rho|$ . If only two depths are used, there is an infinite set of values of the dielectric constant which will match perfectly the two measured values. For this reason data are taken for a number of different depths of liquid sample and a value of the dielectric constant is found which best matches calculated  $|\rho|$  to the measured  $|\rho|$  for all the depths.

The dielectric constant  $\epsilon$  is a complex quantity  $\epsilon' - j\epsilon''$ . The magnitude of the reflectivity  $|\rho|$  is a real function of the complex variable  $\epsilon$ . Fitting this function to the measured values of  $|\rho|$  is done by means of a nonlinear two dimensional least squares fit. The method used to obtain the least squares fit is one given by Marquardt<sup>2/</sup>. This method uses a linear combination of the Taylor series method and the gradient method (method of steepest descent). An appropriate algorithm is given which determines which of the two methods is given the greatest emphasis.

For the same reason that there is an infinite set of perfect fits with two depths, there is an infinite set of minima and maxima of the sum of the squares of the errors. The presence of the gradient method in the linear combination of methods prevents converging on a maximum but the method will in general converge on the minimum which is closest to the initial value of  $\epsilon$  (not necessarily the smallest minimum). For this reason the starting value of  $\epsilon$  must be chosen carefully and when convergence is completed a check must be made to be sure the correct minimum has been found. The only satisfactory way found to perform this check is graphically.  $|\rho|$  is plotted versus depth (for the value of  $\epsilon$  found by convergence) with the measured values of  $|\rho|$  superimposed. It is quite obvious visually whether the smallest minimum has been found.

This geometry of the liquid sample provides good data for analysis as long as the value of  $\epsilon$  is such that the curve of  $|\rho|$  versus depth has pronounced minima. This is the case with water and low concentrations of KOH. With high concentrations of KOH, however, the minima completely disappear. With no good features in the data, the minima of the sum of the squares of the errors become very shallow. In this condition very small errors in the raw data are magnified in the answer.

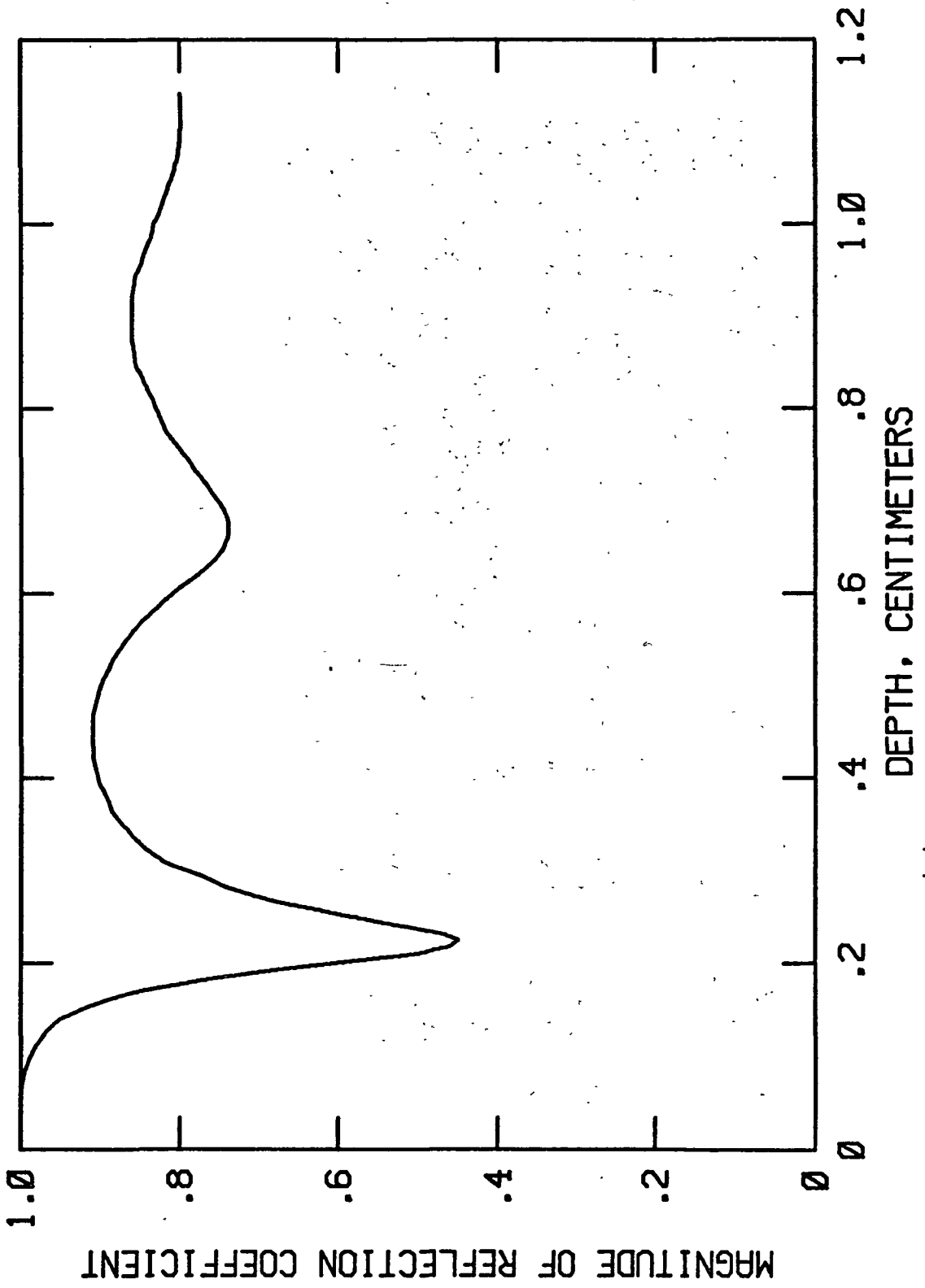


Figure 3---  $|\rho|$  versus depth for  $\epsilon = 70.18 - j29.95$ .

## 9. Presentation of data

The results of the measurement of the dielectric constants of electrolytes are shown in figures 4-72. These show the real and imaginary parts of the dielectric constants of water and KOH in concentrations from 5 to 30 weight percent. The results are presented by frequency band with increasing concentration within each band.

The results for pure water show a value of  $\epsilon'$  of about 80 at low frequencies to about 25 at high frequencies.  $\epsilon''$  varies from about 15 to about 30. The water results show considerable statistical scatter at the higher frequencies. This scatter occurs because the curve of  $|\rho|$  versus depth has no pronounced minima, causing the least squares fit to be ill-conditioned. In this condition any small statistical errors in the data are magnified. In general, however, the values obtained for water agree quite closely with published values.<sup>3/</sup>

The results for KOH solutions show a decrease in  $\epsilon'$  with increasing concentration, and  $\epsilon''$  increases with increasing concentration. The greatest elevation of  $\epsilon''$  occurs at low frequencies. This also agrees with what might be expected from published literature.<sup>4/</sup>

These results plus visual observation of the  $|\rho|$  versus frequency x-y recordings showed no evidence of any absorption peaks.

The results for higher concentrations show statistical scatter for the same reason previously mentioned. This condition probably cannot be overcome except by modifying the measurement method to allow a measurement of the signal transmitted through the sample as well as that reflected from it.

## 10. Electrode measurements

To make measurements of the reflectance of electrodes, a waveguide cell was designed. This design was a modification of the cell used for measurements on electrolytes. Strips of electrode material were spot welded to metal plates which were inserted between the waveguide and the short circuit assembly containing the precision micrometer. In this way the height of electrolyte in the cell could be adjusted precisely. The strips of electrode material form the waveguide short circuit in this configuration.

Extensive measurements were made on the waveguide cell with standard nickel cadmium electrode and 30 percent by weight KOH electrolyte over the frequency range 2.6-3.95 GHz. In order to obtain proper electrochemical performance from this cell it was found necessary to nickel plate all metal parts in contact with the electrolyte and spot weld the electrodes onto pure nickel plates.

The first measurement made was with the dry electrodes. In this case the reflectivity was not observably different from the reflection from a pure nickel plate. Next the electrolyte was added to the cell and it was activated. Then reflection measurements were made with the electrolyte adjusted level with the surface of the electrode so that the entire electrode was wet but there was no appreciable thickness of the electrolyte for the microwave signal to pass through. Measurements were made with the cell fully charged, fully discharged, half charged, during charging and during discharging.

In no case was the reflection observably different from the dry electrode. In addition the same battery cycles were repeated without the microwave signal present and no differences in the terminal properties were observed. Because of limited time these measurements were not extended to the other frequency ranges.

#### 11. Conclusion

Electromagnetic interactions with electrochemical cells can be divided into two types; those where energy is absorbed and converted to heat and those where the radiation couples to something which directly affects the properties of the cell. The energy absorption can be calculated for a given geometry from the properties of the materials making up the cell. Some of these properties were measured in this study. The second type of interaction is harder to characterize, but if it is present it must be observable because of its effects on the electromagnetic radiation or its effect on the characteristics of the cell.

In this study nothing was observed which suggested any interaction of the second type. Also, there was no evidence of any peaks of energy absorption in any of the data taken in this study.

#### References

1. Roberts, S. and Hippel, A. von: "A New Method of Measuring Dielectric Constants and Loss in the Range of Centimeter Waves," J. Appl. Phys., 1946, 17, p. 610.-
2. Marquardt, Donald W.: "An Algorithm for Least-Squares Estimation of Nonlinear Parameters," J. Soc. Indust. Appl. Math., 1963, 11, No. 29, p. 431.
3. Harvey, A. F.: Microwave Engineering (Academic Press, New York, 1963), p. 248.
4. *ibid*, p. 249.

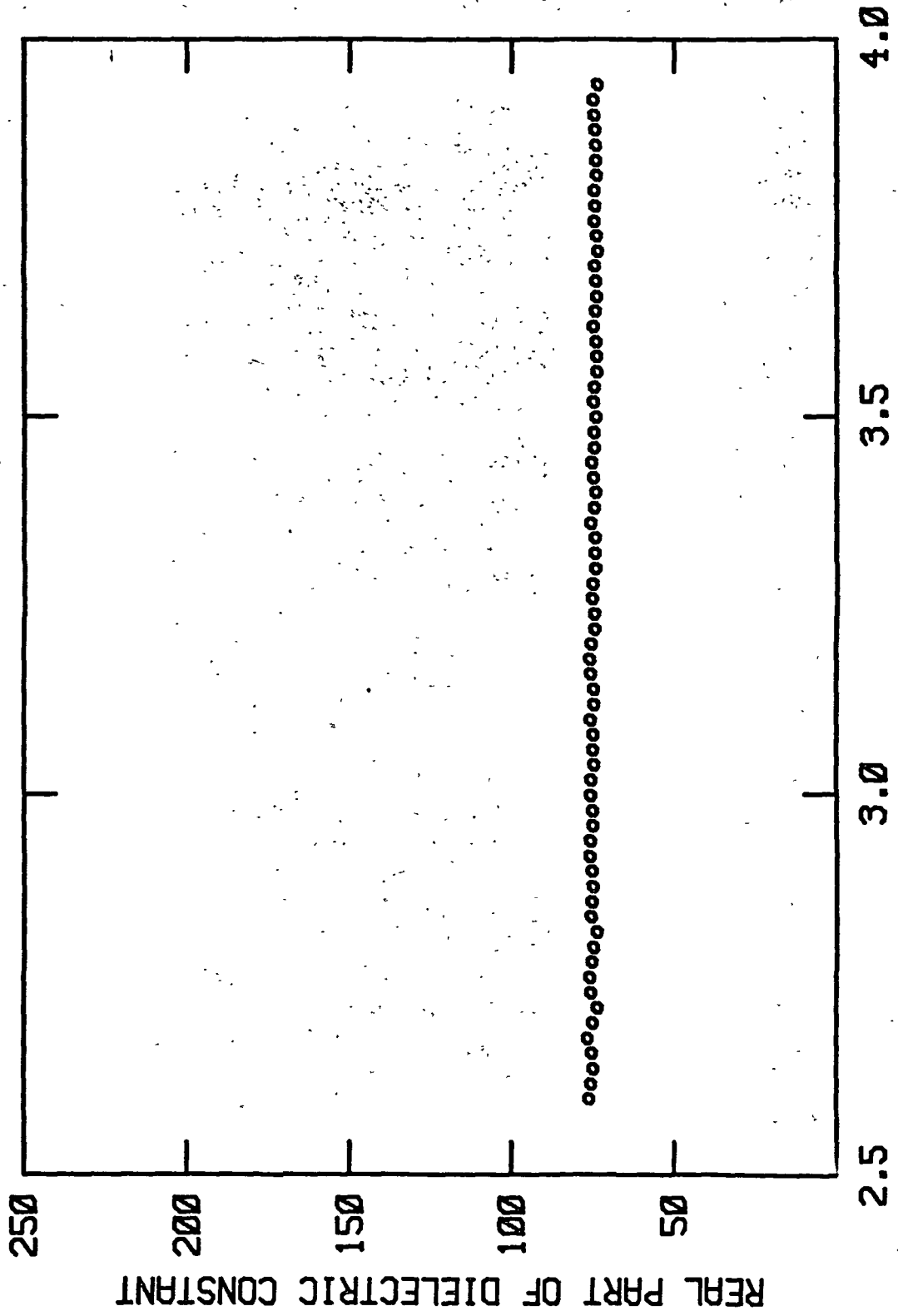


Figure 4.--Water.

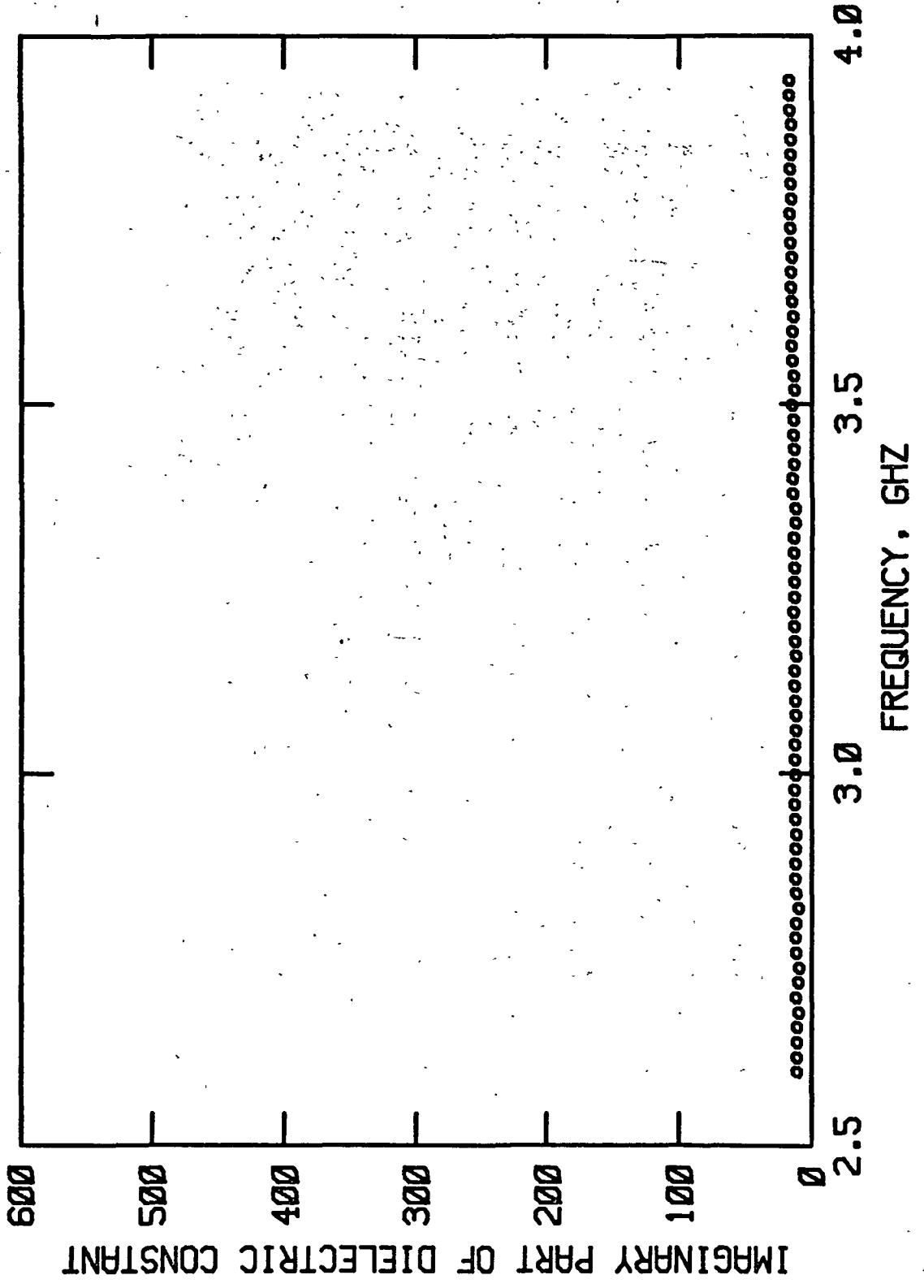


Figure 5.--Water.

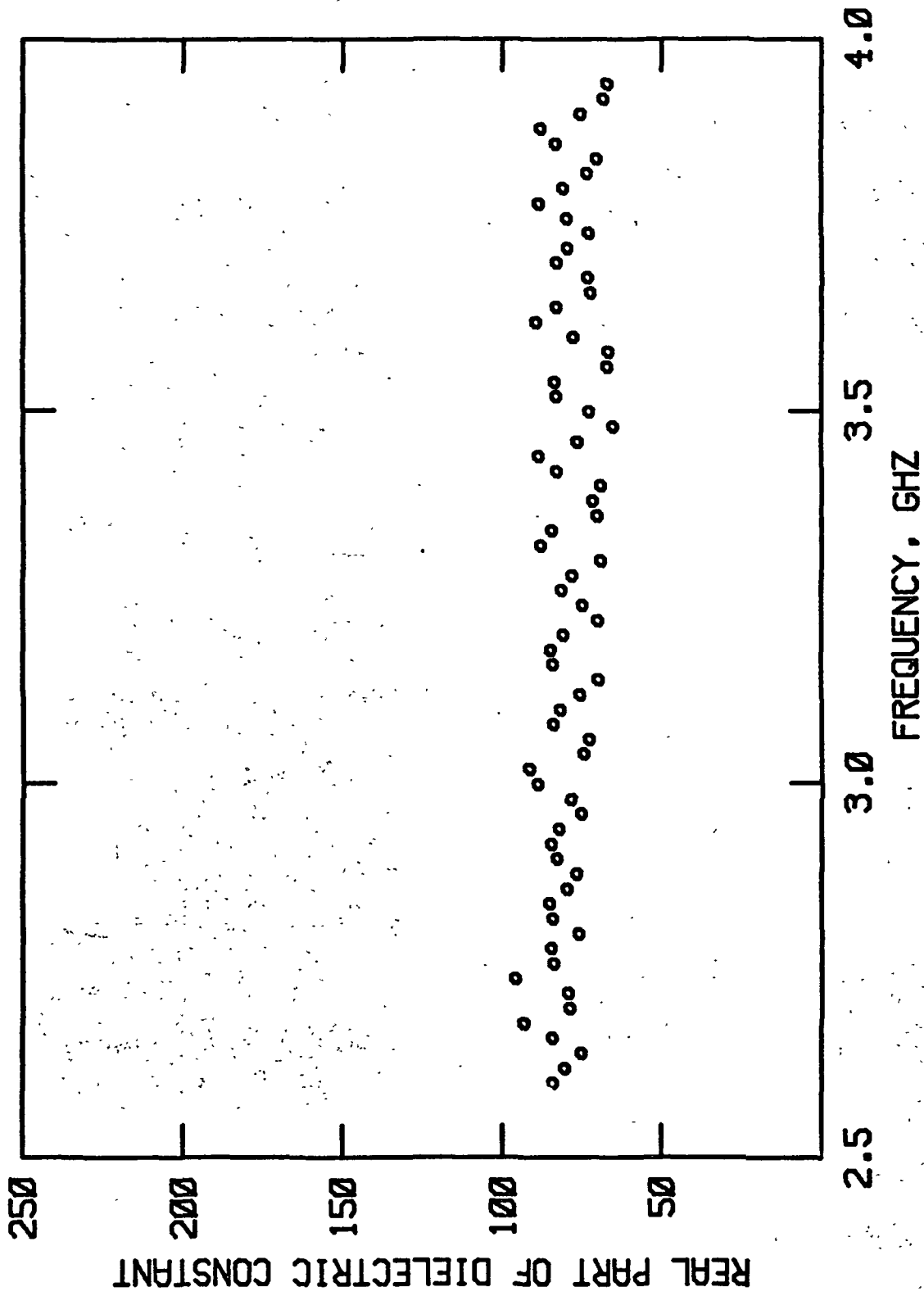


Figure 6.-- 5 percent KOH.



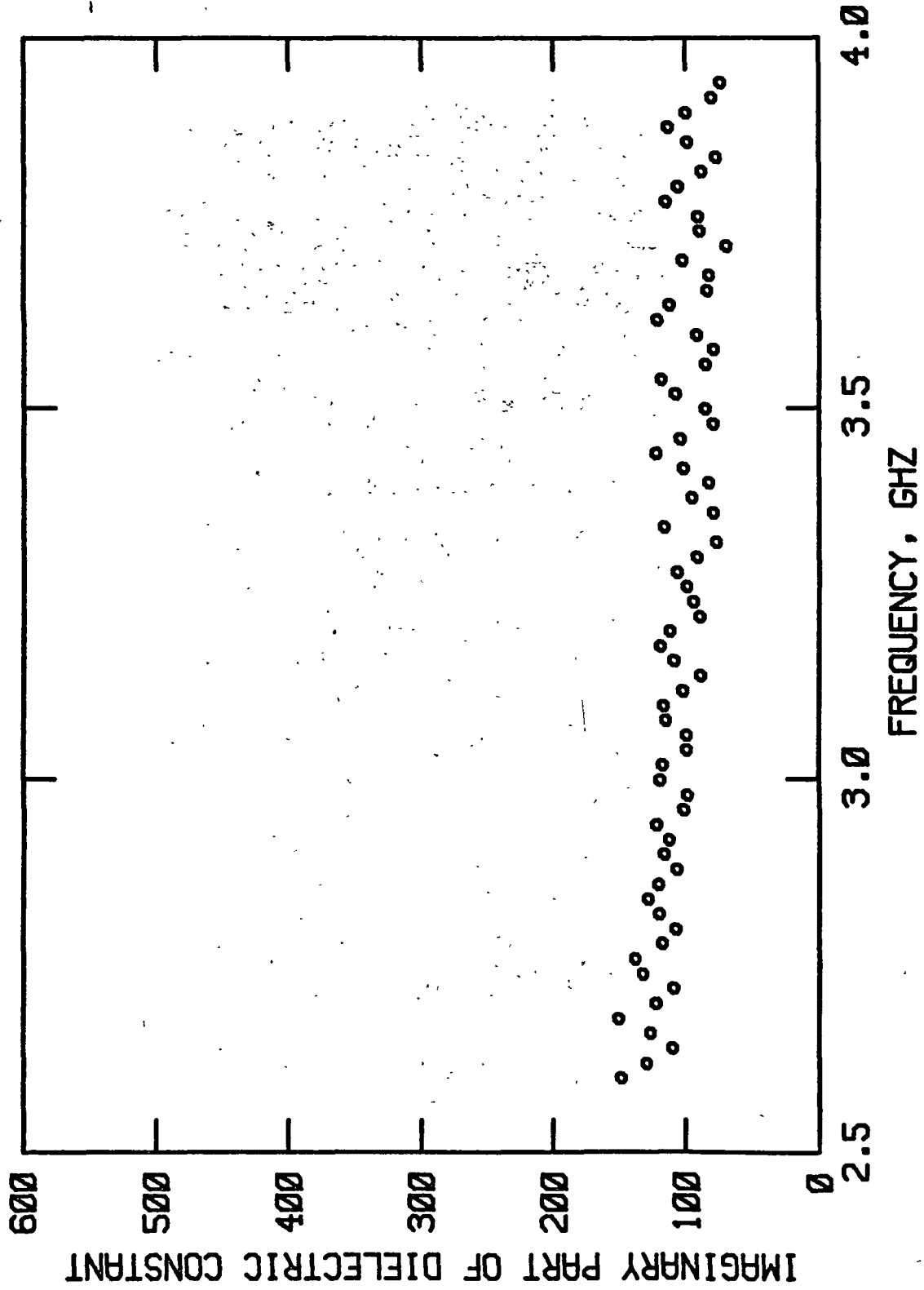


Figure 7.-- 5 percent KOH

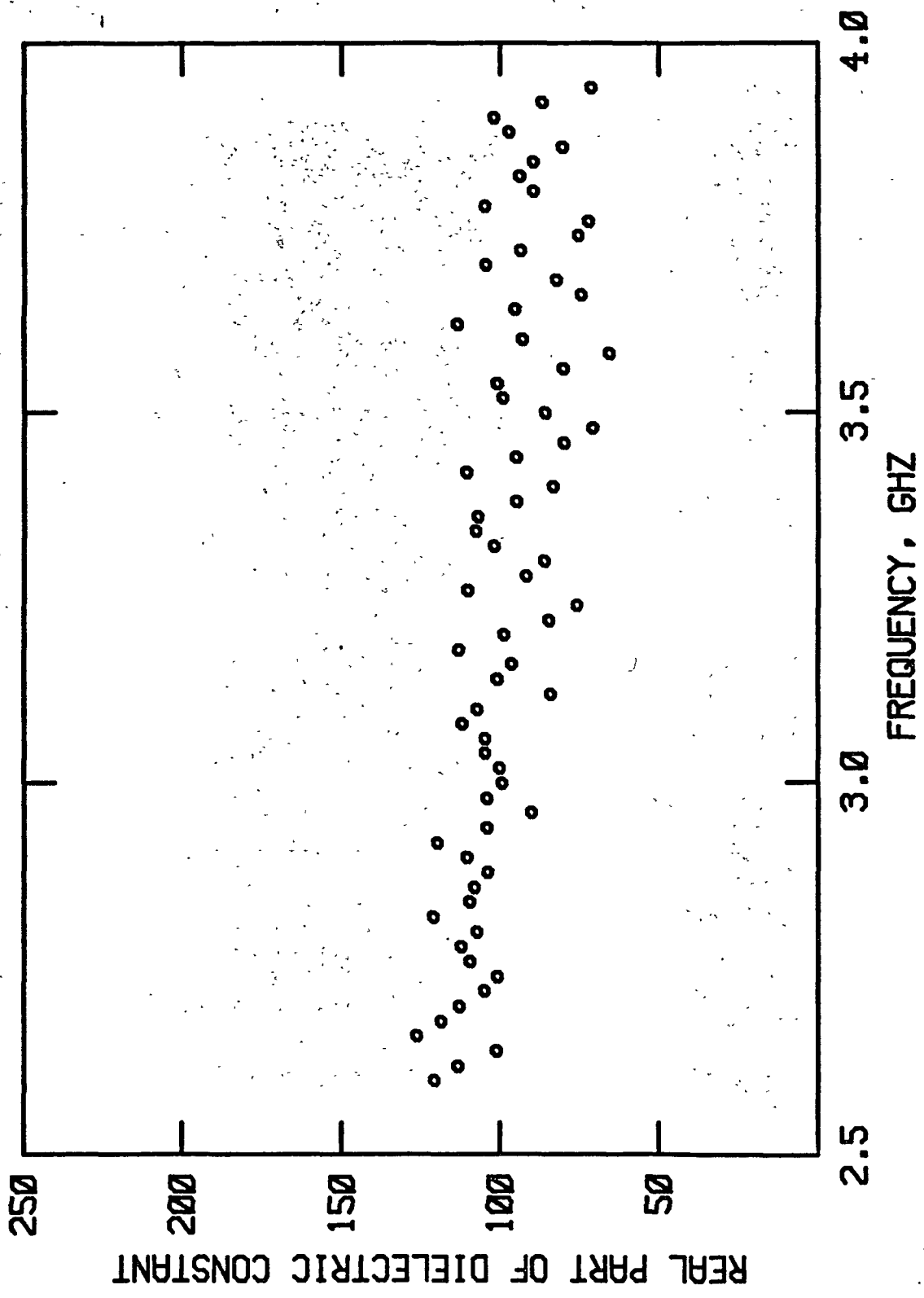


Figure 8.--- 10 percent KOH.

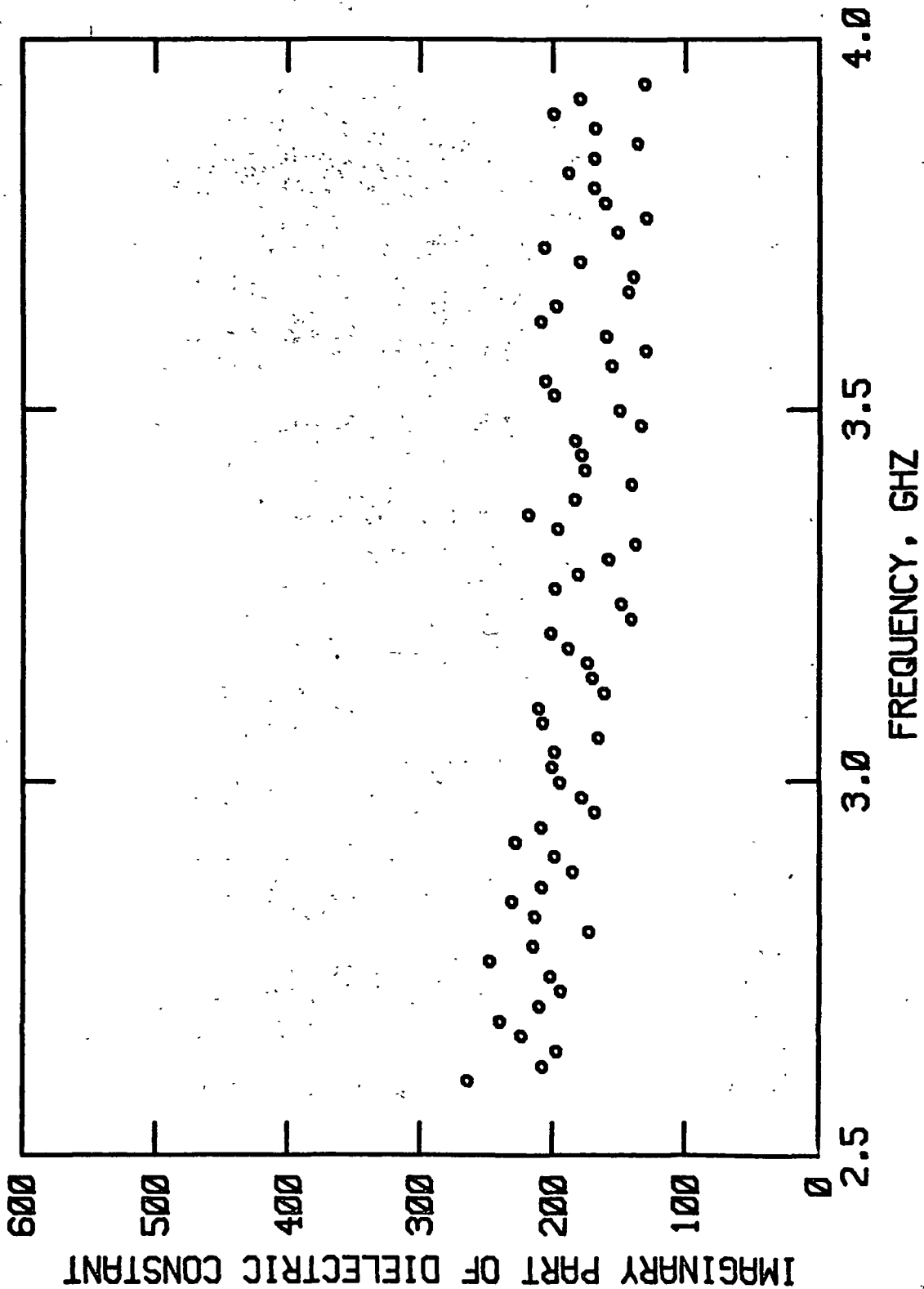


Figure 9.--- 10 percent KOH.

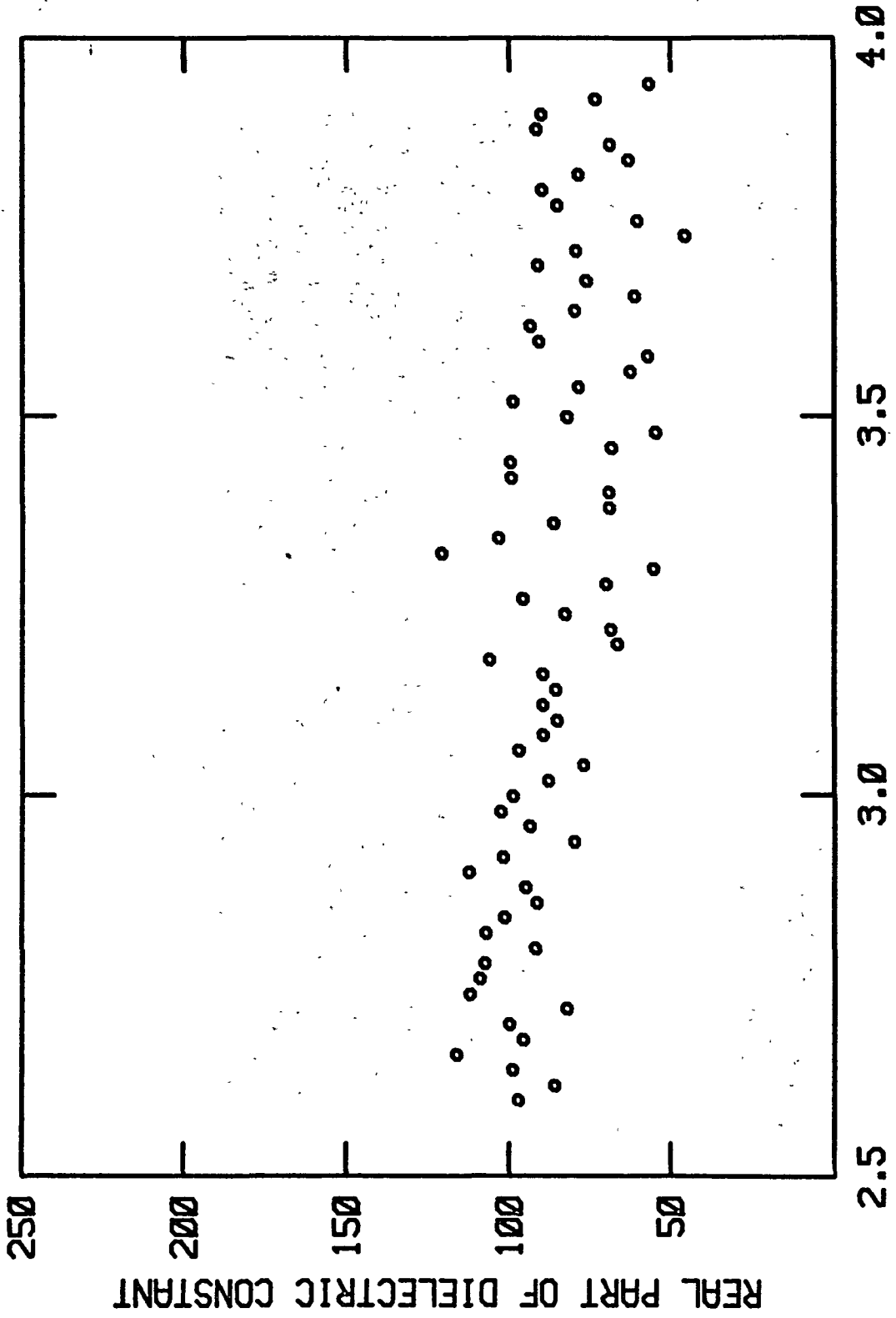


Figure 10.-- 15 percent KOH.

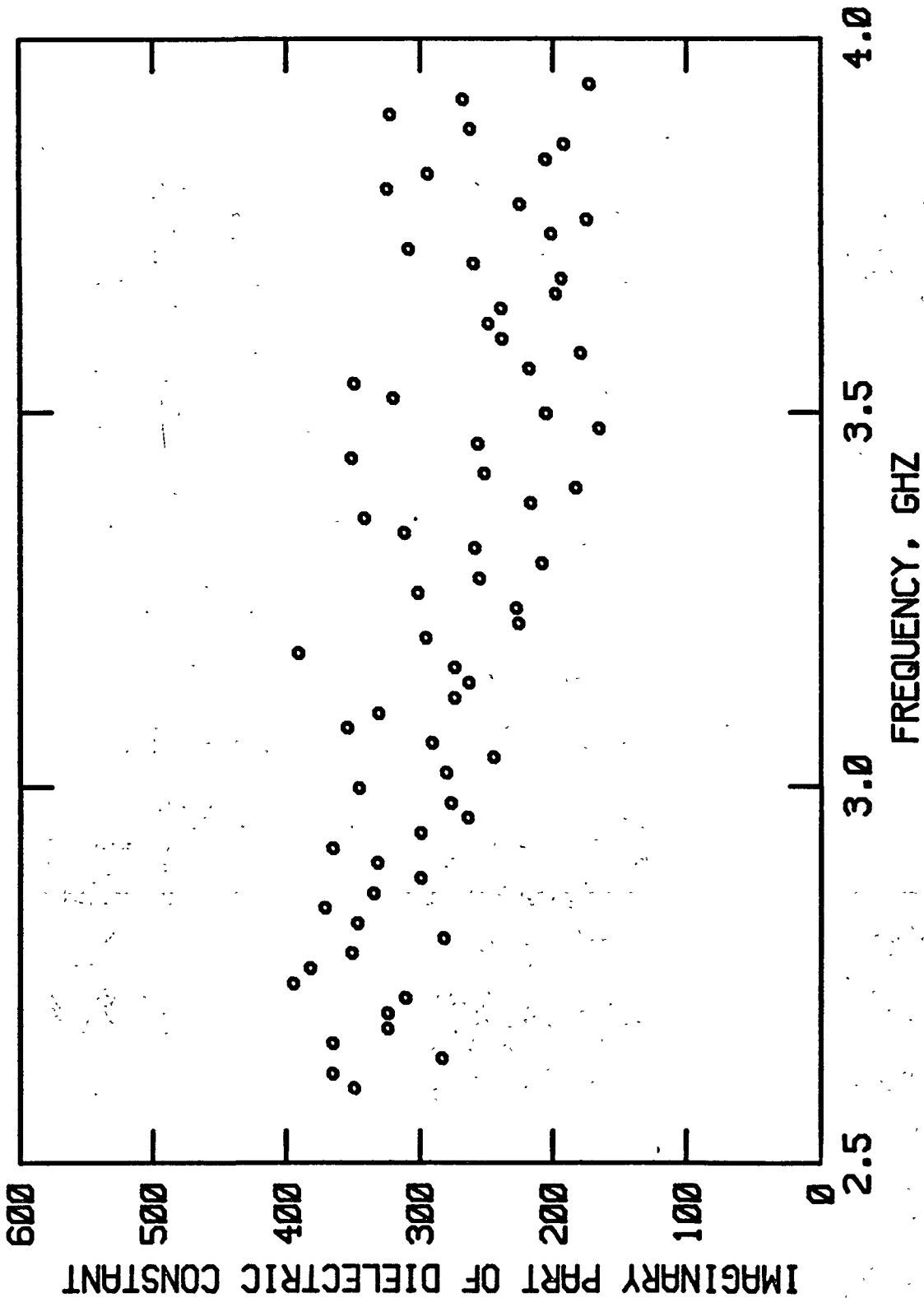


Figure 11.--15 percent KOH.

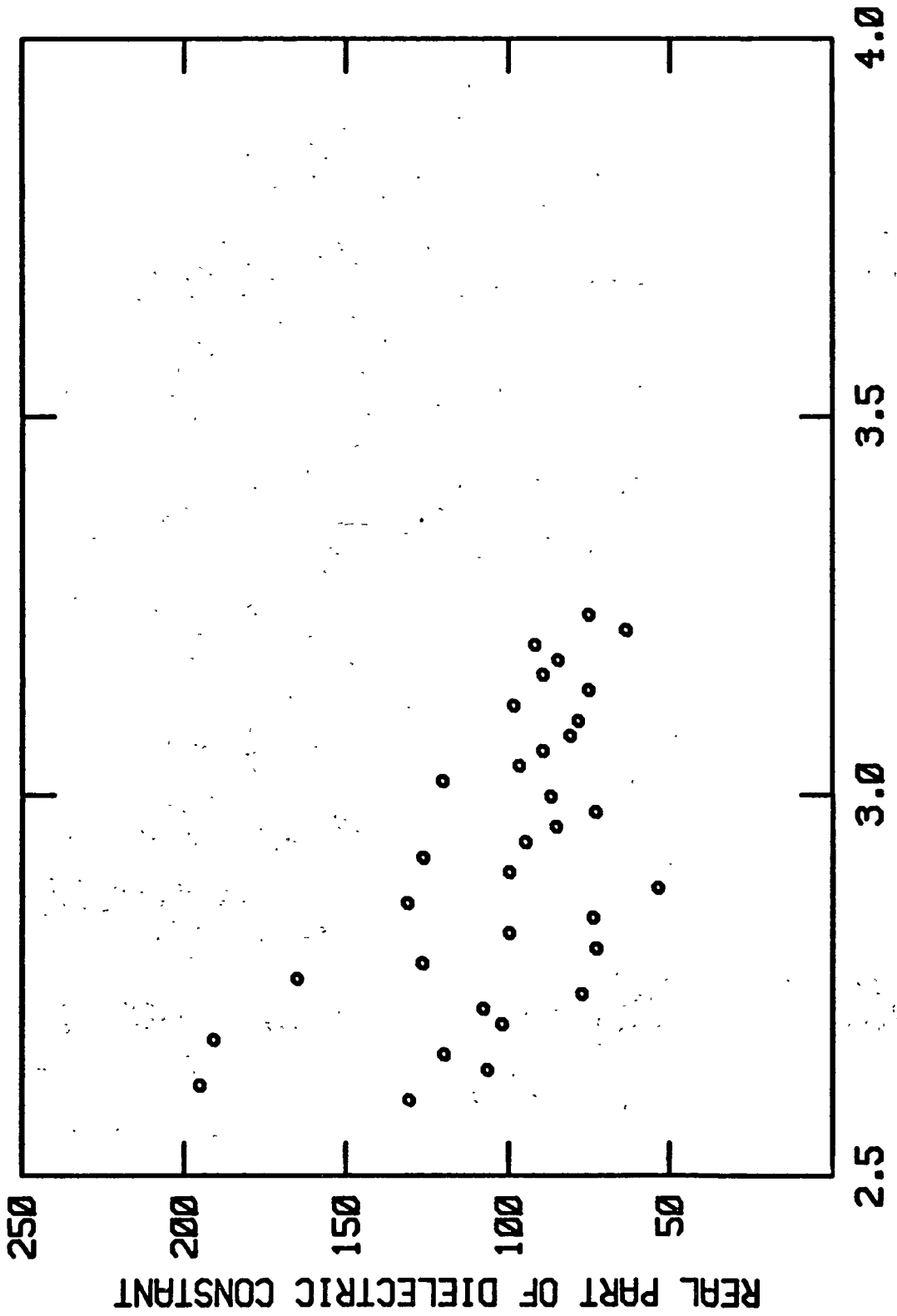


Figure 12.-- 25 percent KOH.

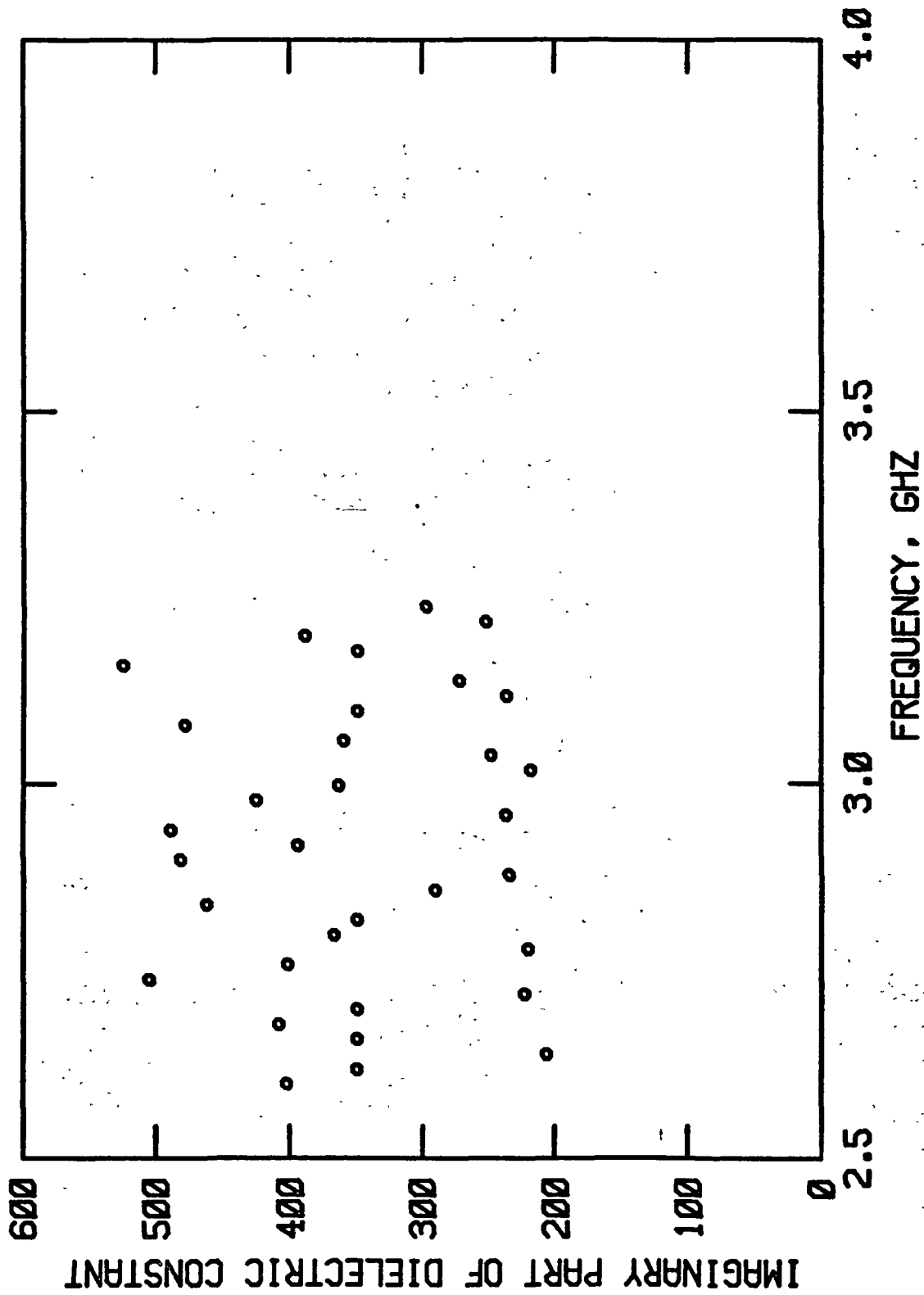


Figure 13.-- 25 percent KOH.

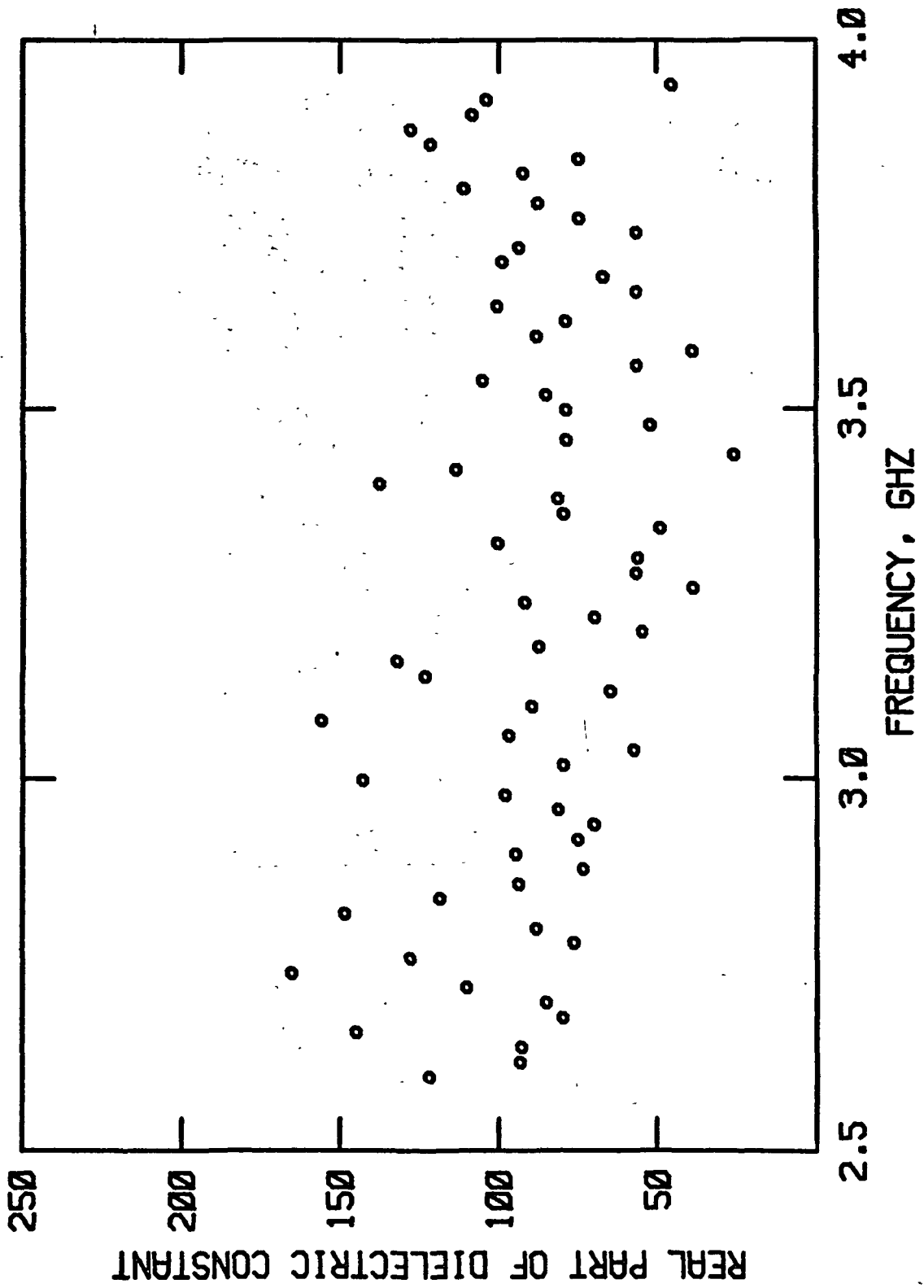


Figure 14.--30 percent KOH.



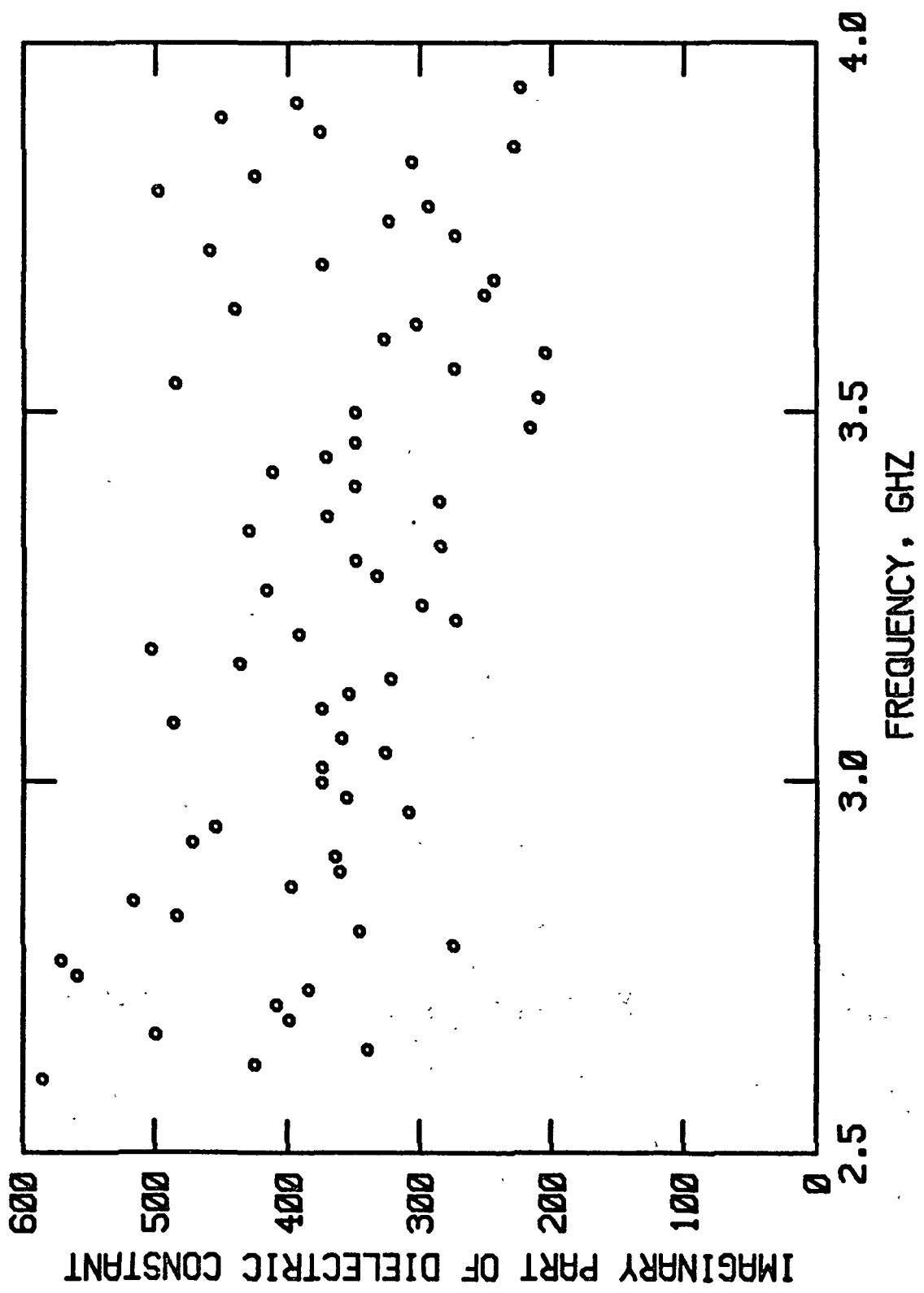


Figure 15.--- 30 percent KOH.

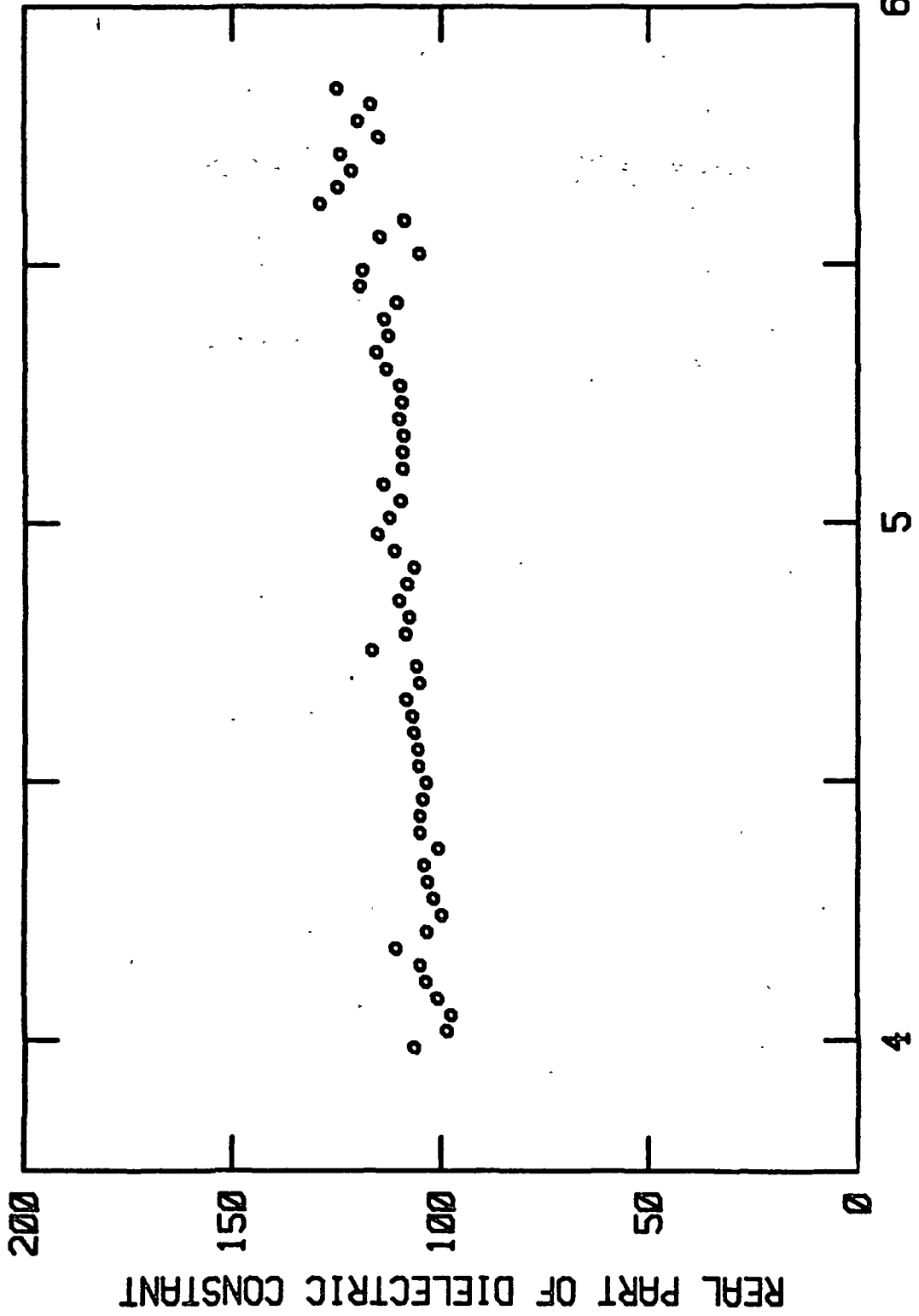


Figure 16.--Water.

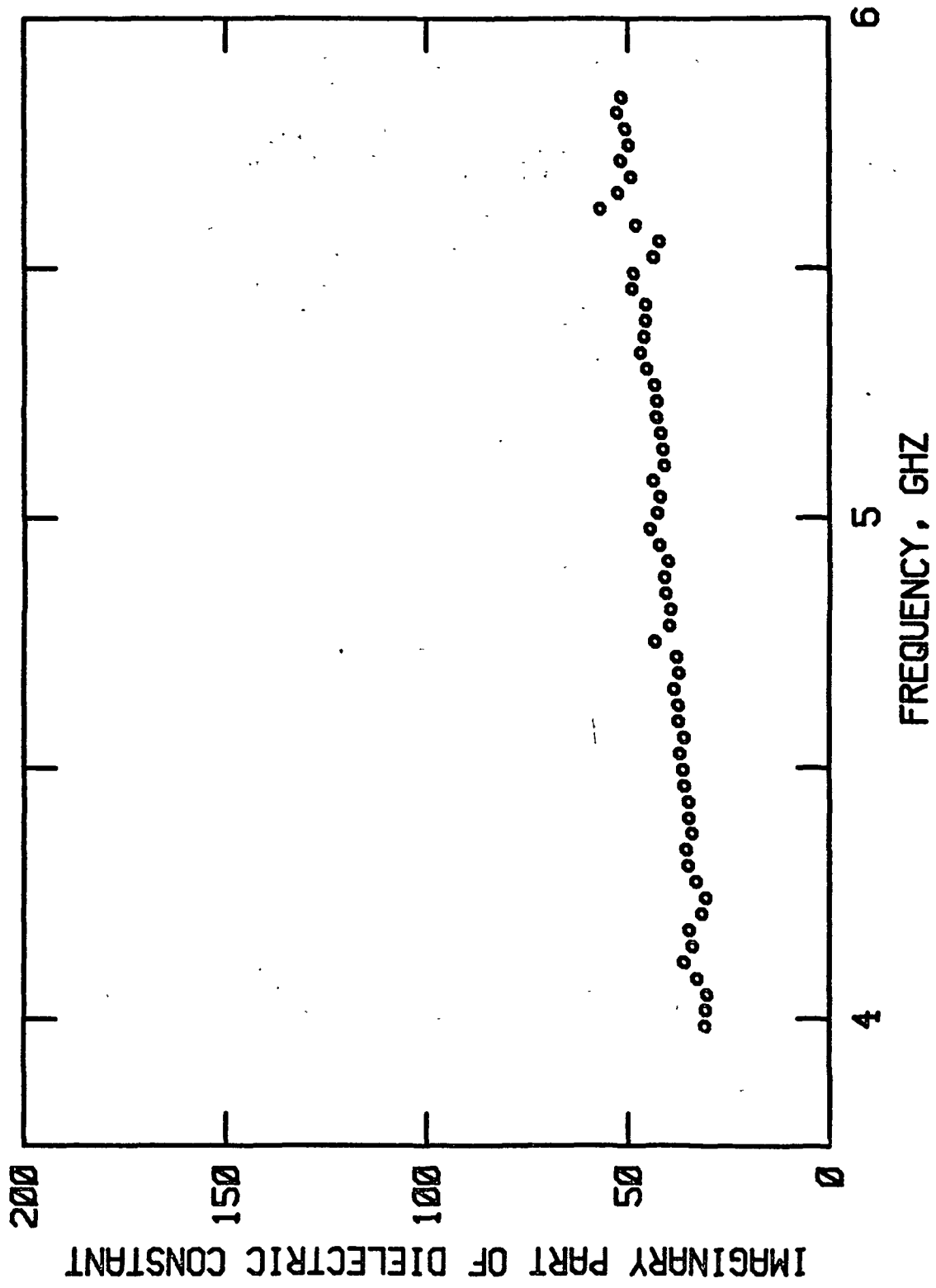


Figure 17.--Water.

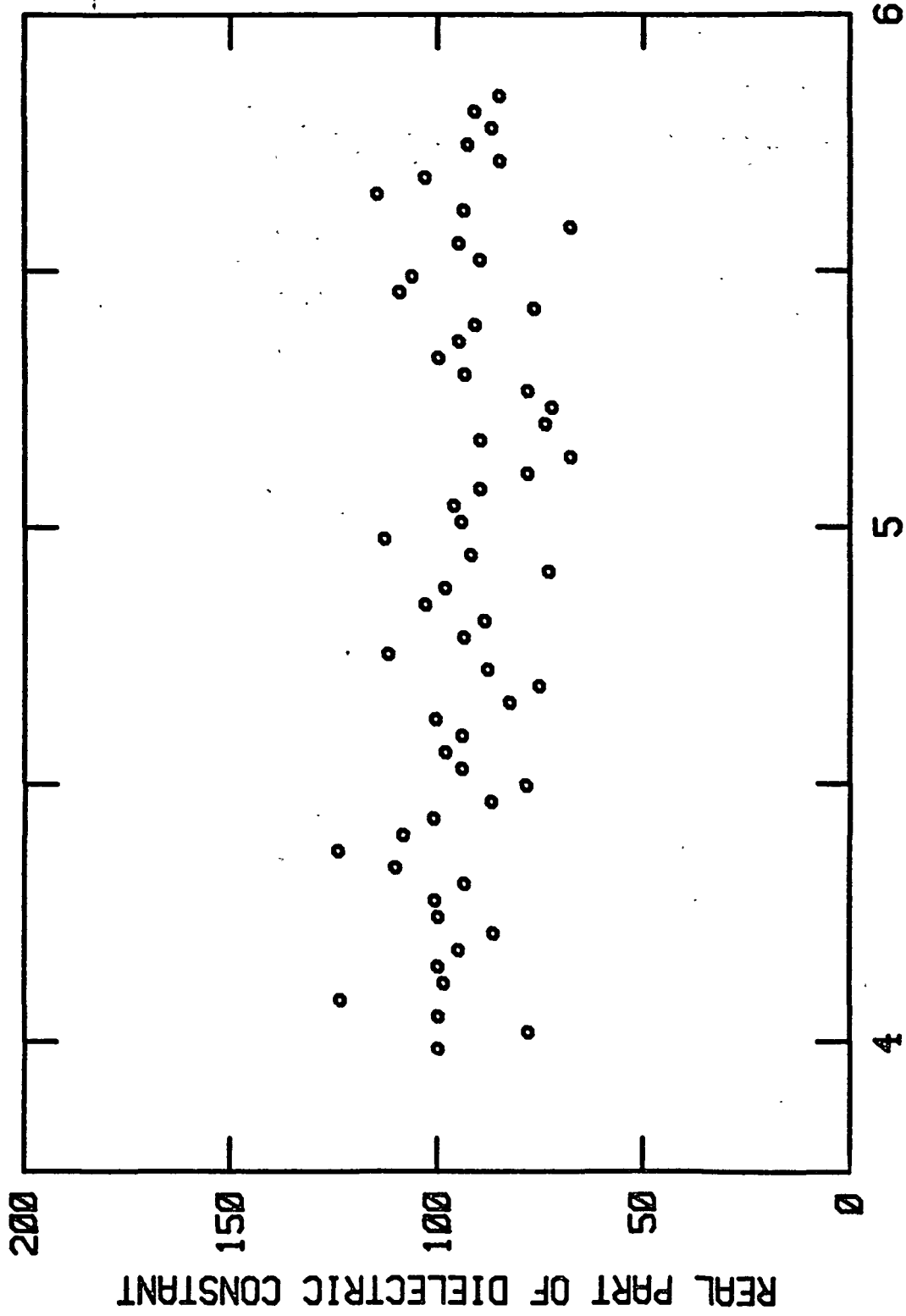


Figure 18.--5 percent KOH.

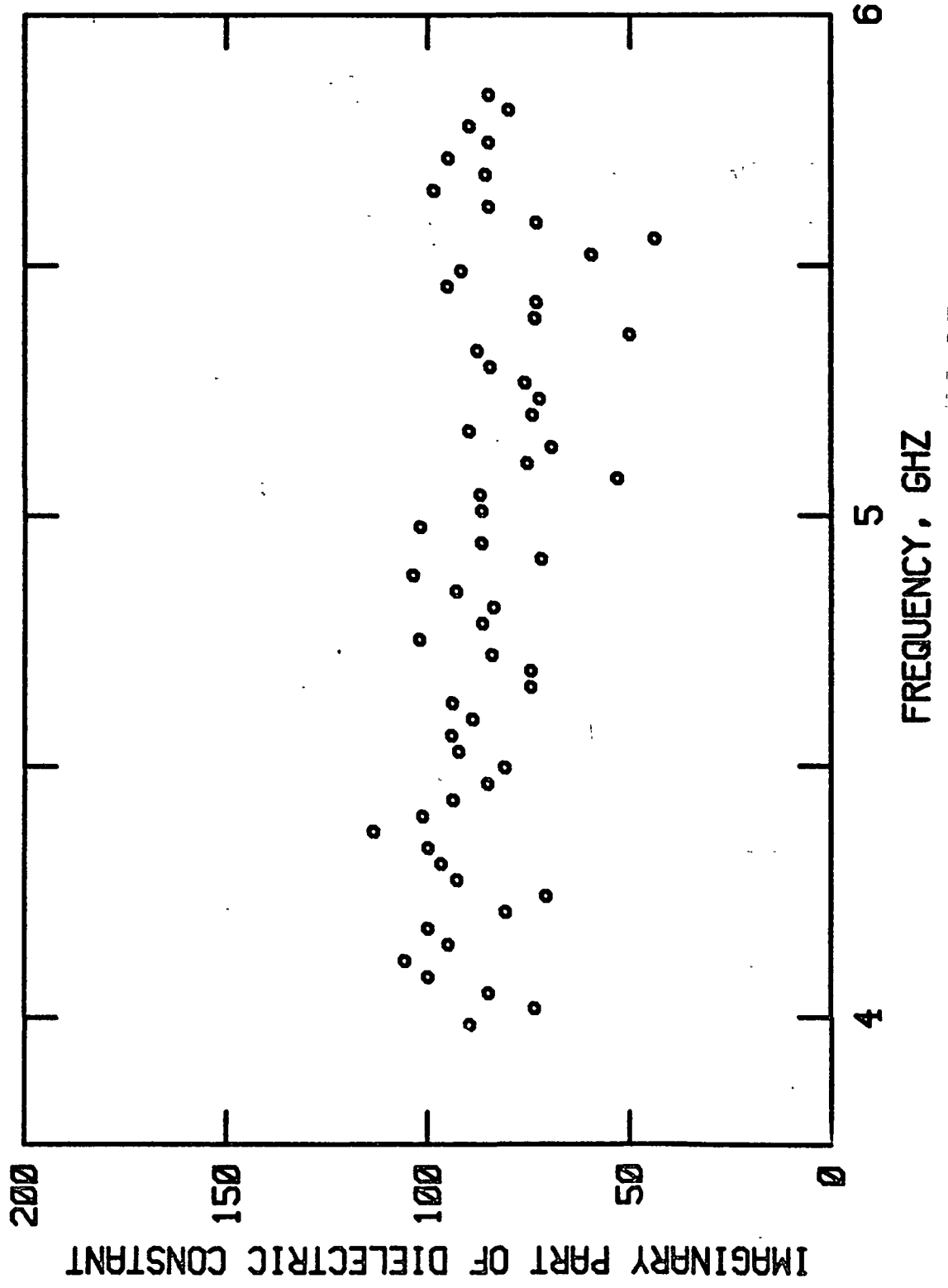


Figure 19.--5 percent KOH.

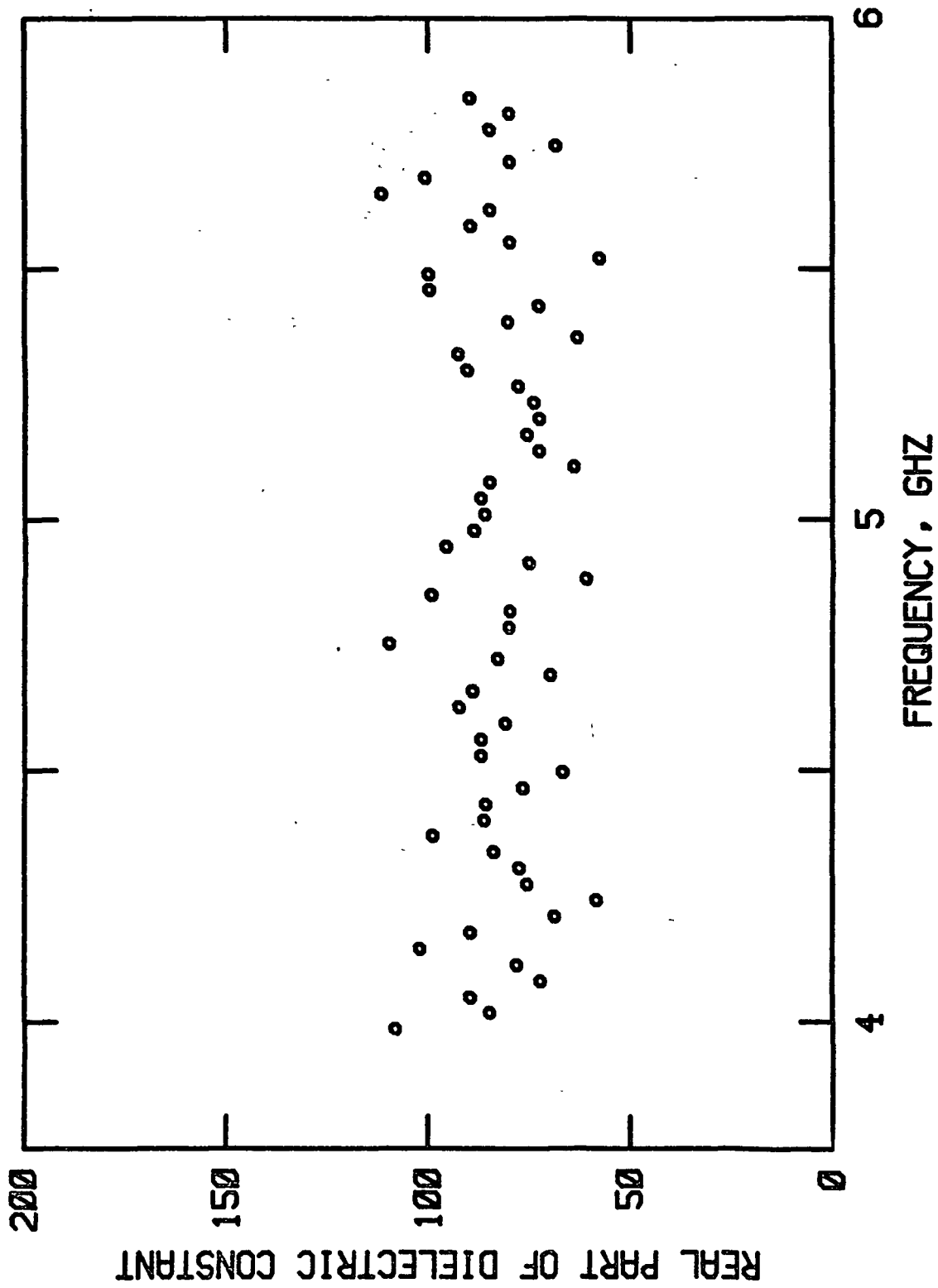


Figure 20.--10 percent KOH.

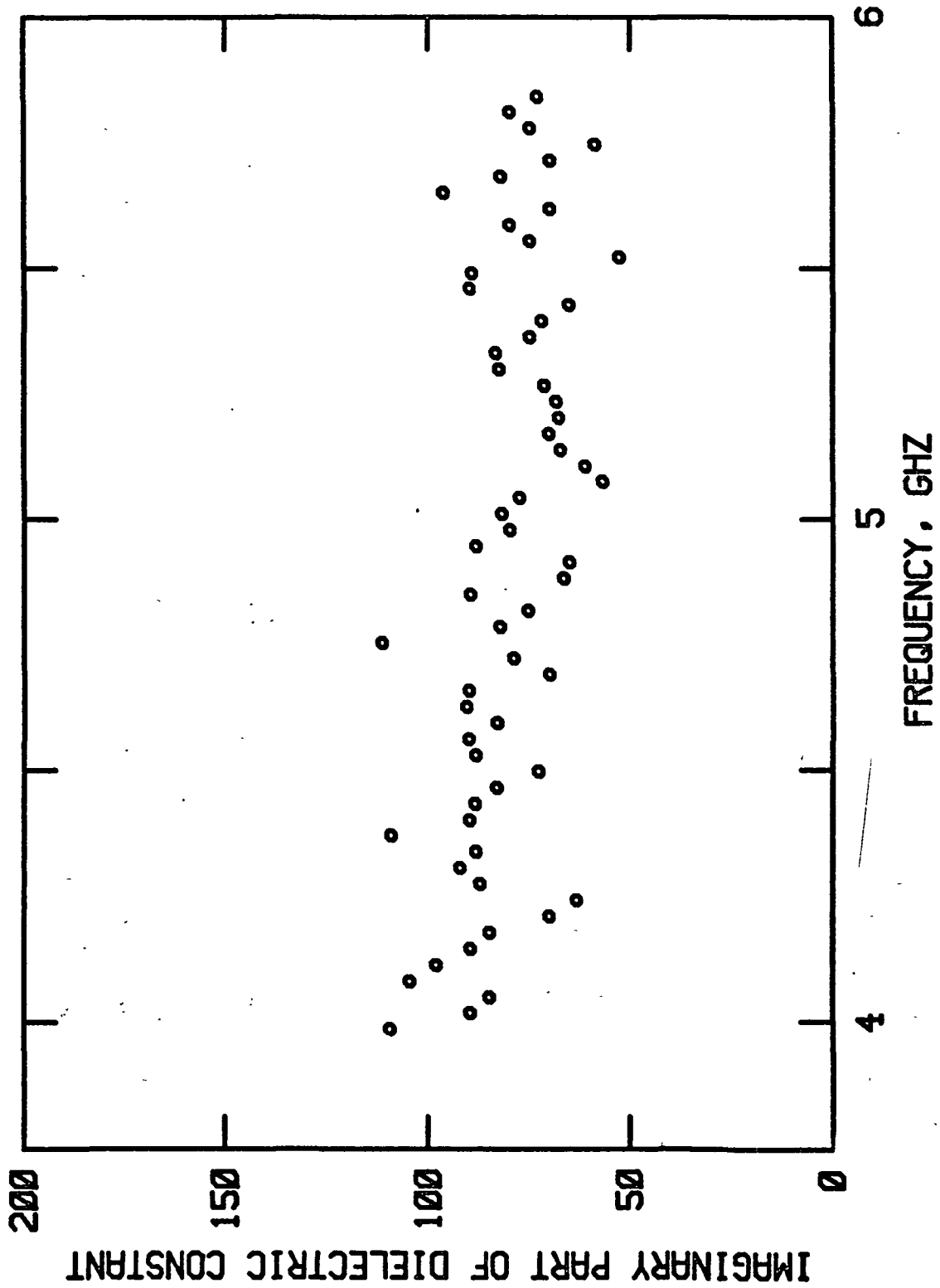


Figure 21.--10 percent KOH.

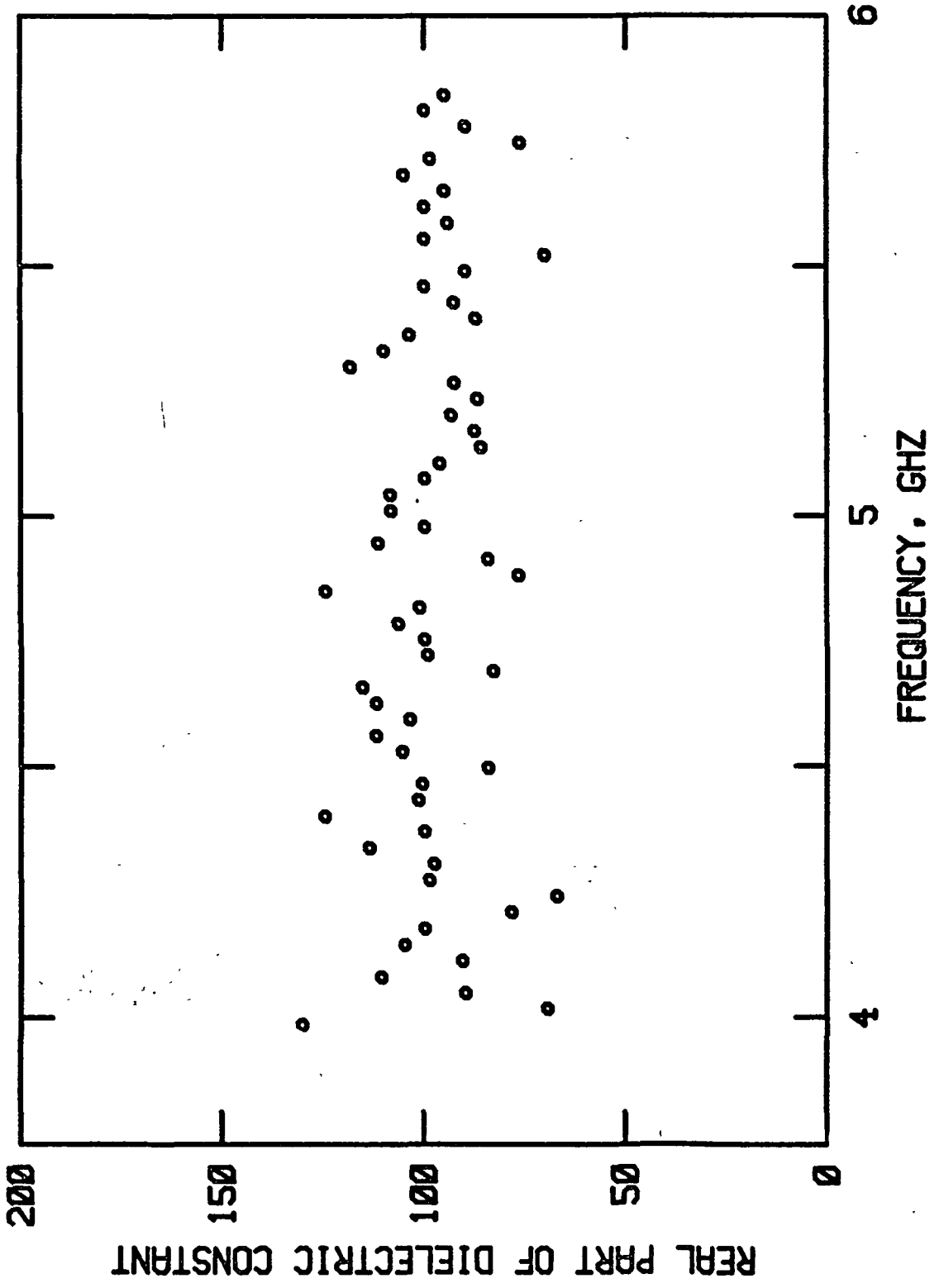


Figure 22.--15 percent KOH.



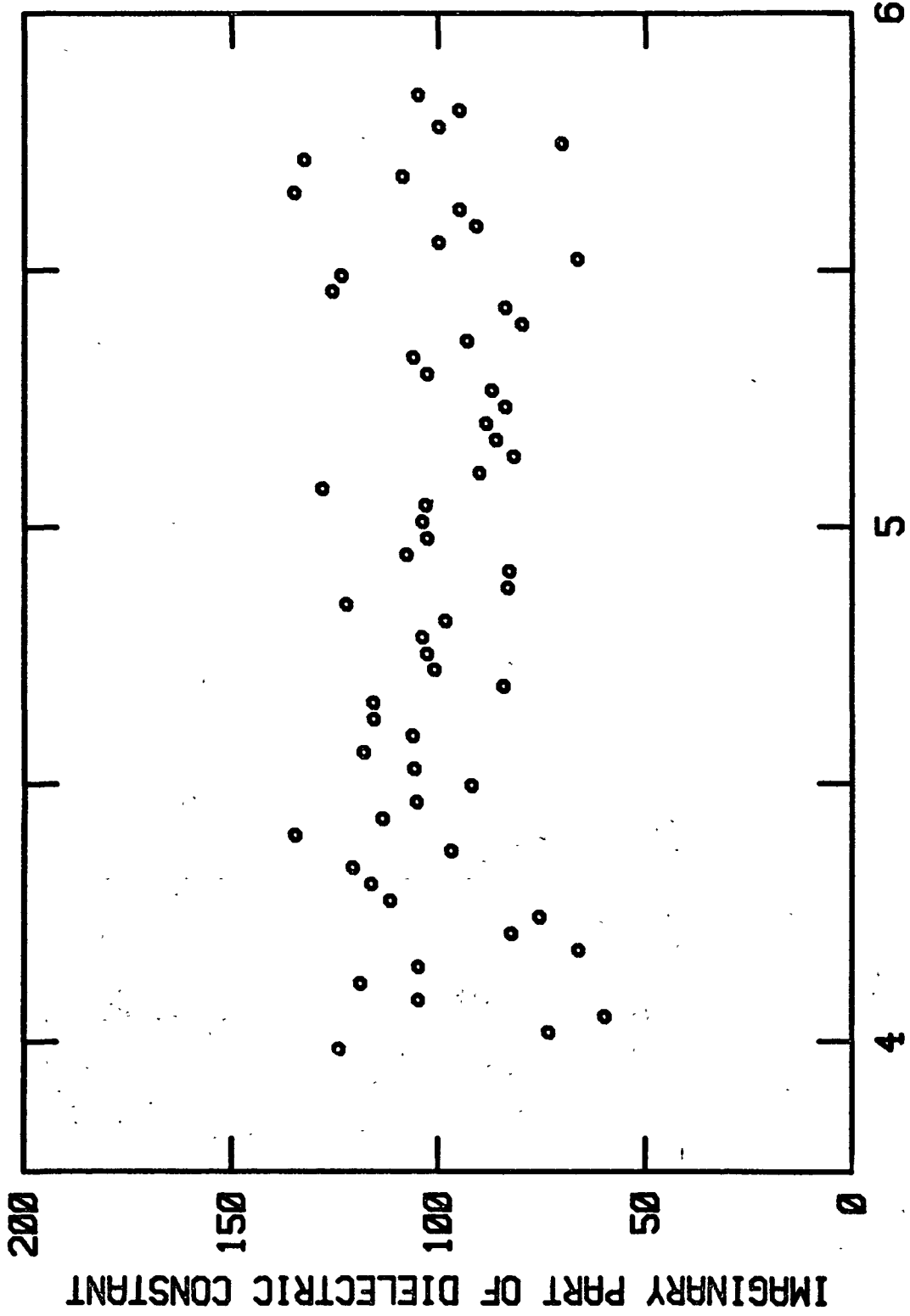


Figure 23.--15 percent KOH.

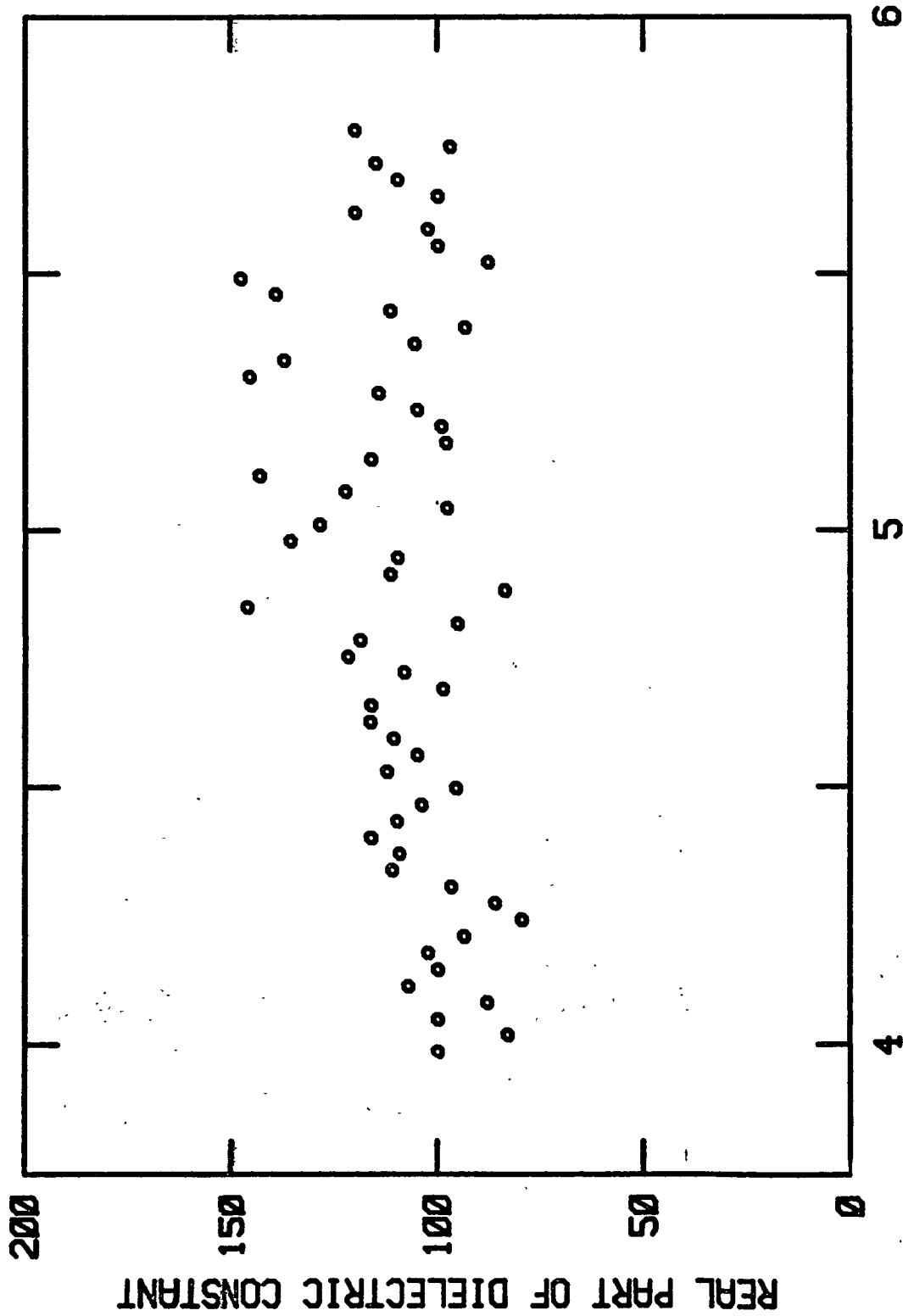


Figure 24.--20 percent KOH.

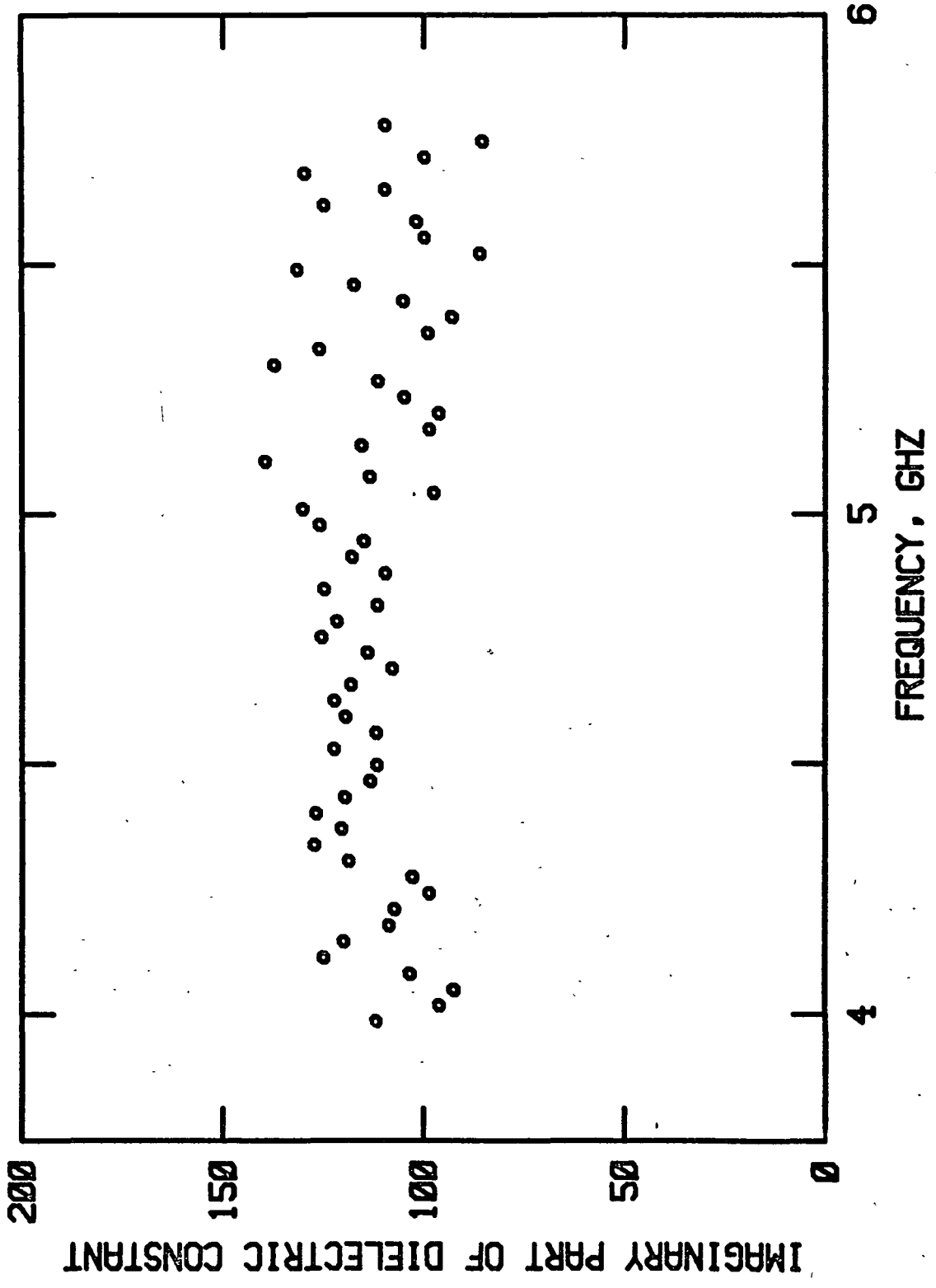


Figure 25.--20 percent KOH.

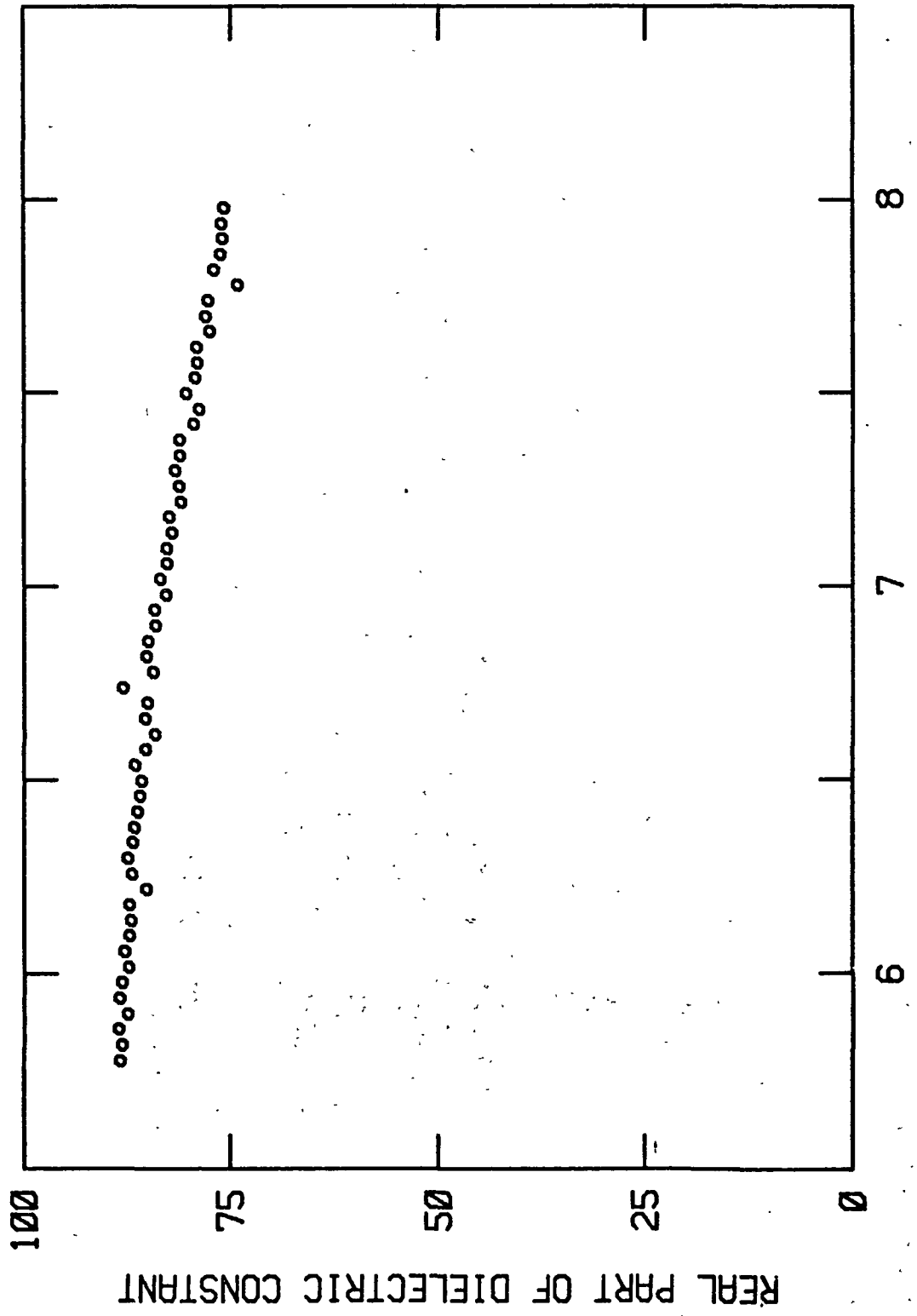


Figure 26.--Water.

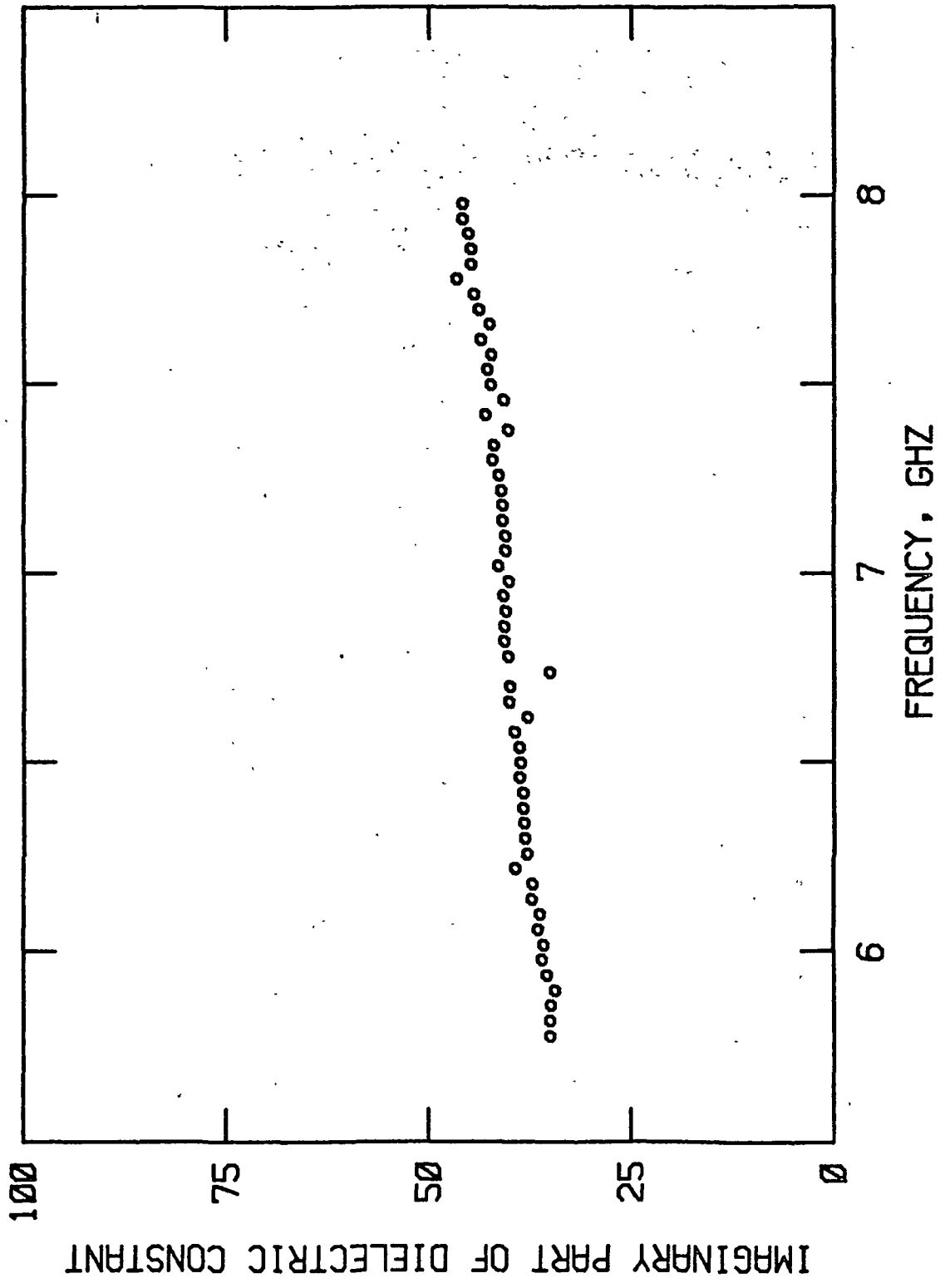


Figure 27.--Water.

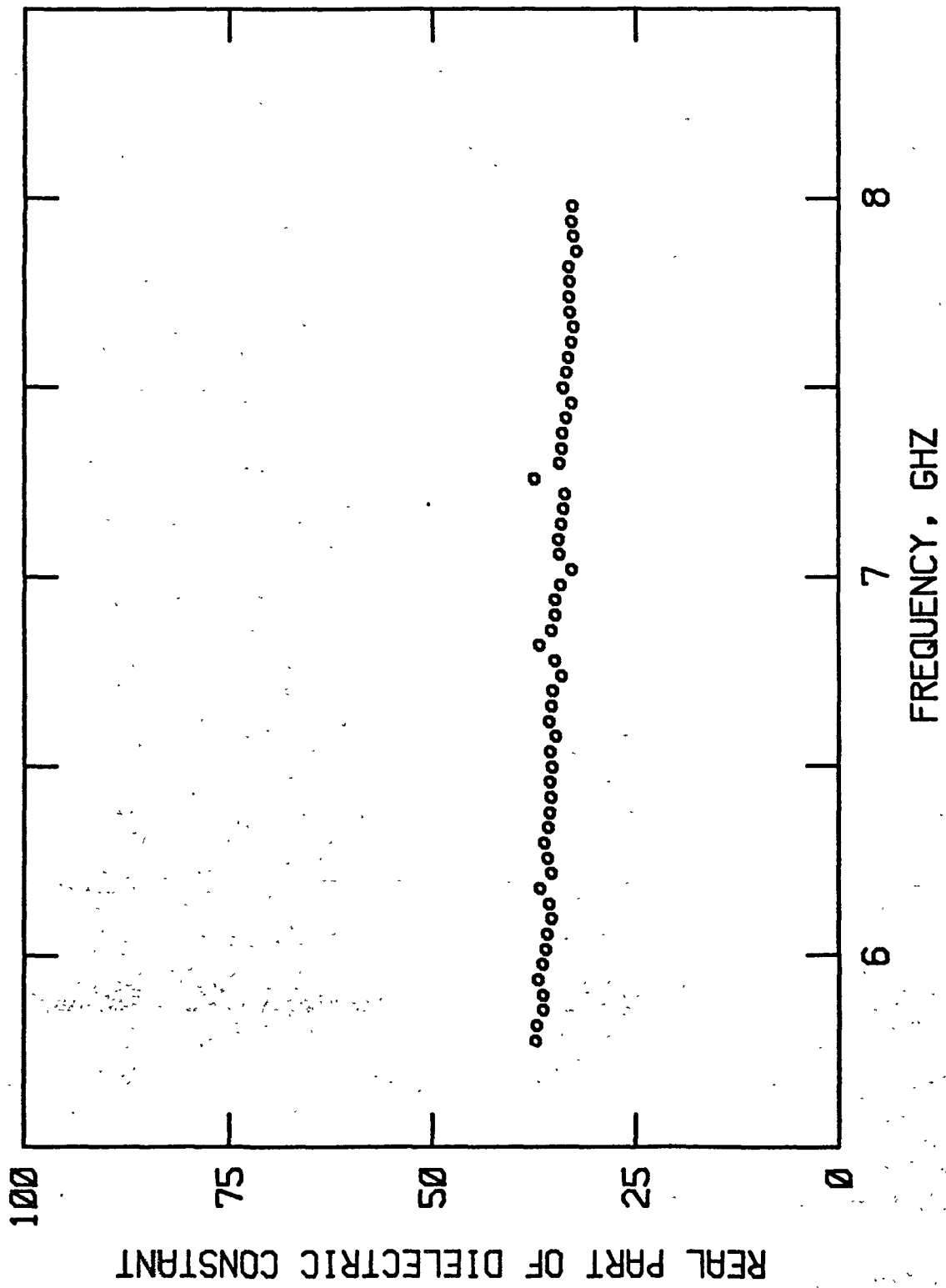


Figure 28.--5 percent KOH.

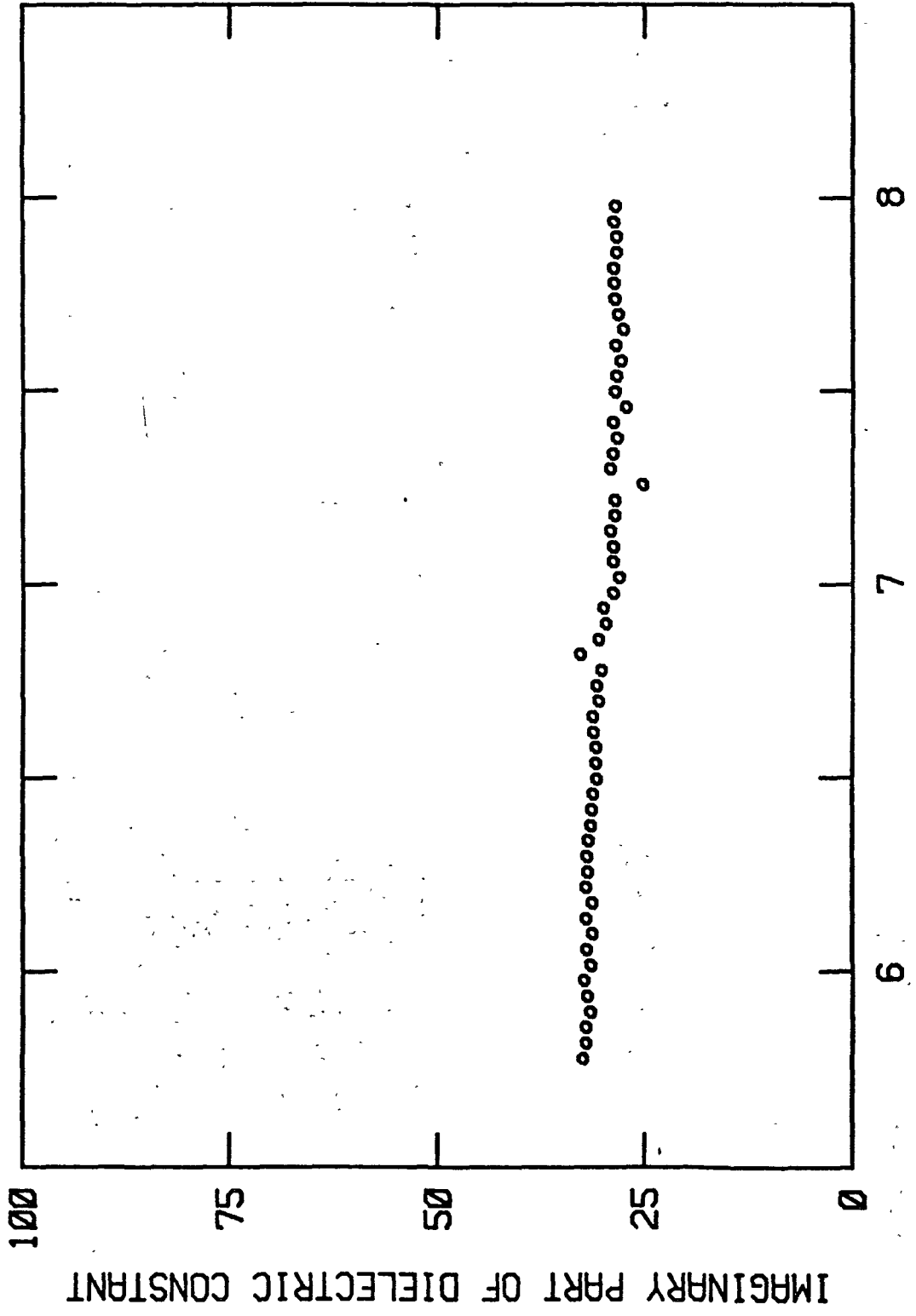


Figure 29.--5 percent KOH.

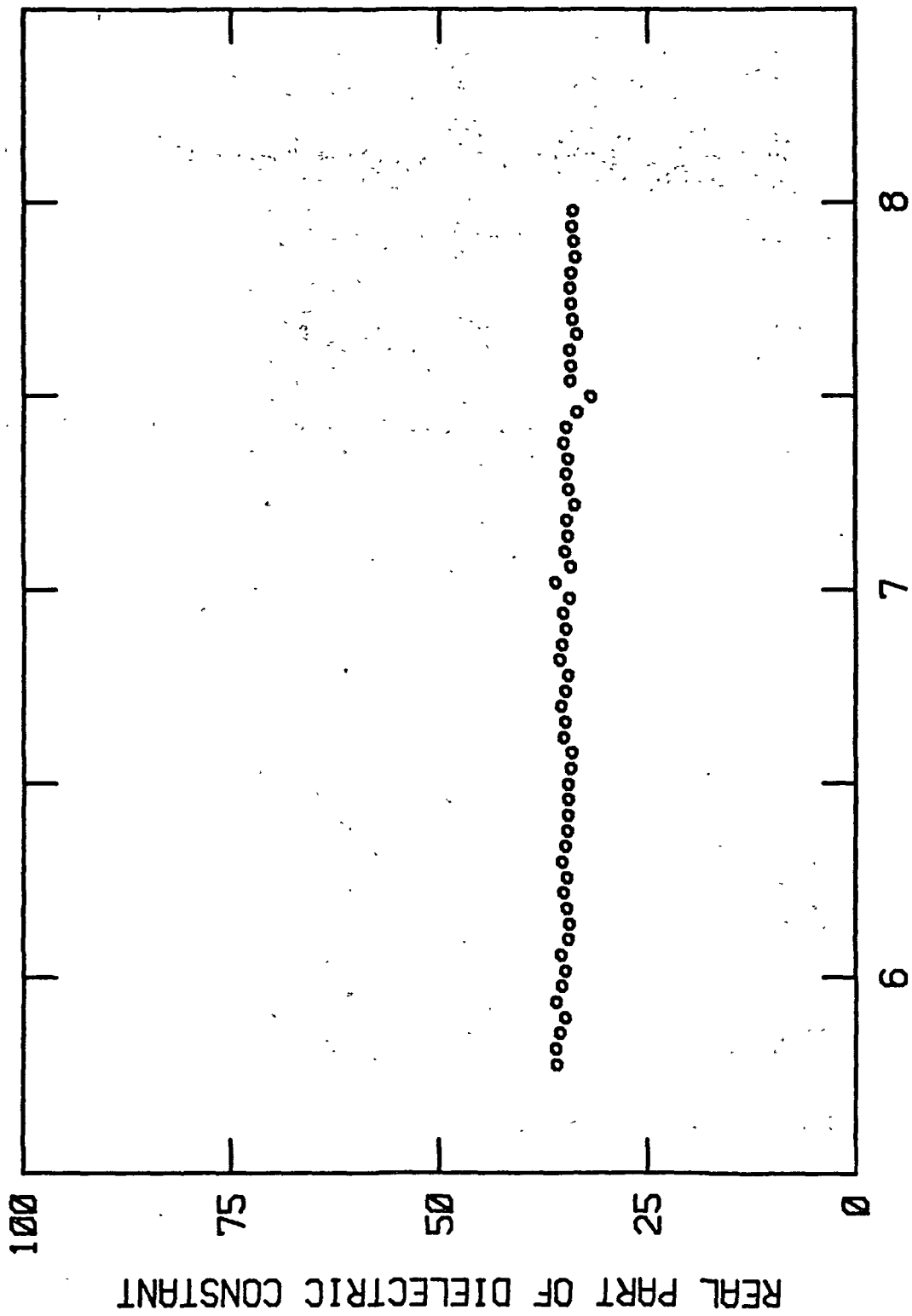


Figure 30.--10 percent KOH.



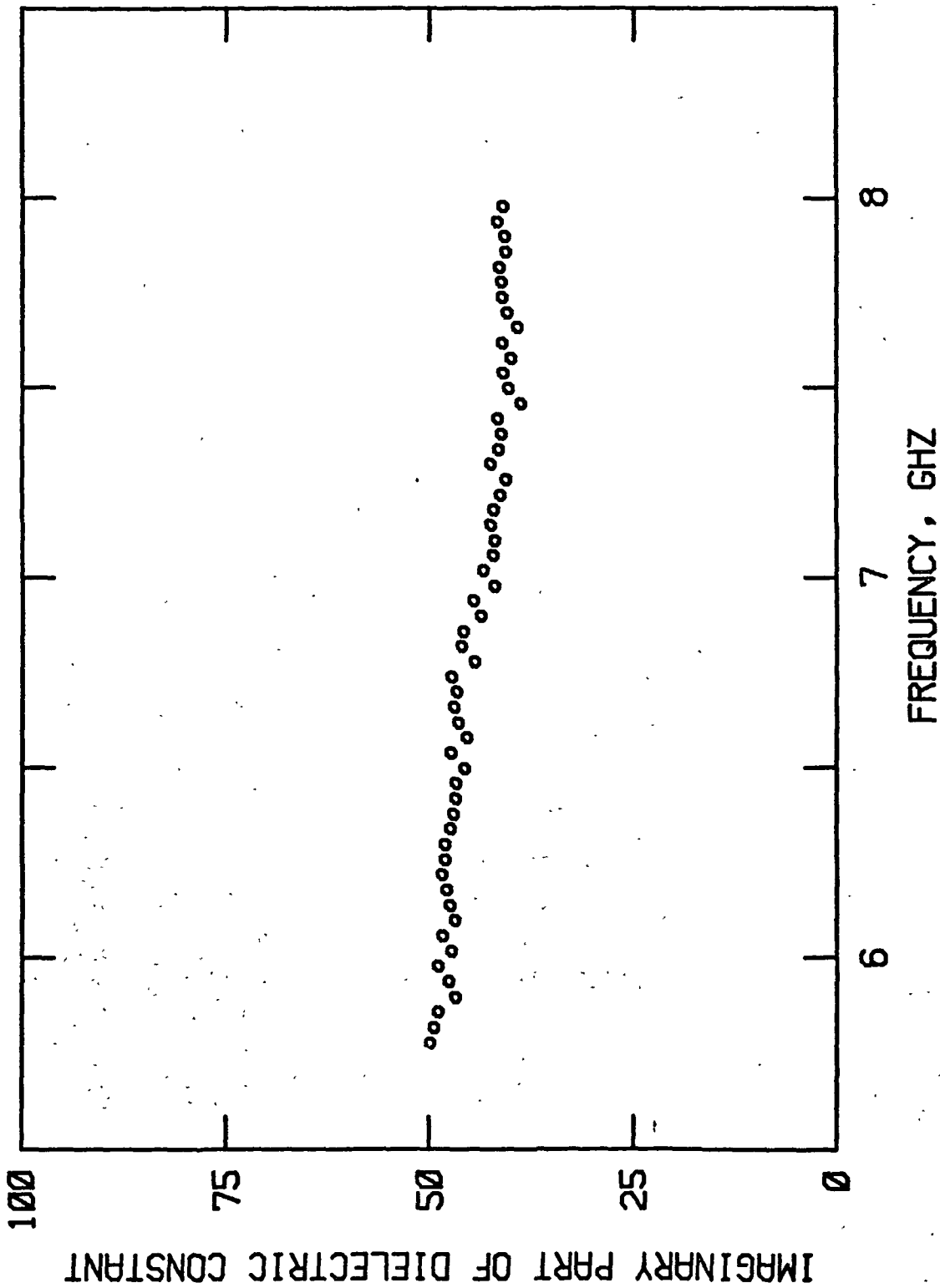


Figure 31.--10 percent KOH.

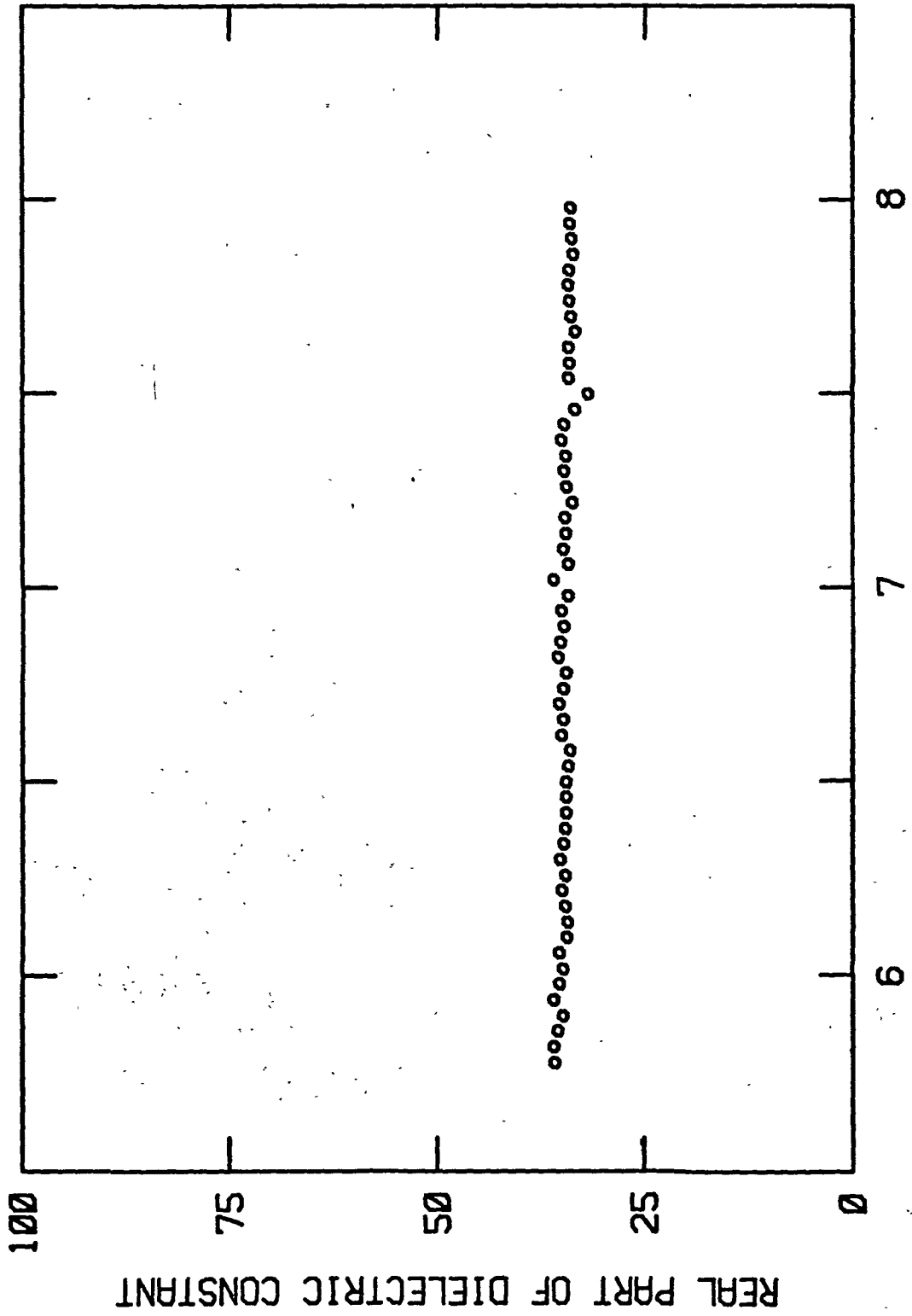


Figure 32.--20 percent KOH.

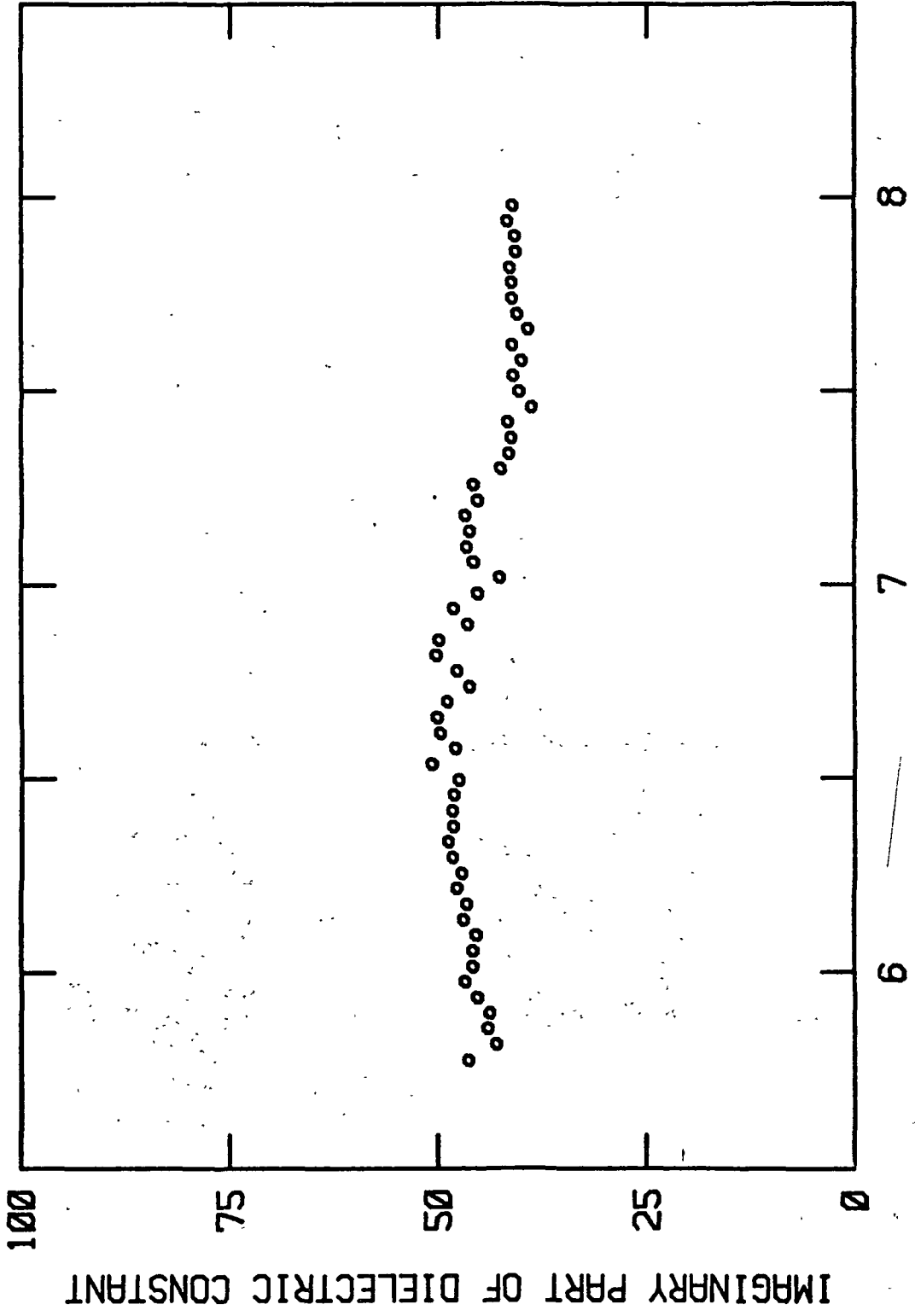


Figure 33.--20 percent KOH.

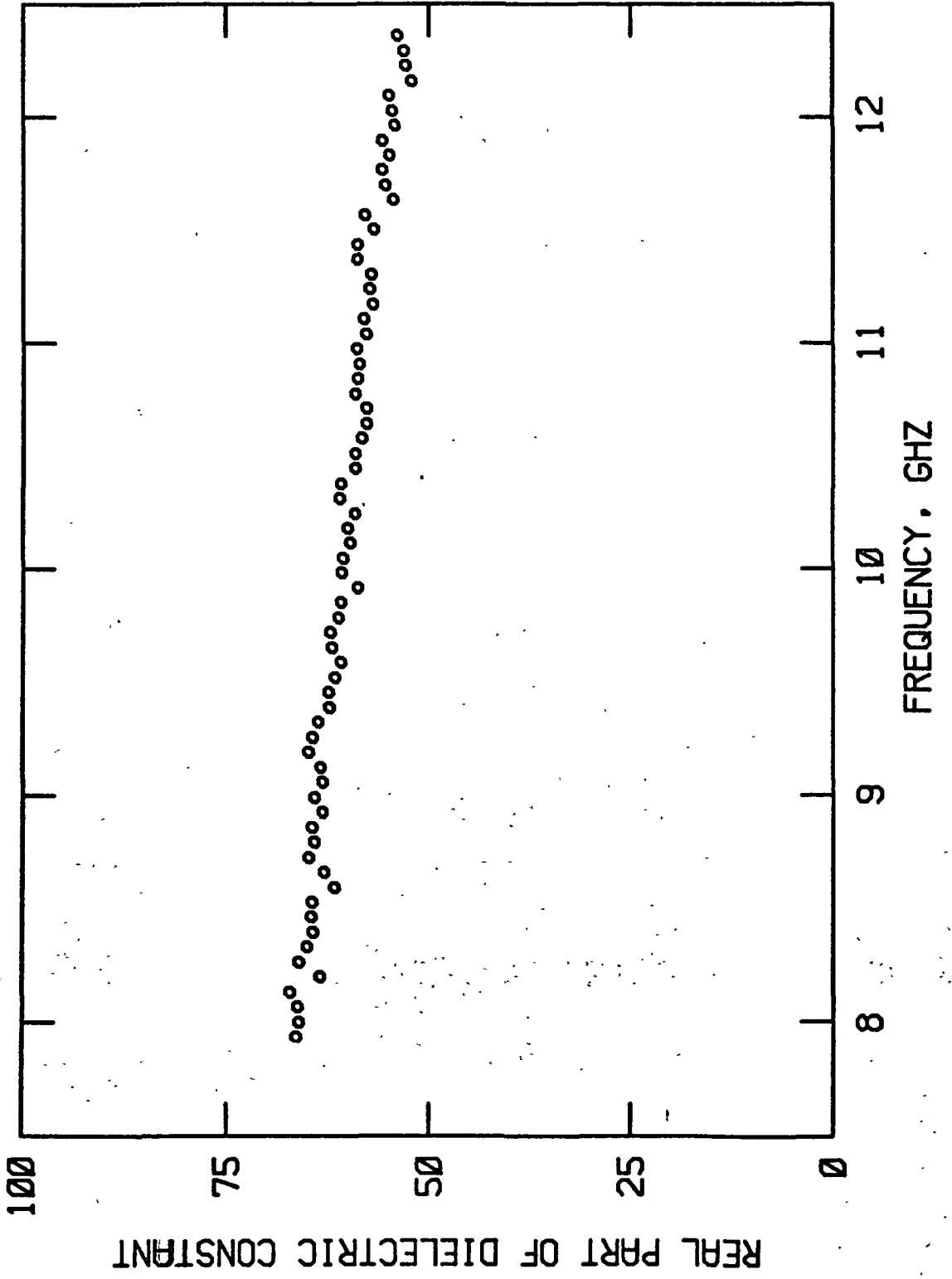


Figure 34. --Water.

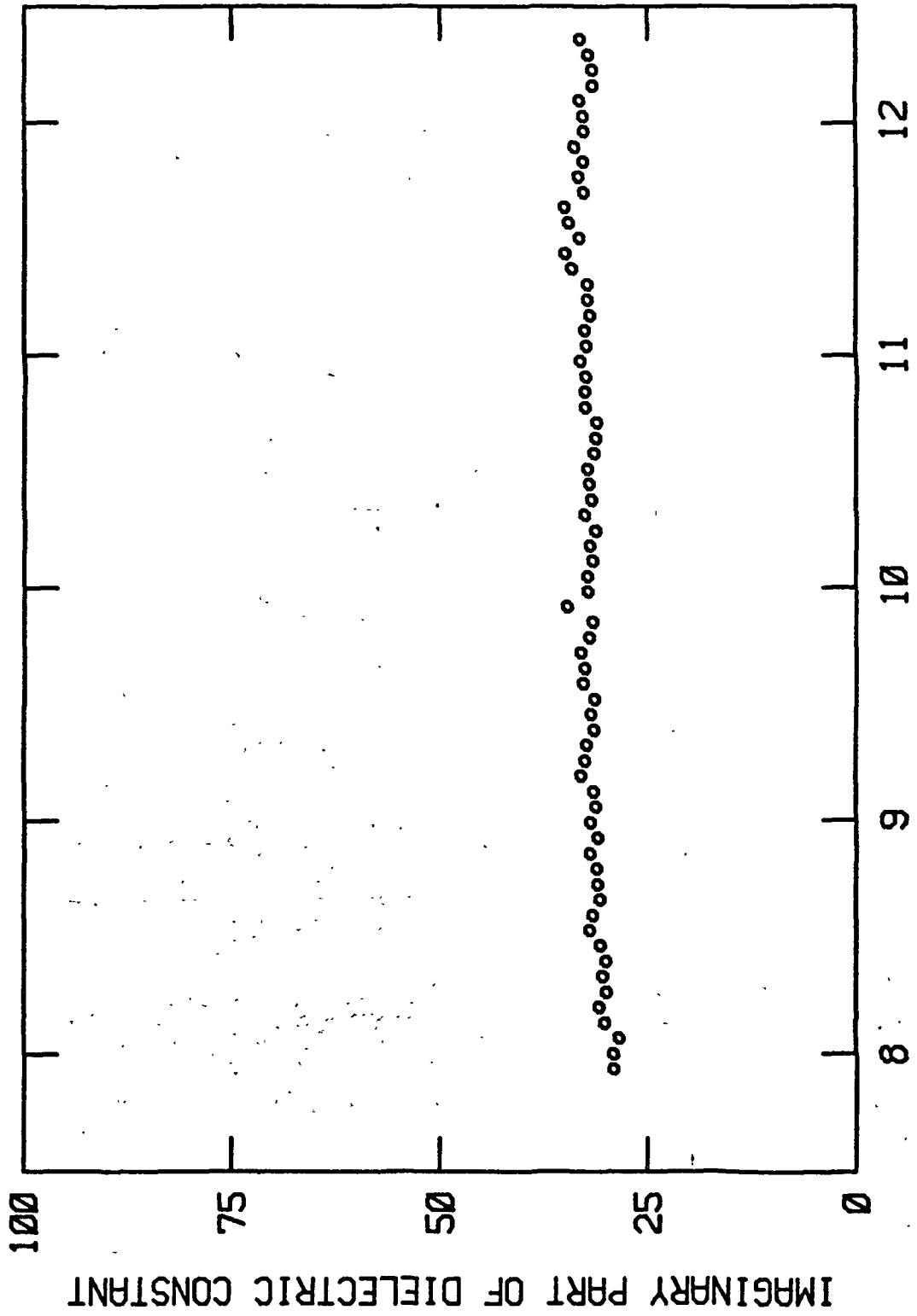


Figure 35.---Water.

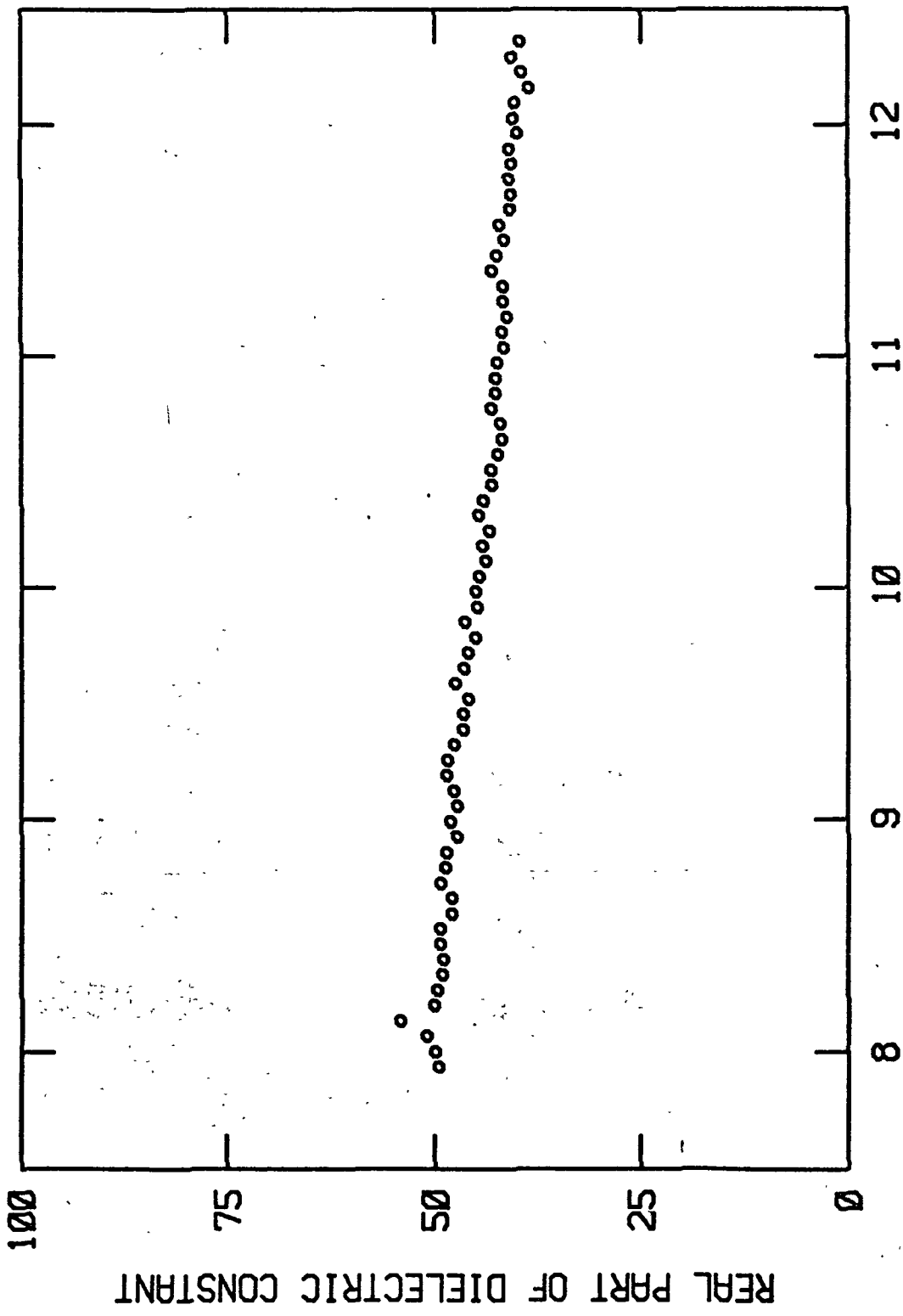


Figure 36.--5 percent KOH.

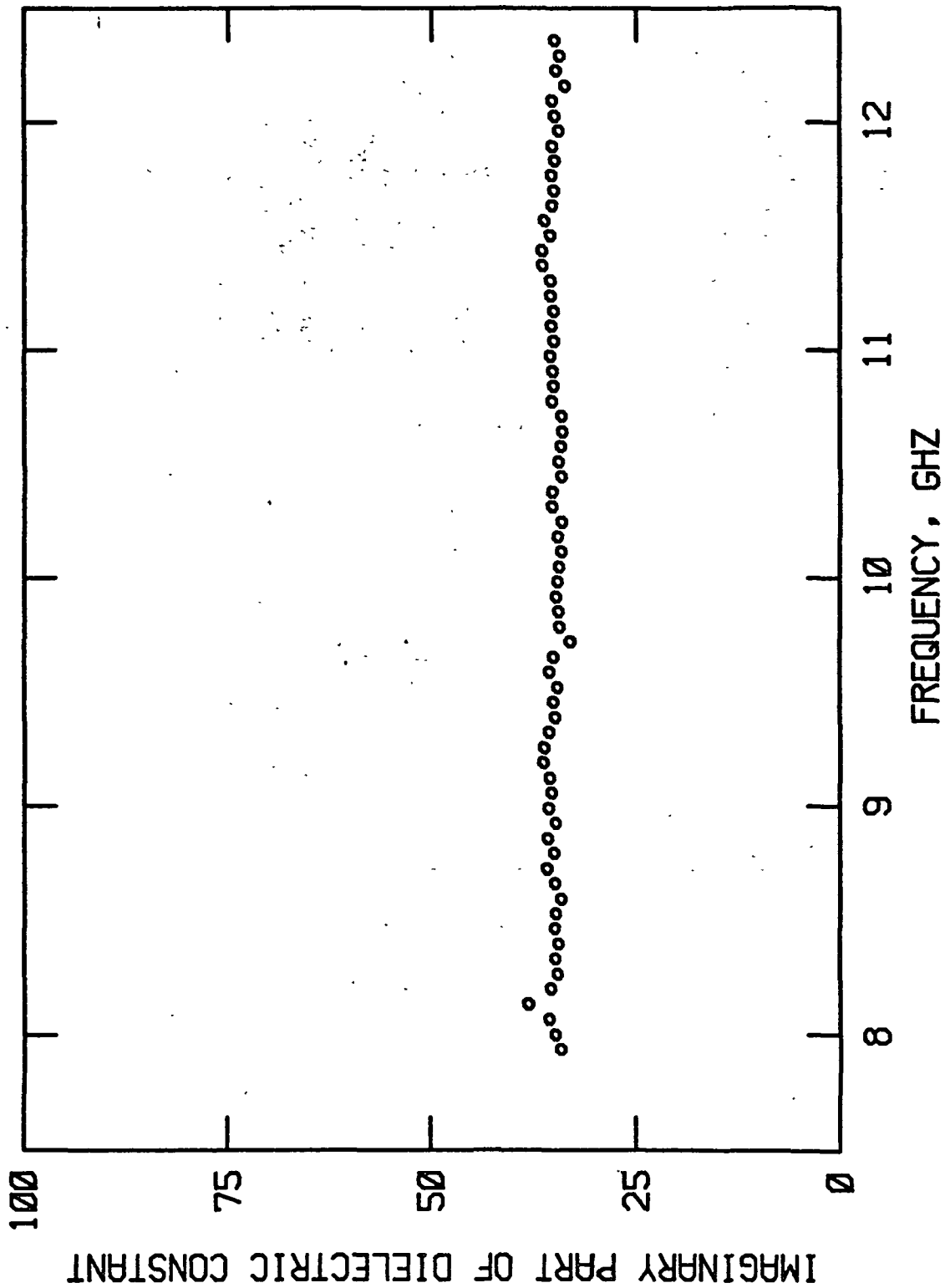


Figure 37.--5 percent KOH.

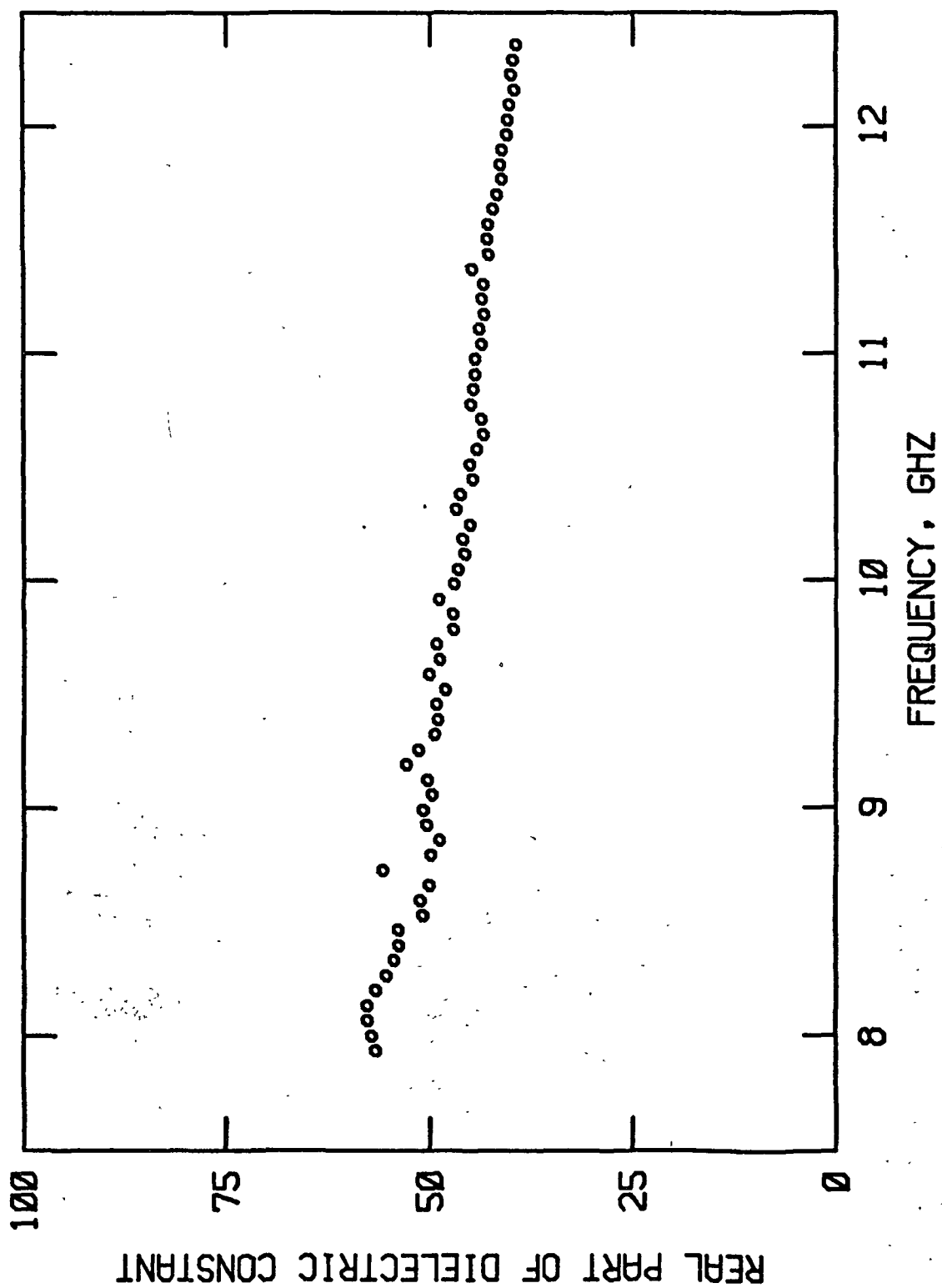


Figure 38.--10 percent KOH.



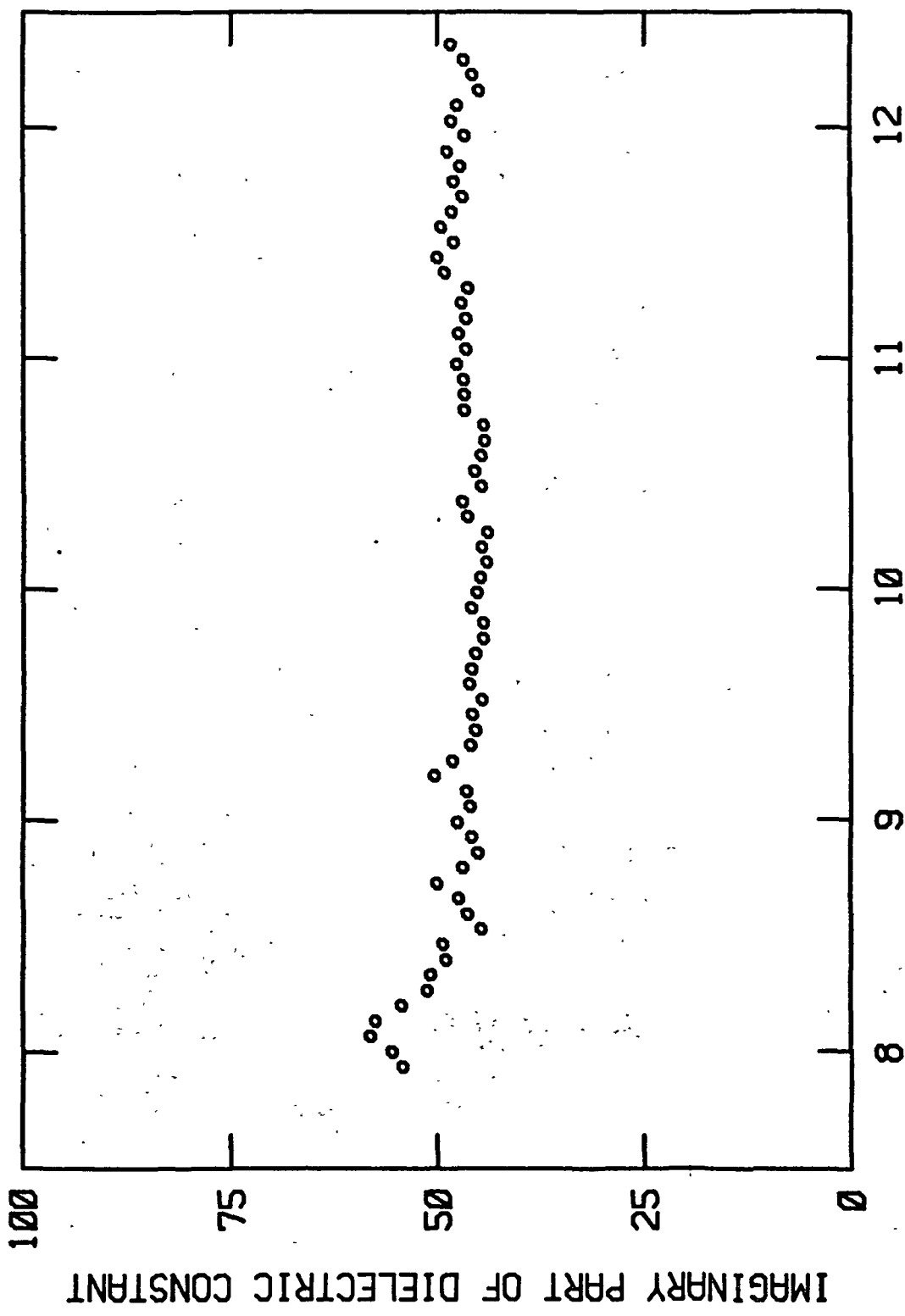


Figure 39.--10 percent KOH.

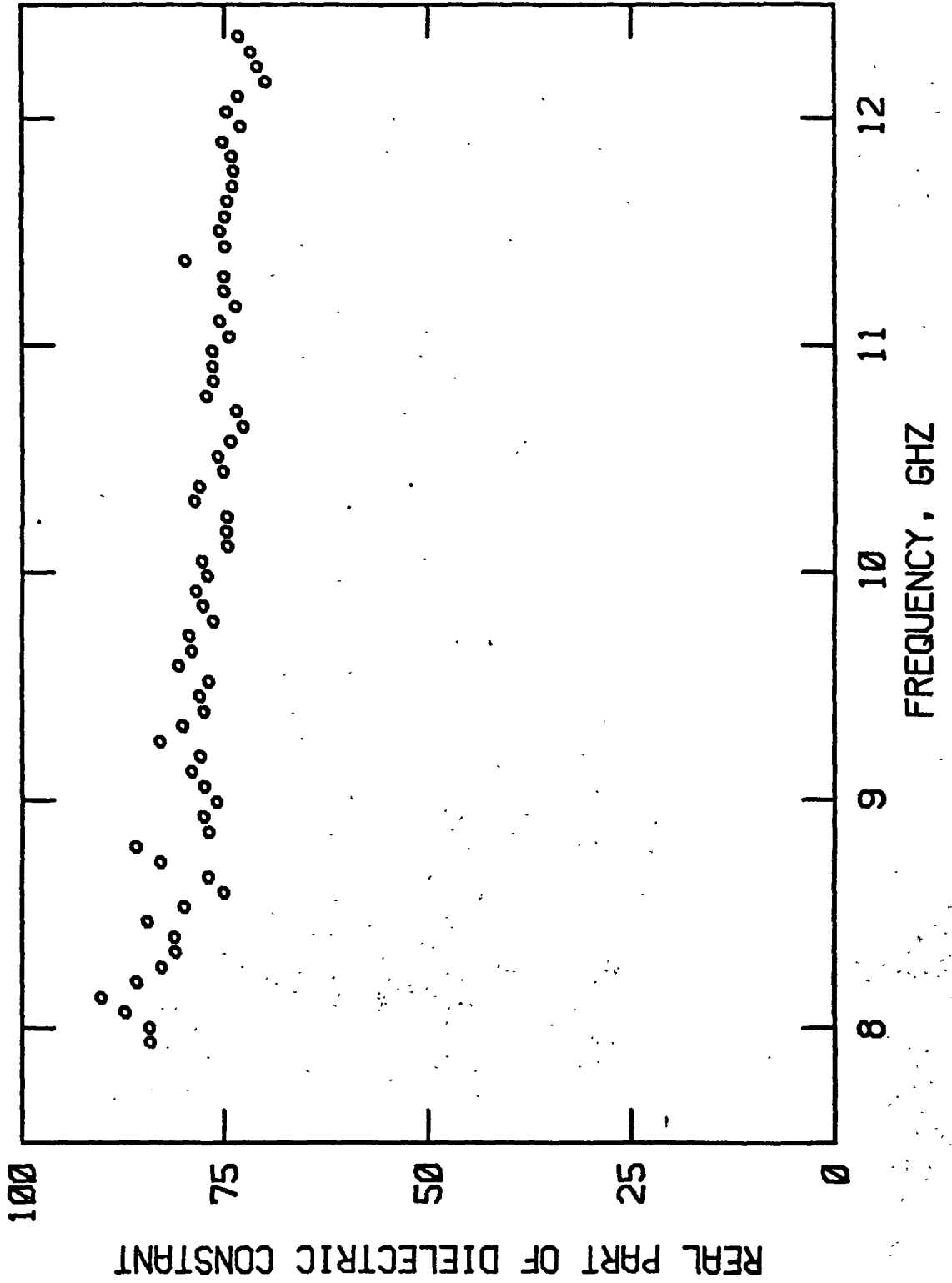


Figure 40.--15 percent KOH.

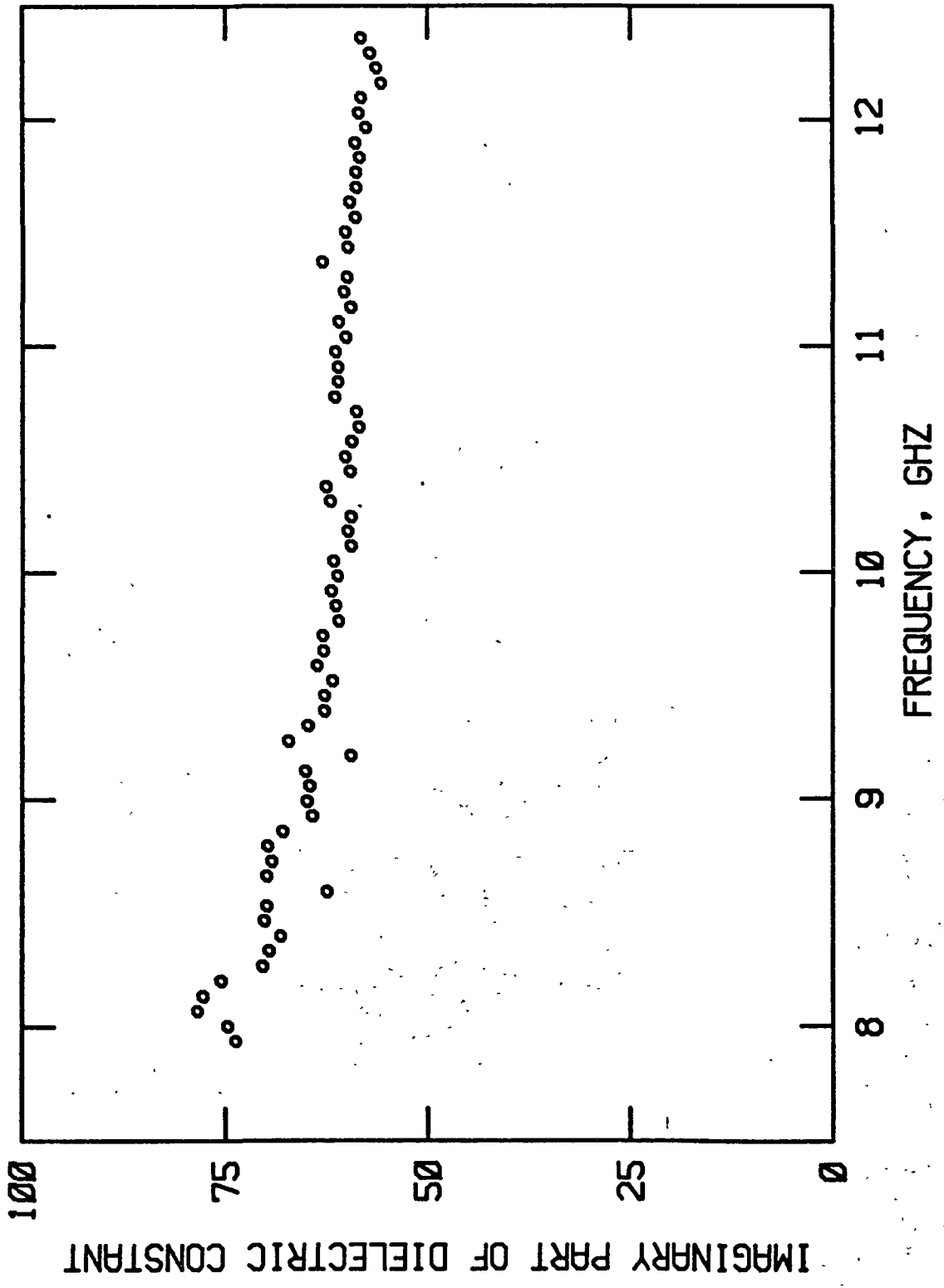


Figure 41.--15 percent KOH.

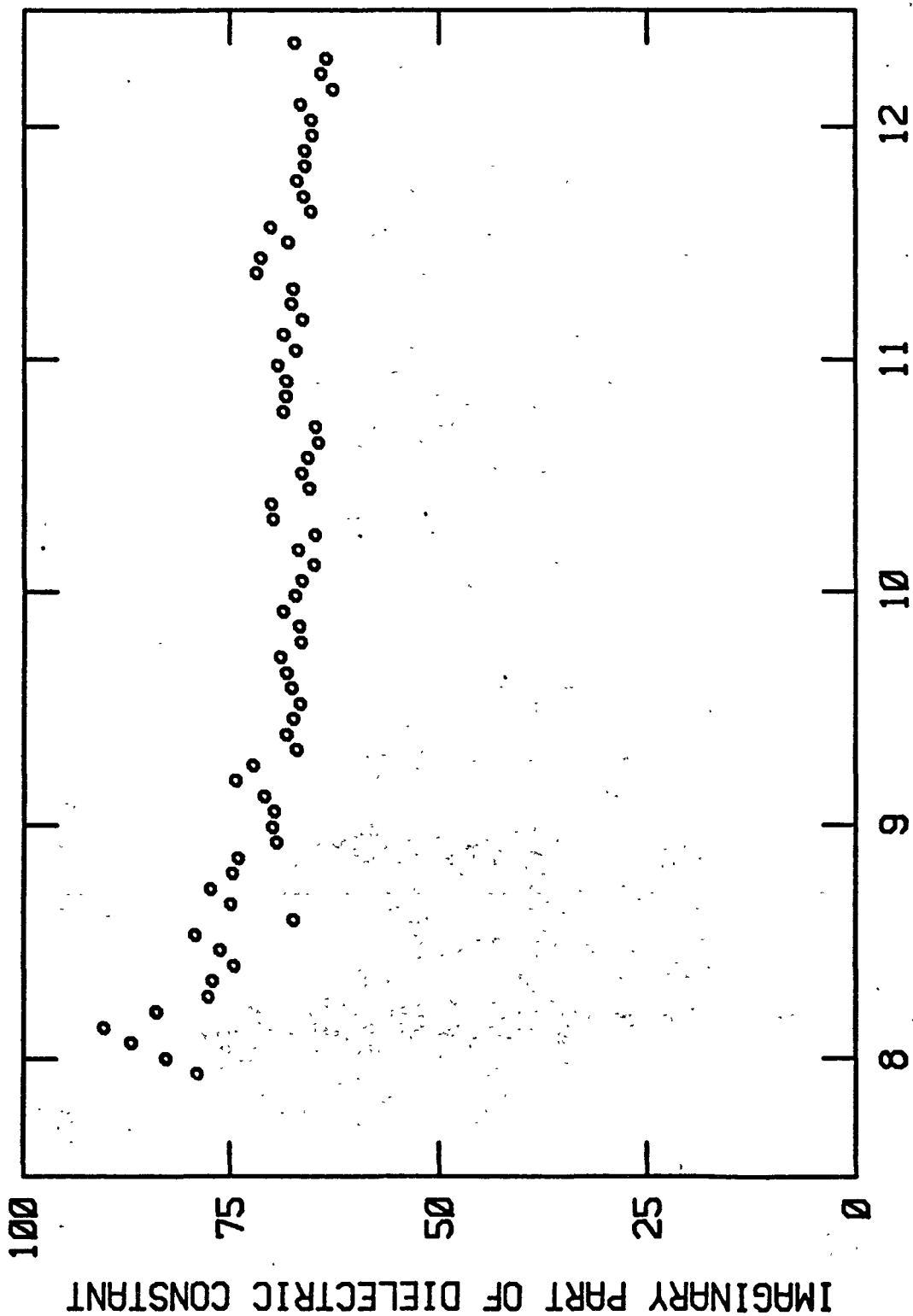


Figure 42.--20 percent KOH.

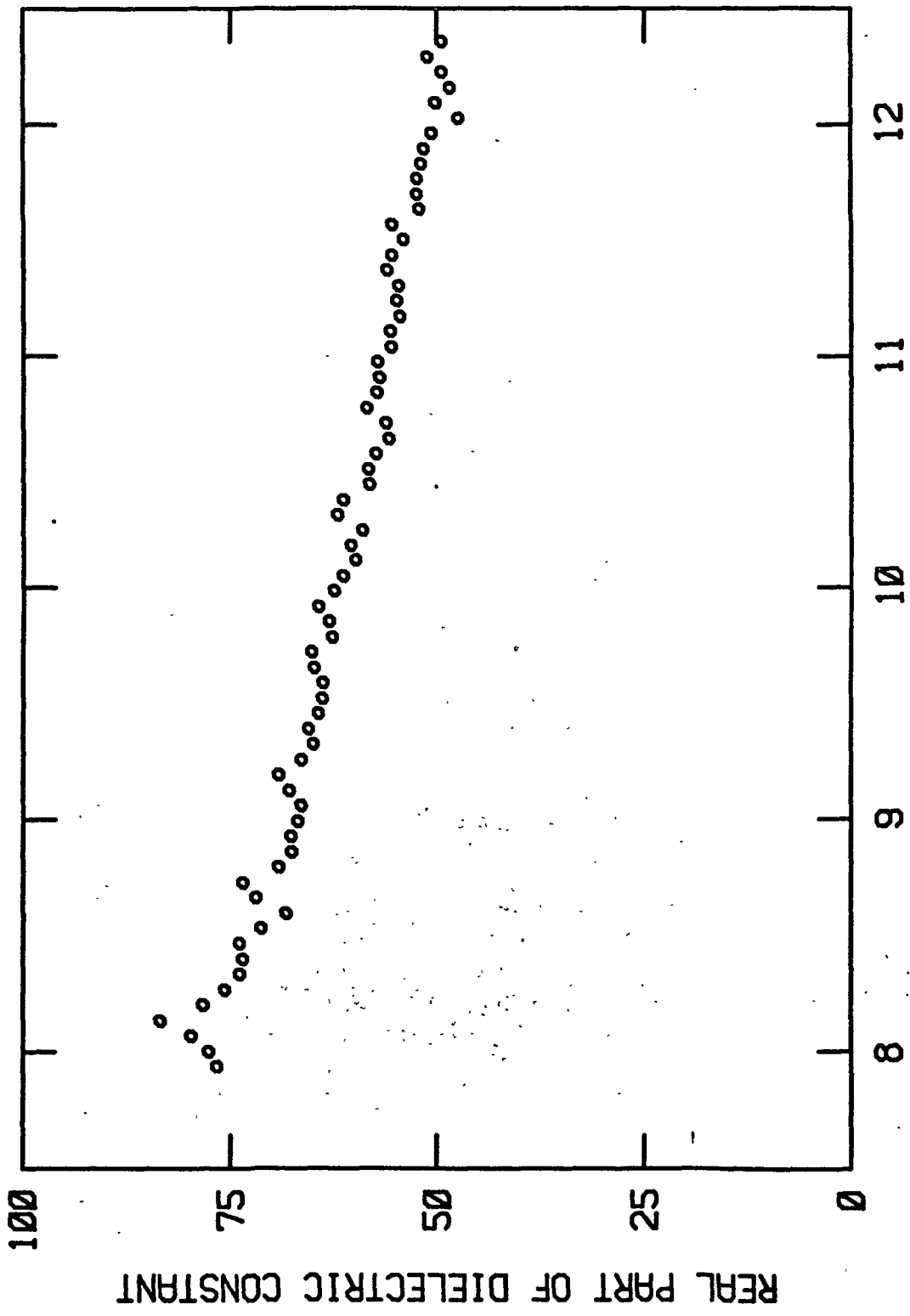


Figure 43.--20 percent KOH.

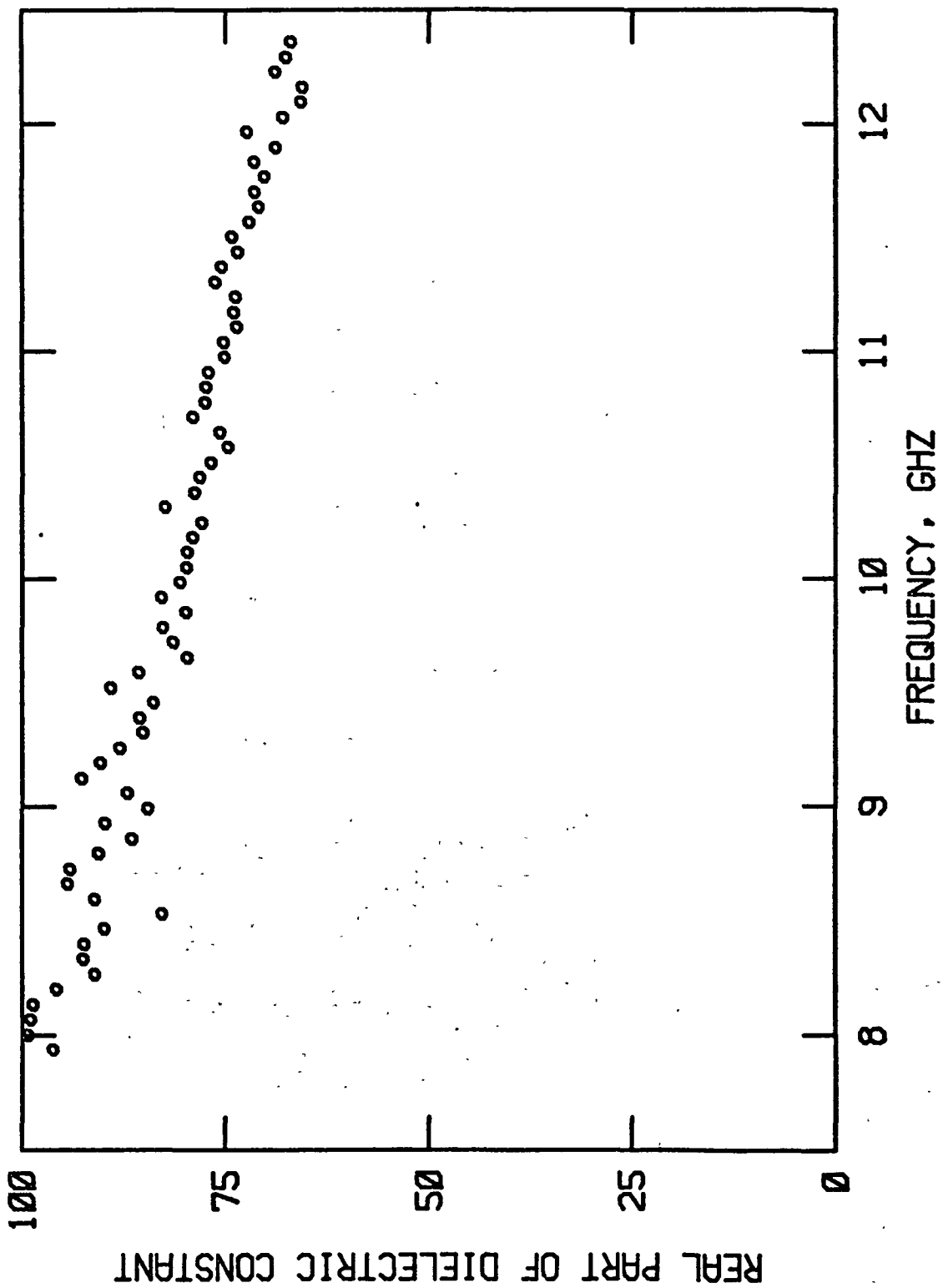


Figure 44.--25 percent KOH.

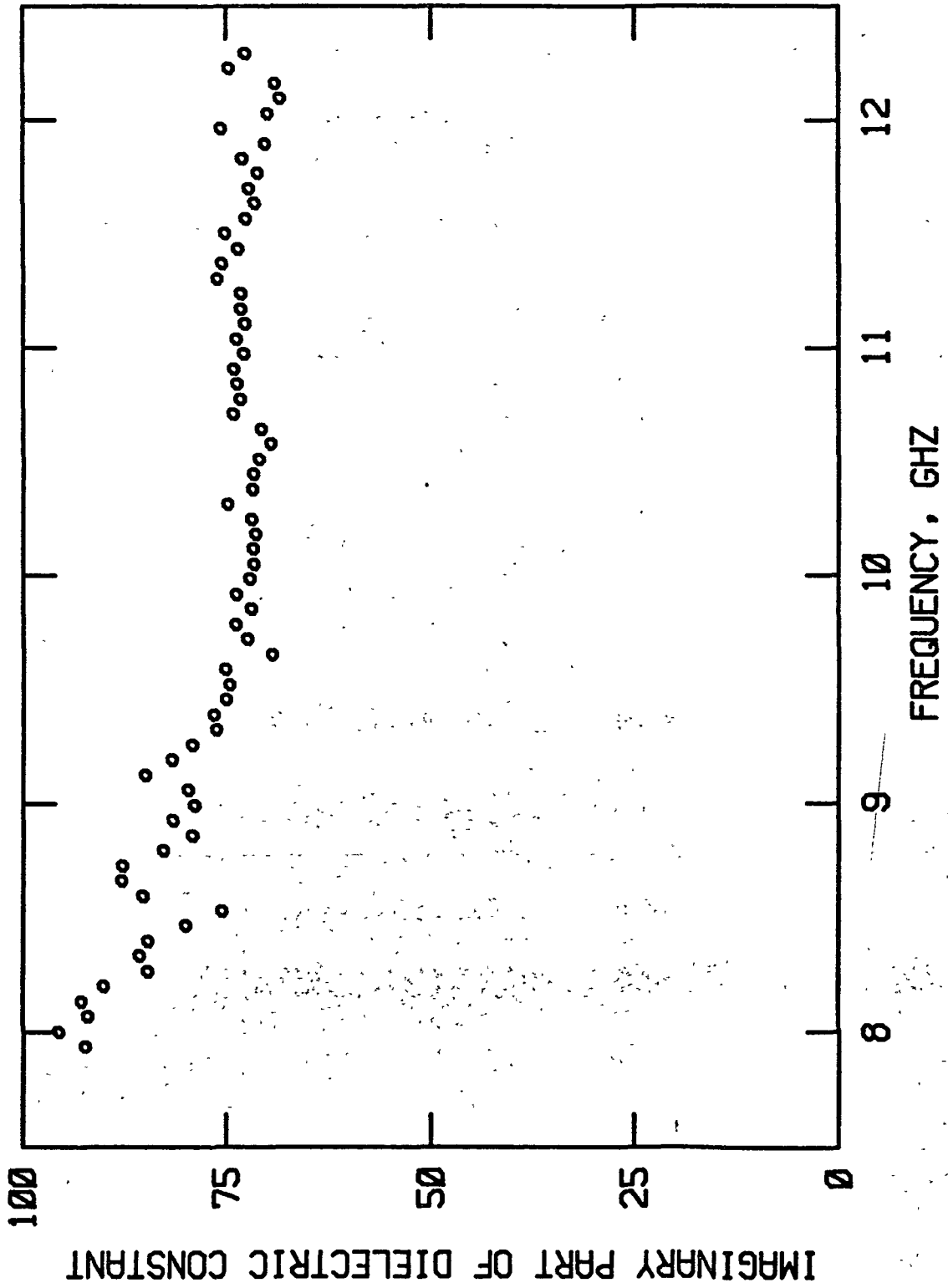


Figure 45.--25 percent KOH.

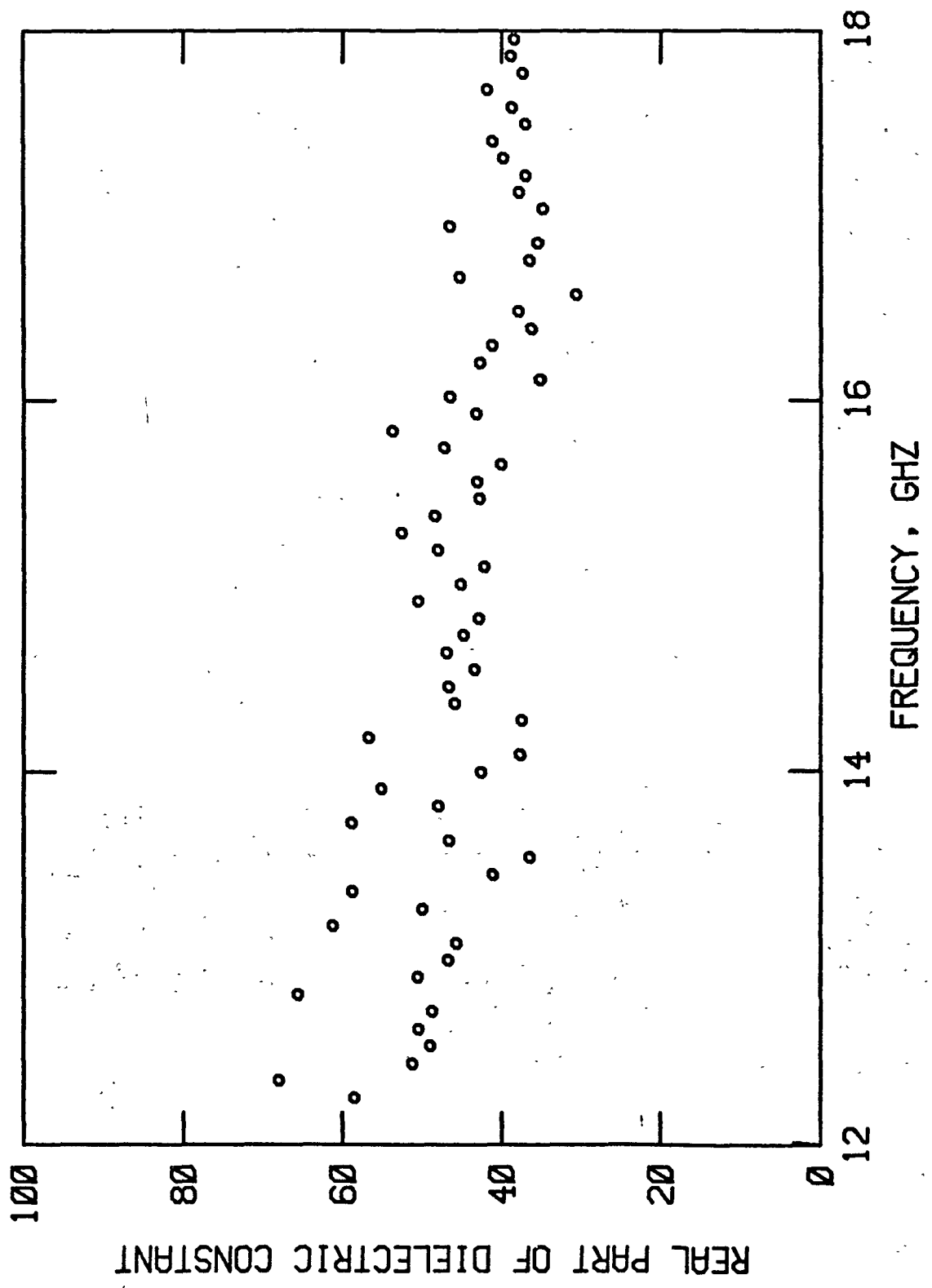


Figure 46.--Water.



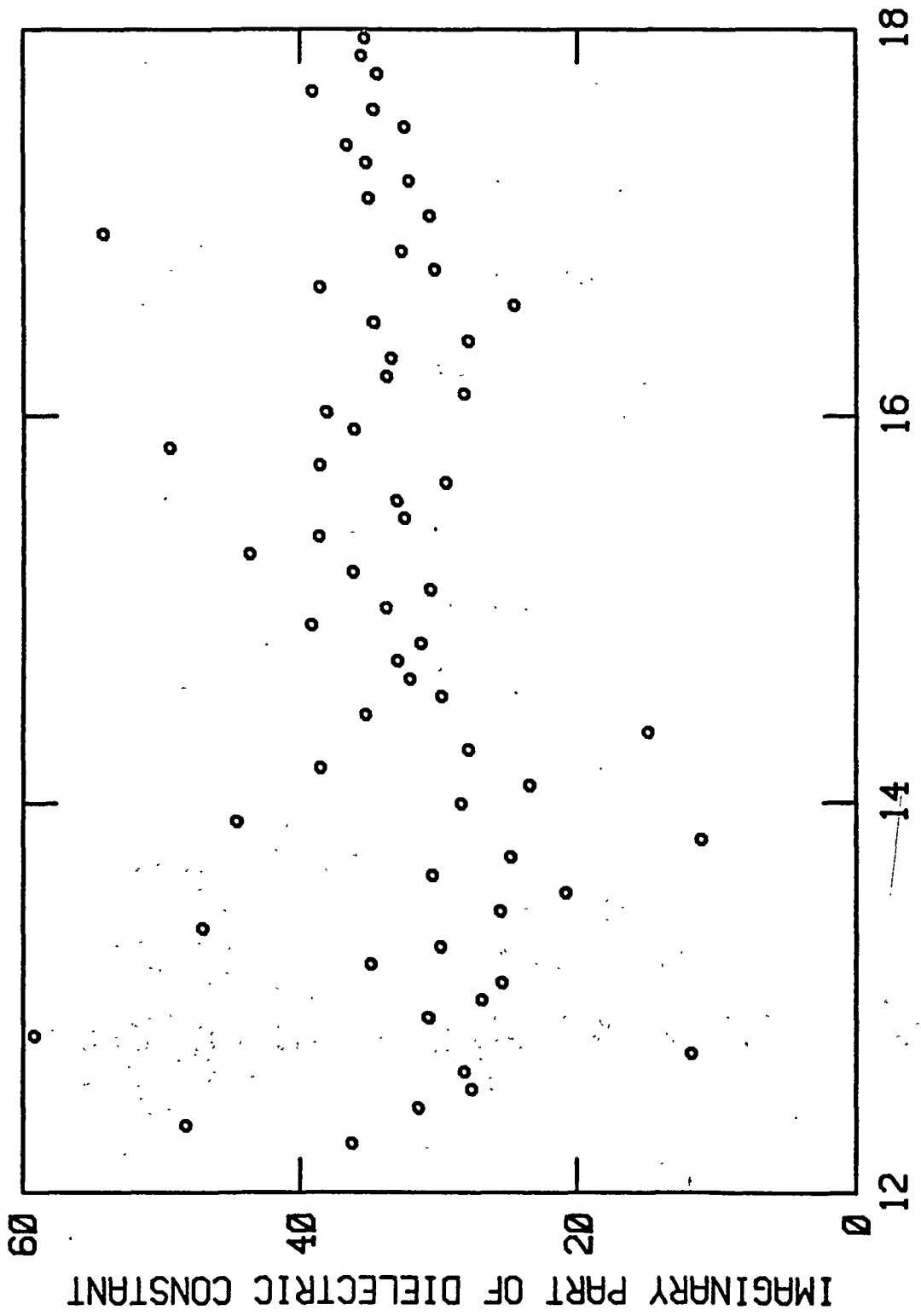


Figure 47.--Water.

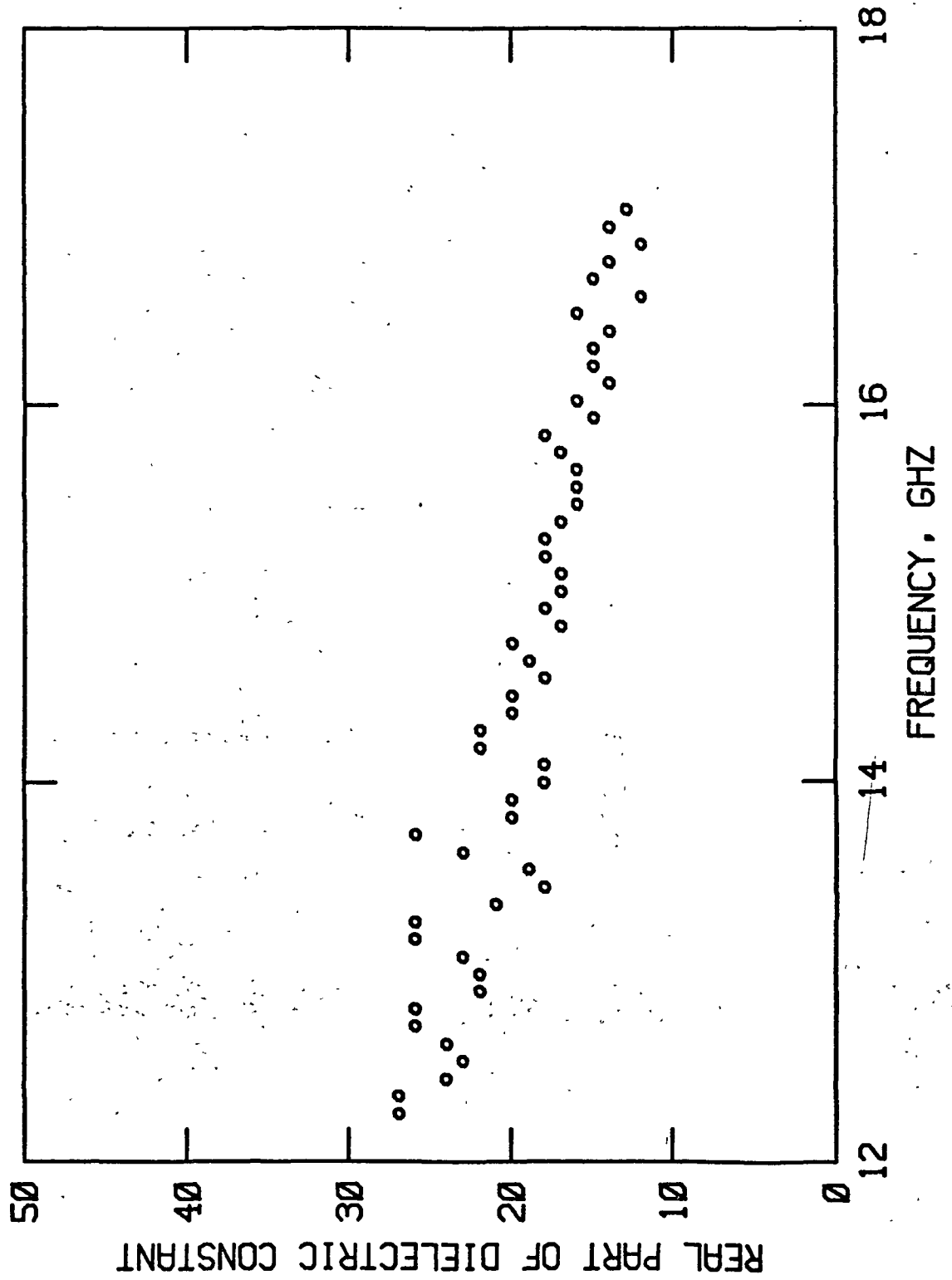


Figure 48.--5 percent KOH.

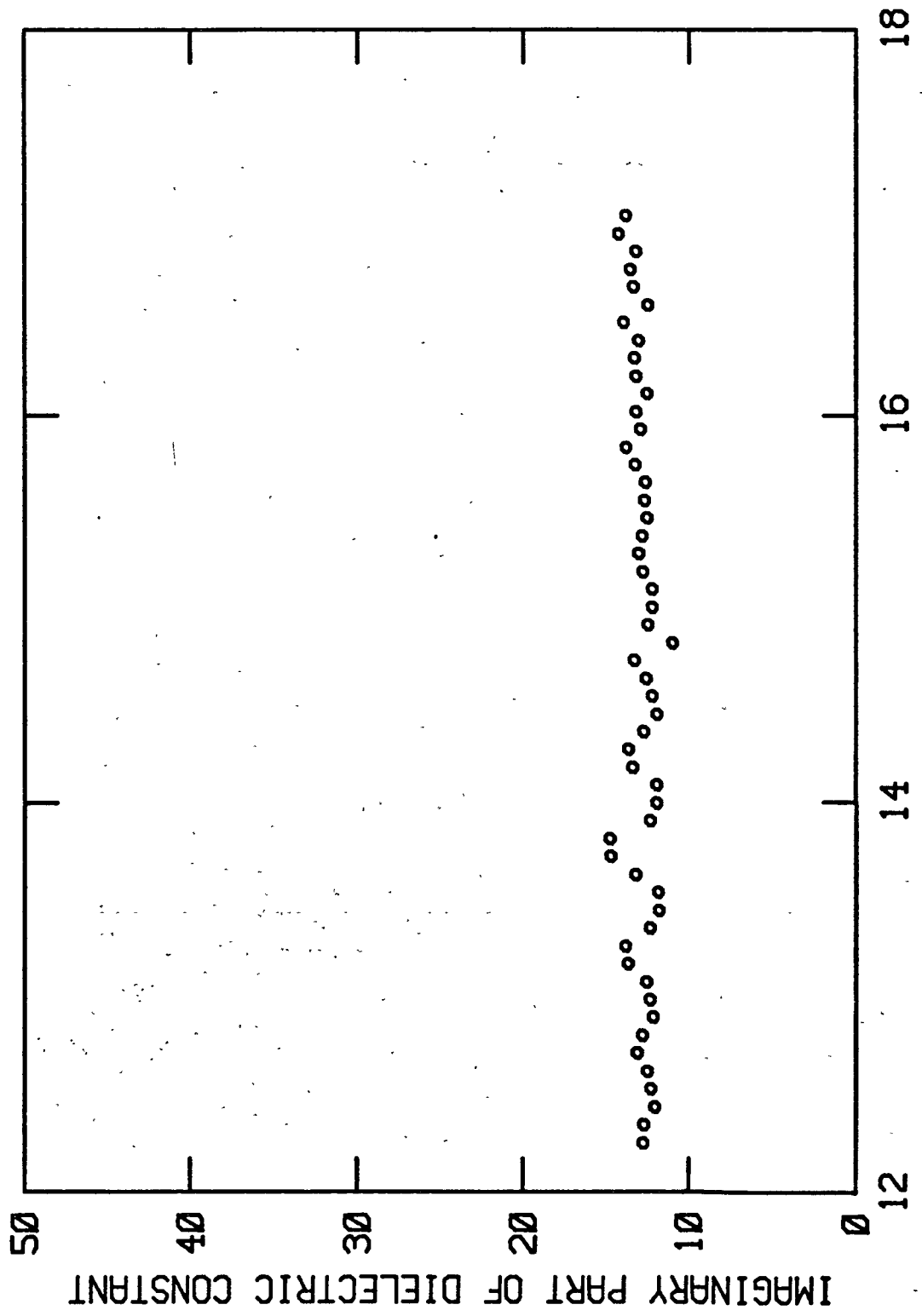


Figure 49.--5 percent KOH.

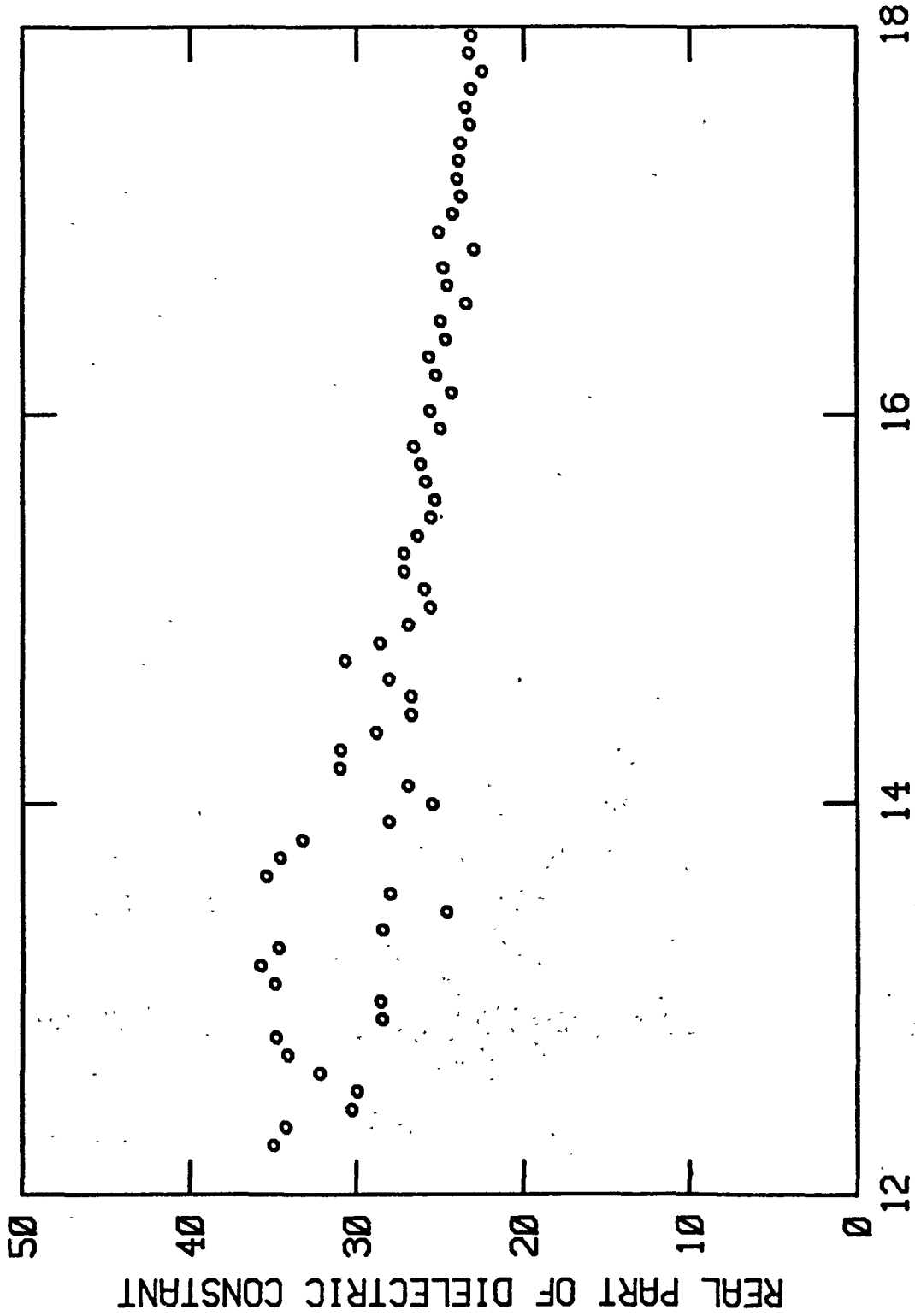


Figure 50. ---10 percent KOH.

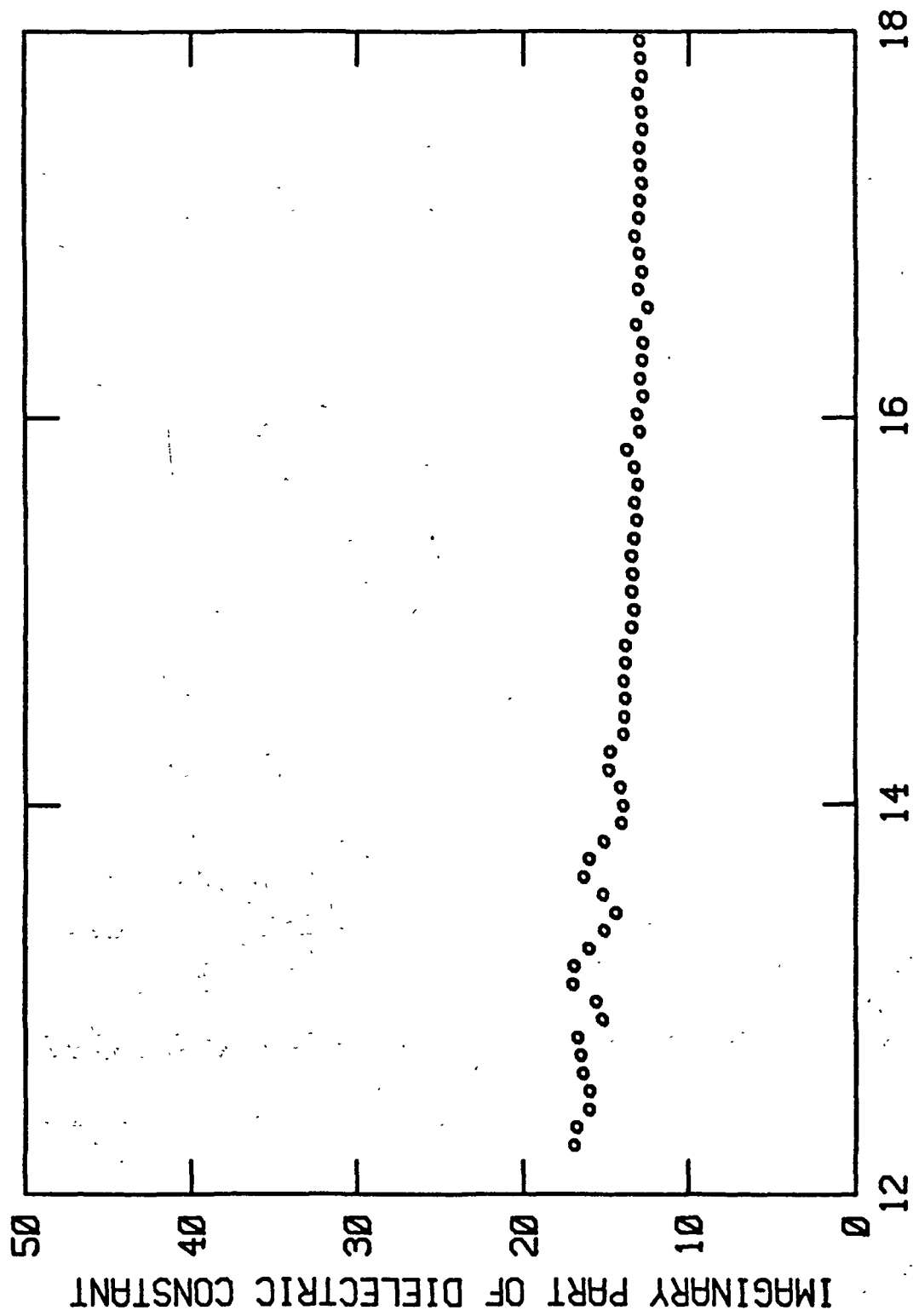


Figure 51.--10 percent KOH.

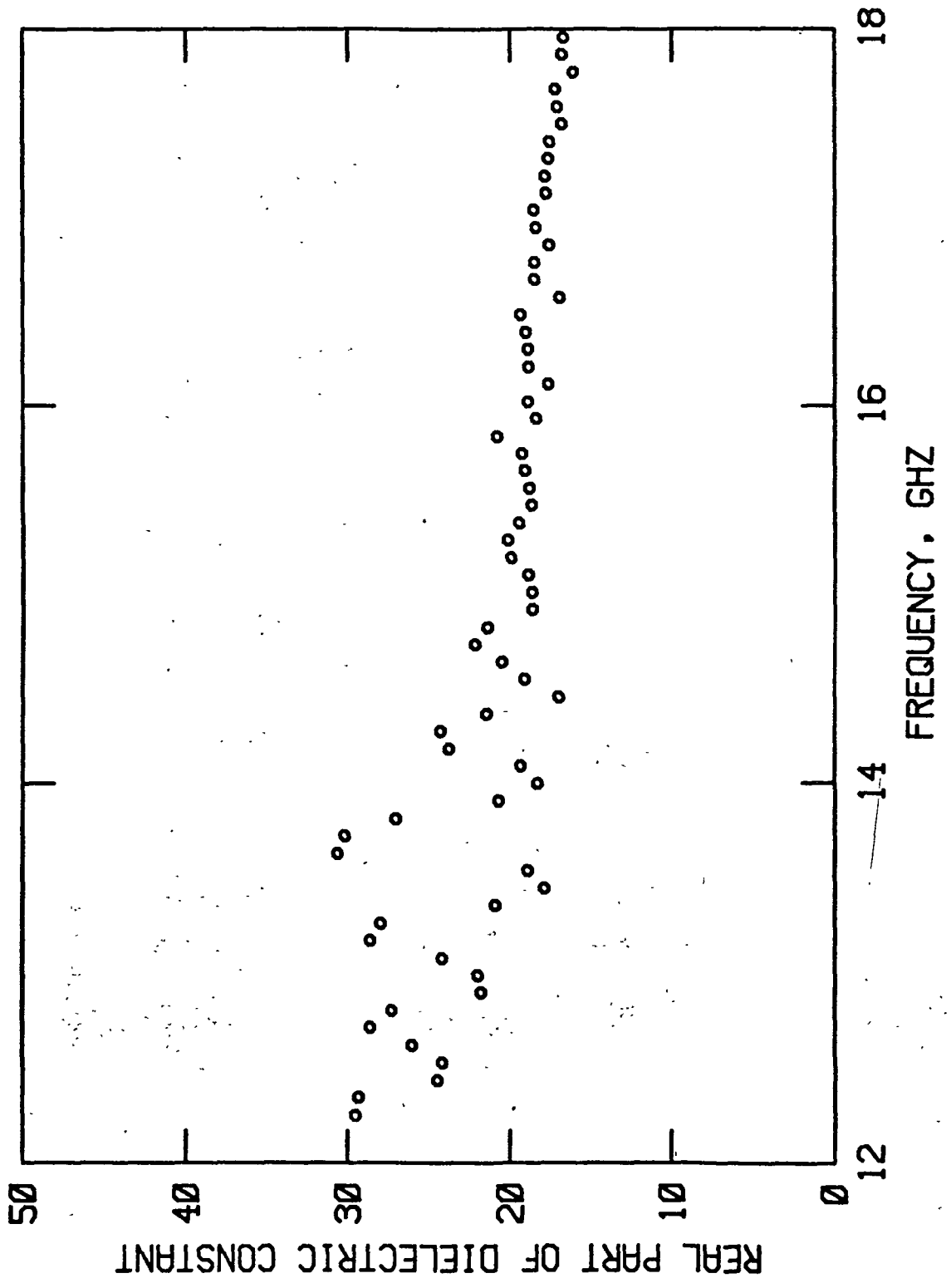


Figure 52.--15 percent KOH.

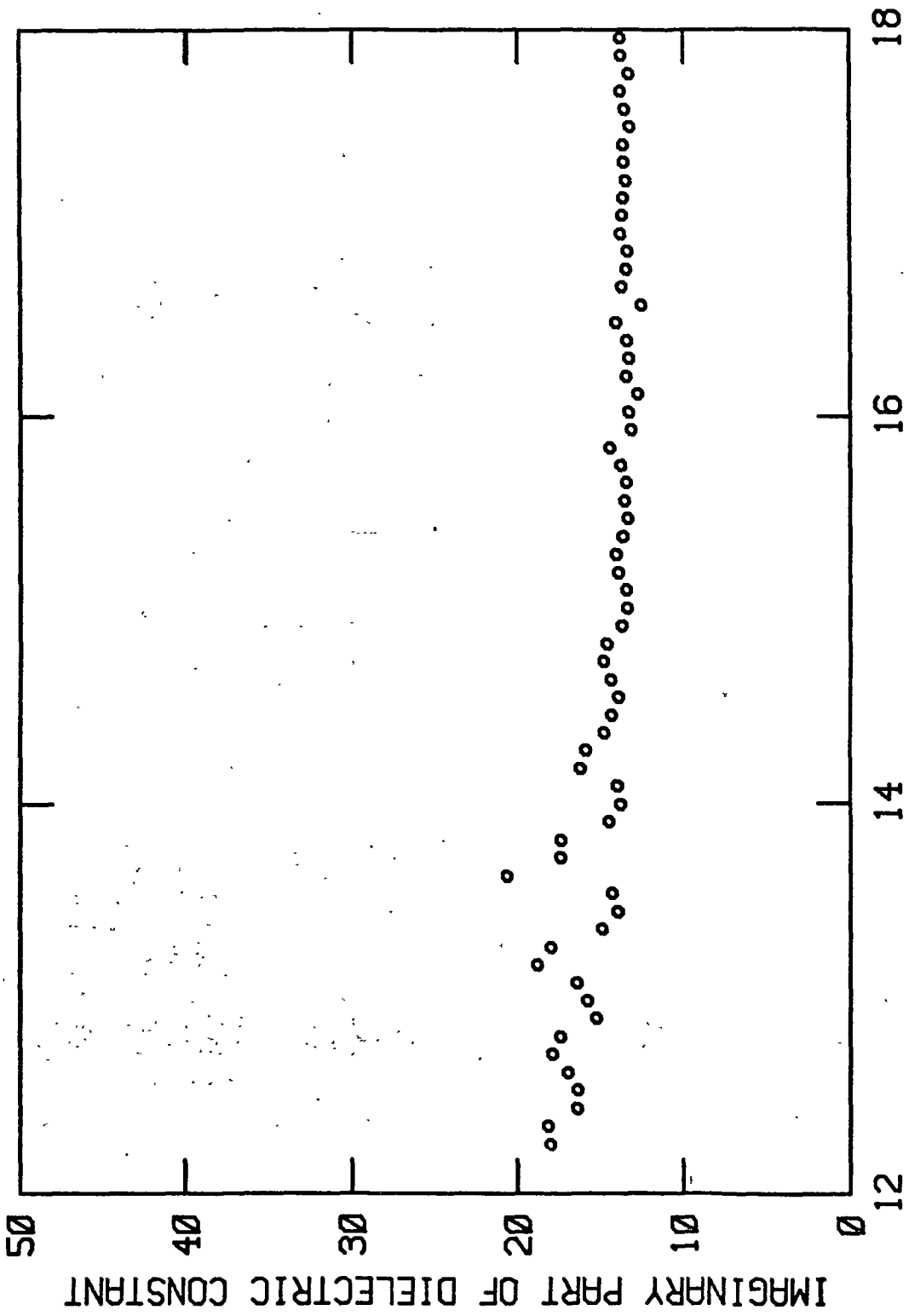


Figure 53, ---15 percent KOH.

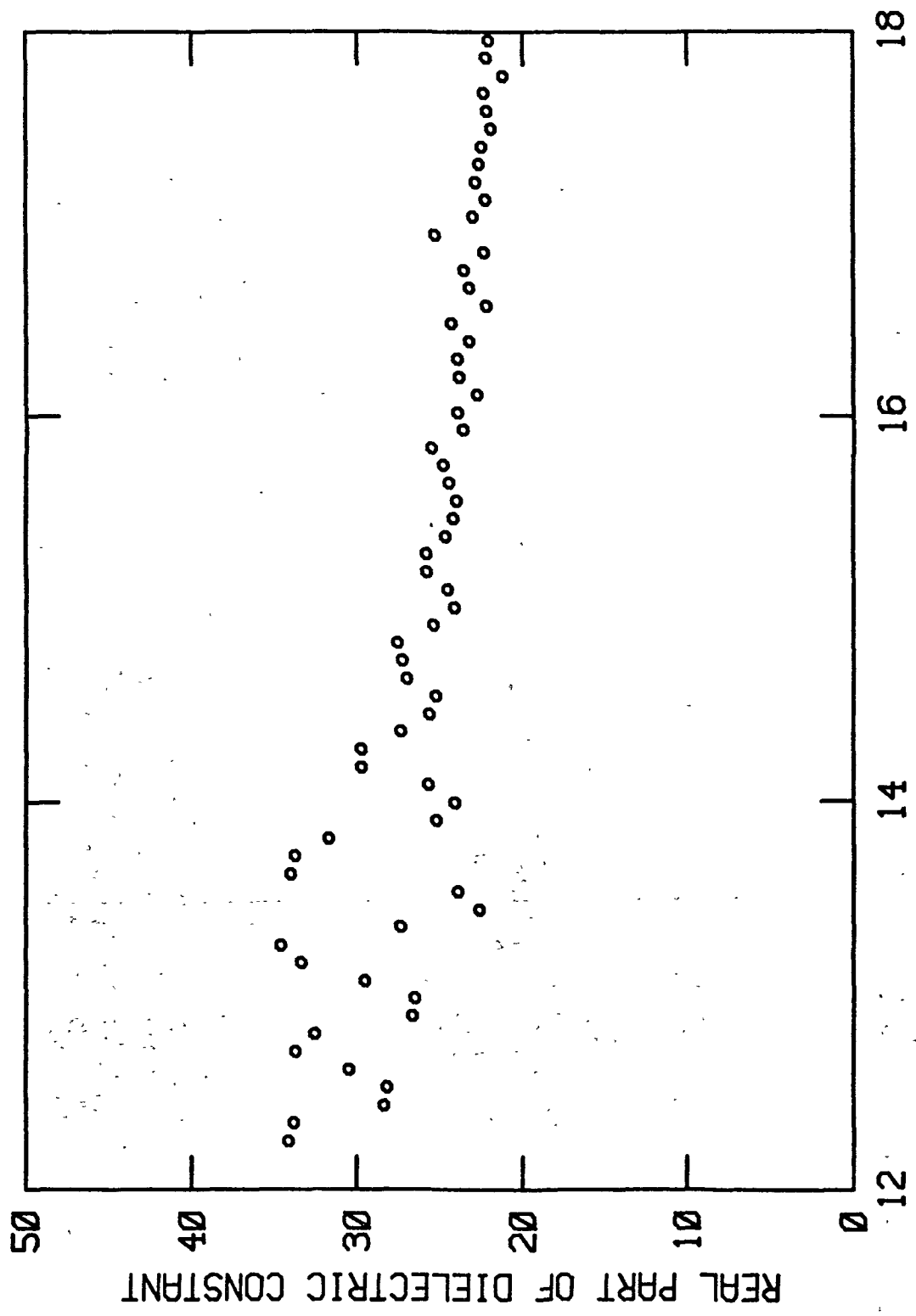


Figure 54, ---20 percent KOH.



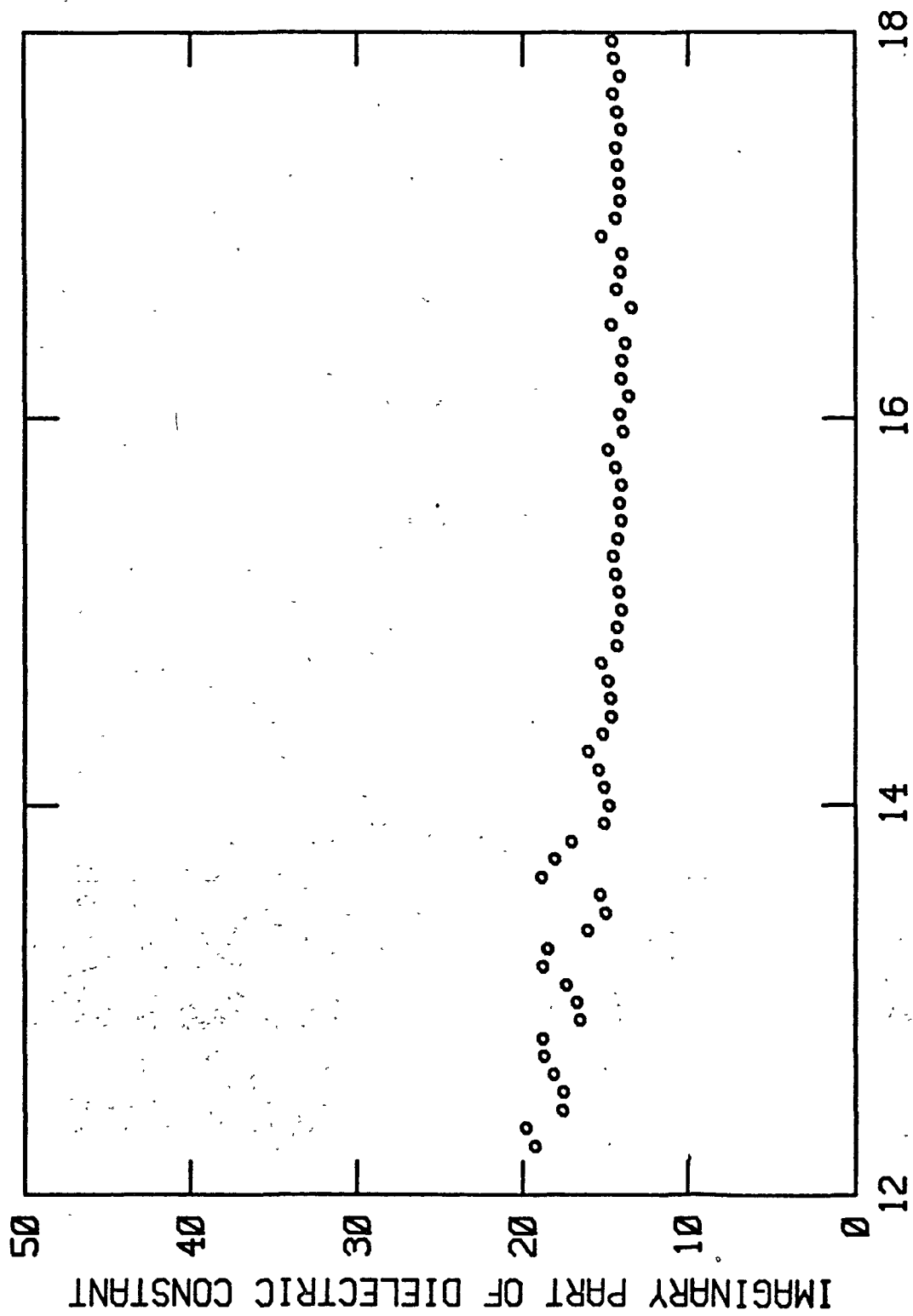


Figure 55.--20 percent KOH.

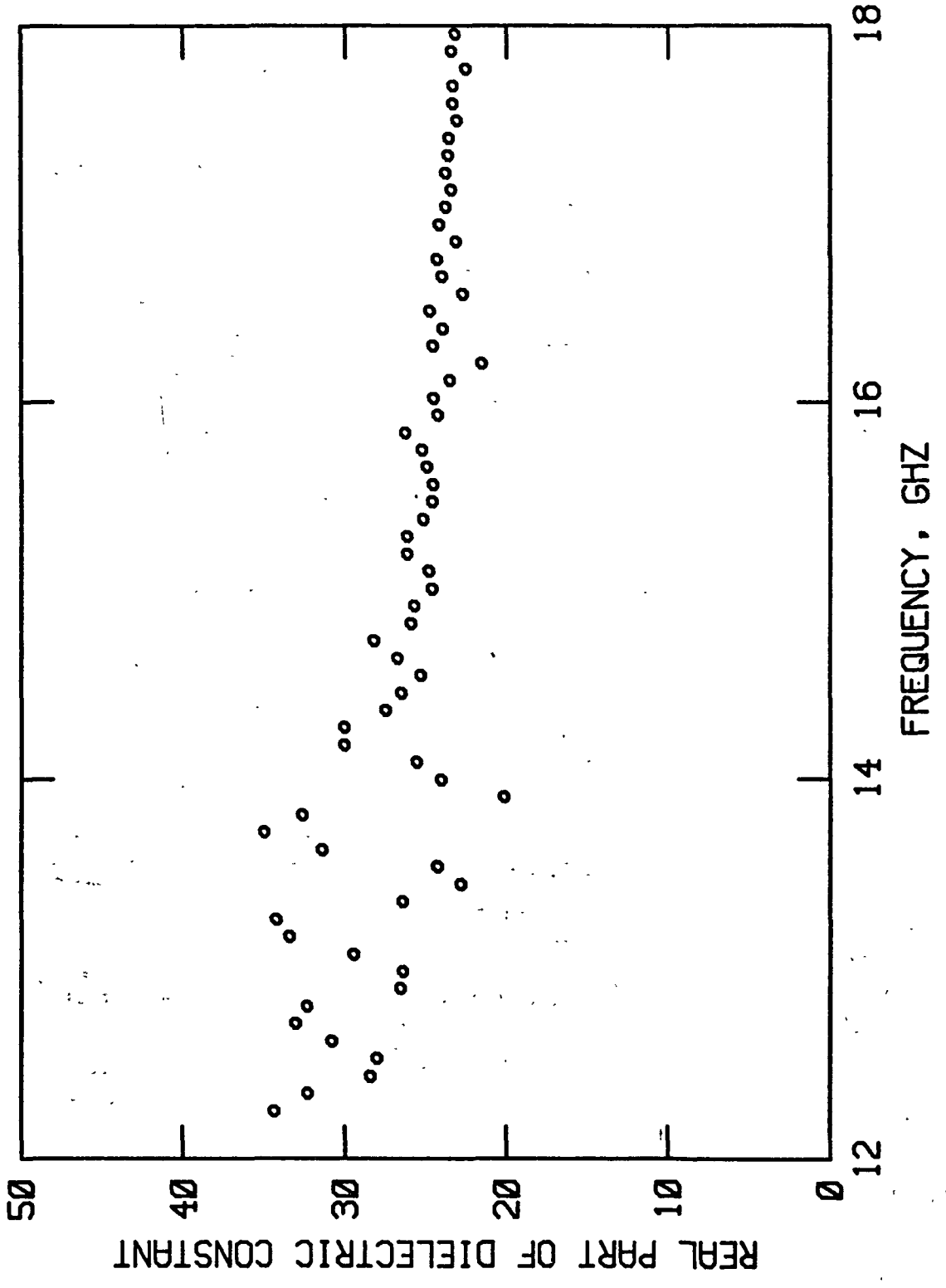


Figure 56.--25 percent KOH.

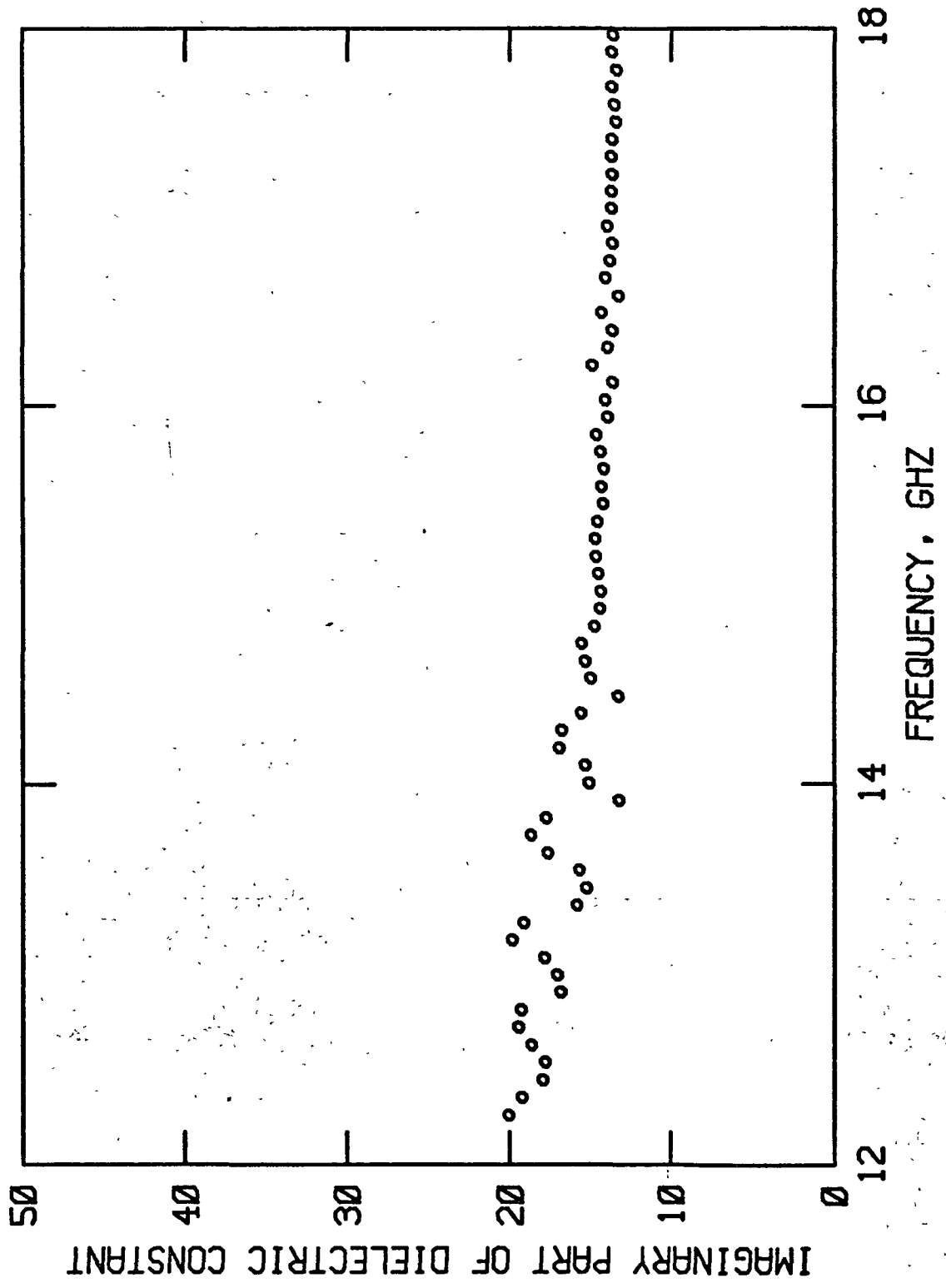


Figure 57.--25 percent KOH.

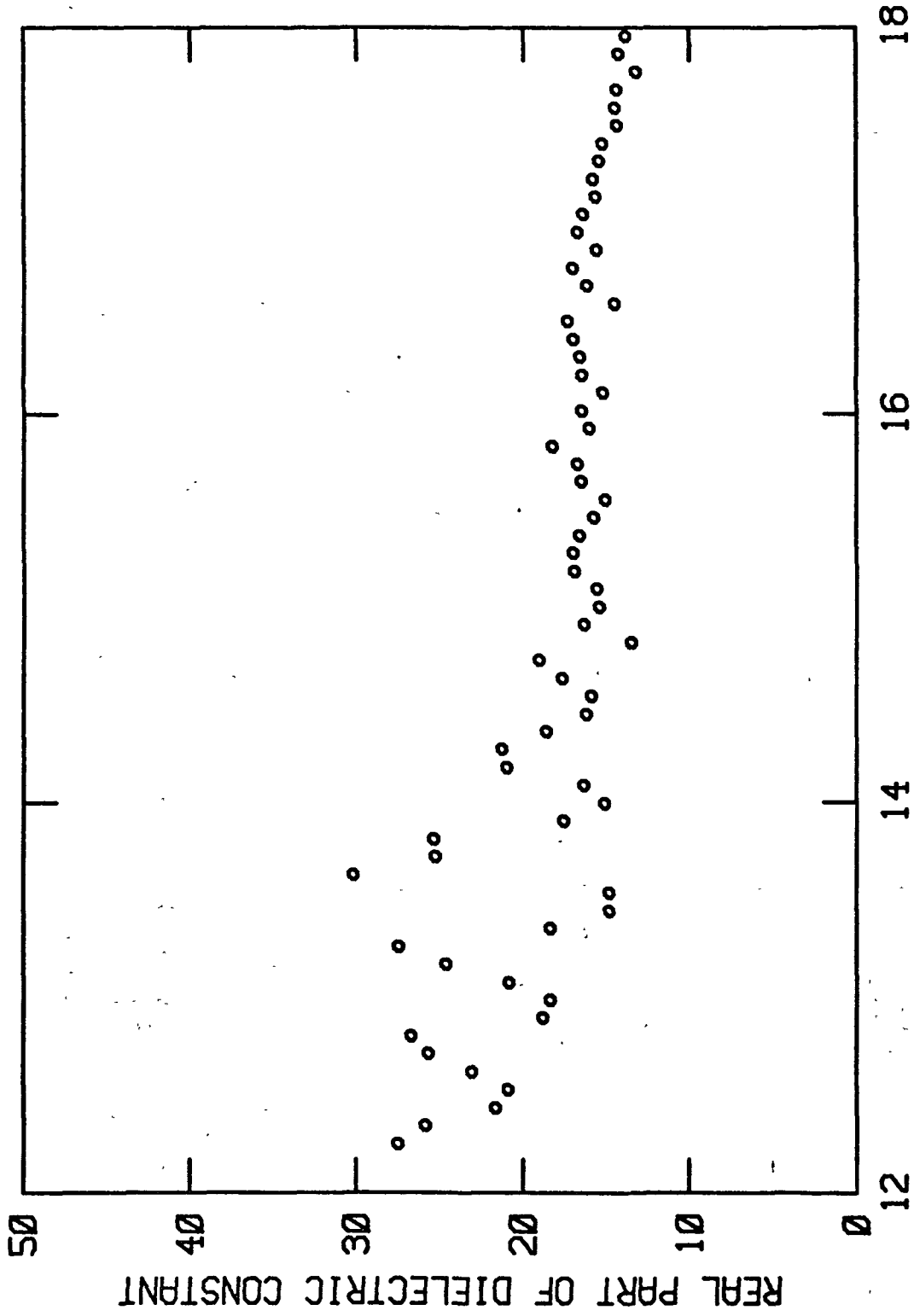


Figure 58.--30 percent KOH.

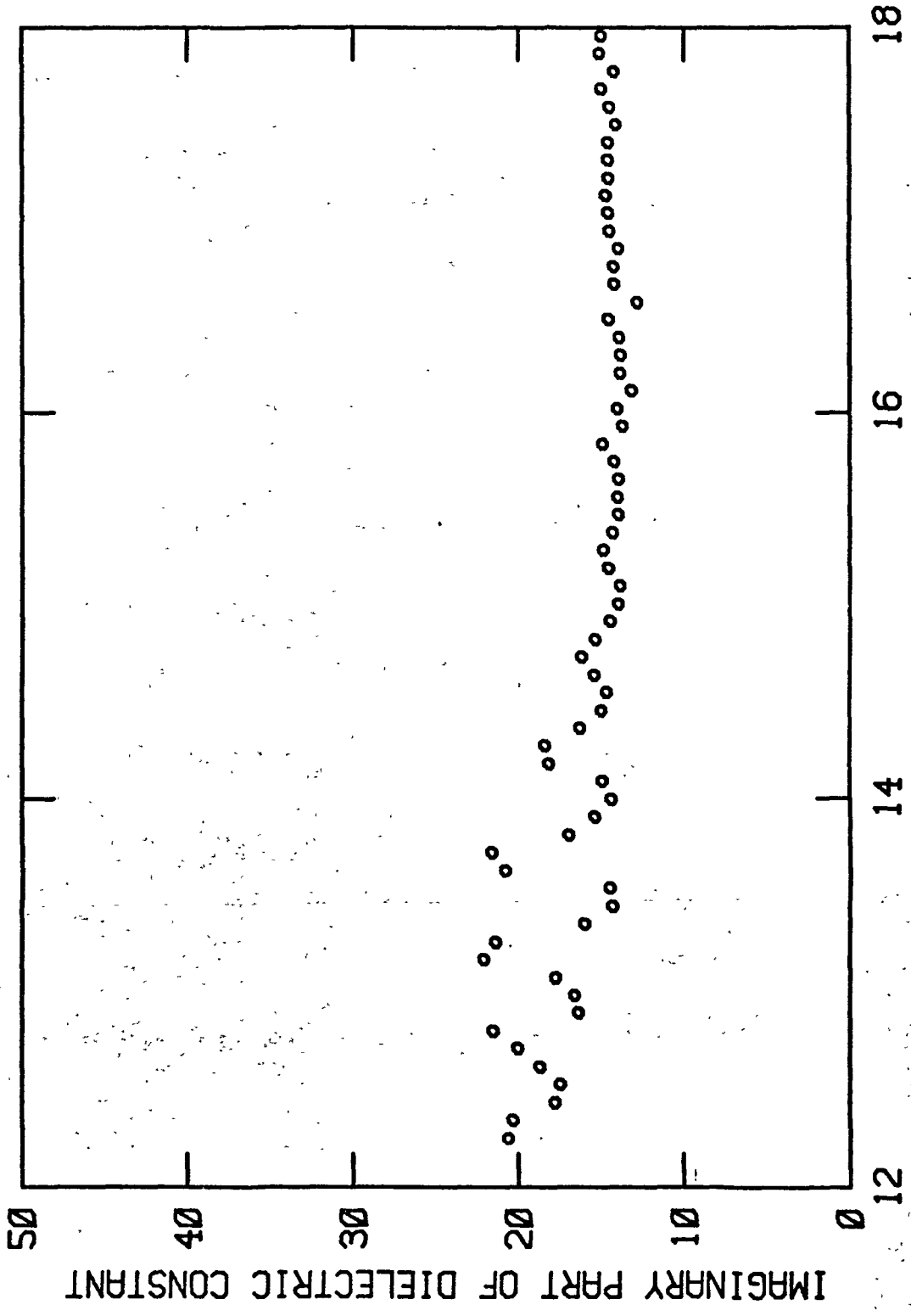


Figure 59.---30 percent KOH.

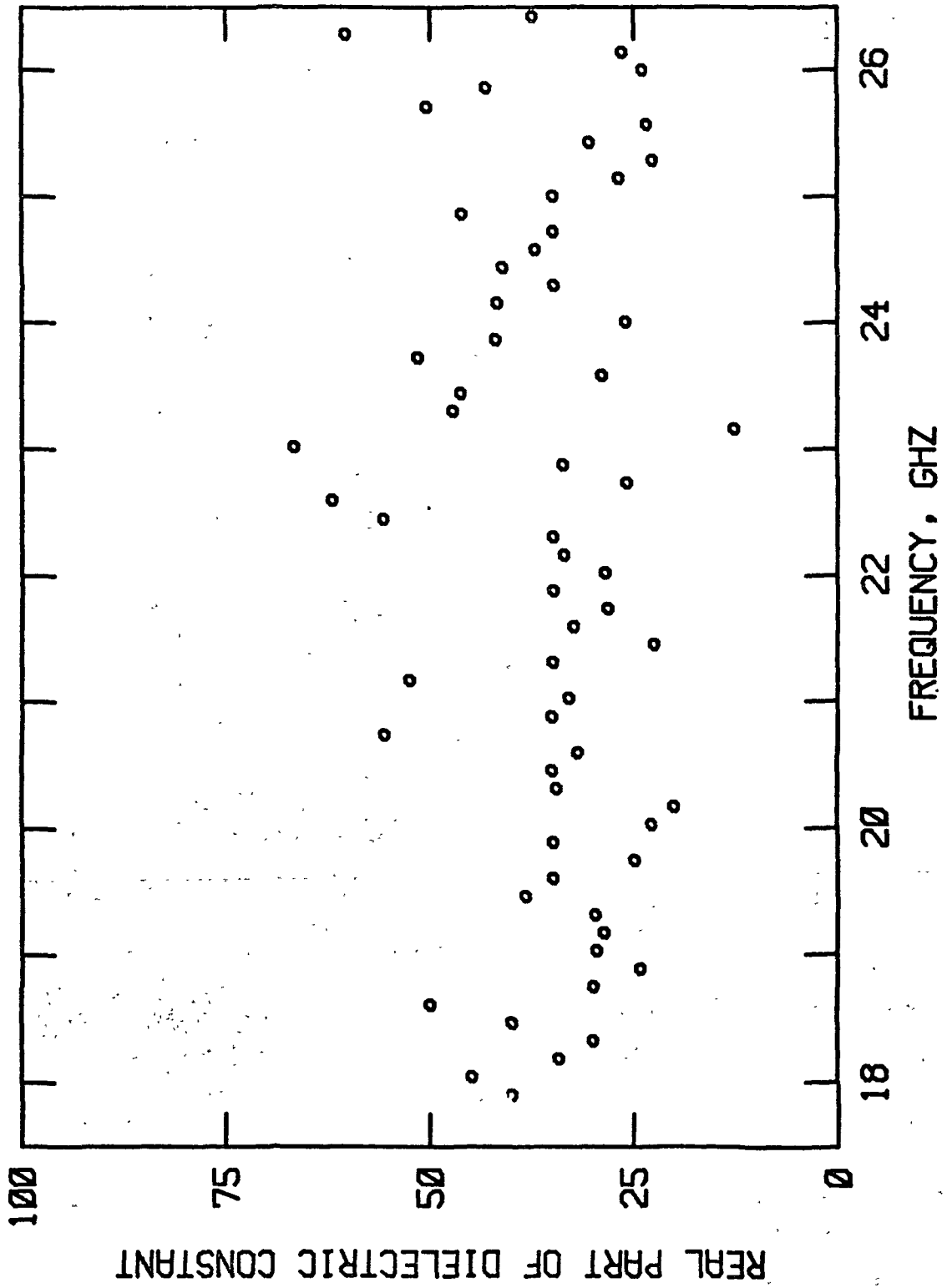


Figure 60.--Water.

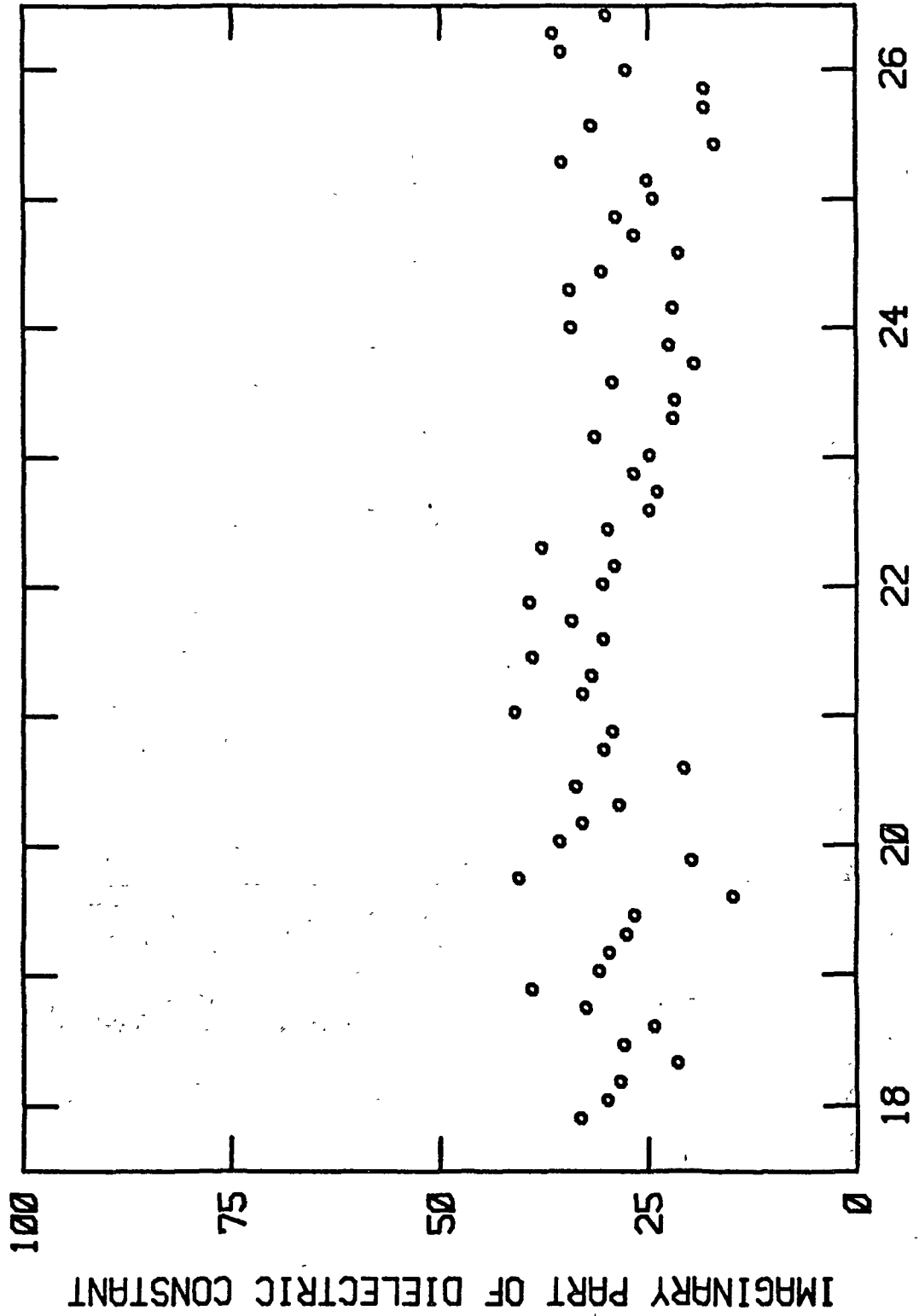


Figure 61.--Water.

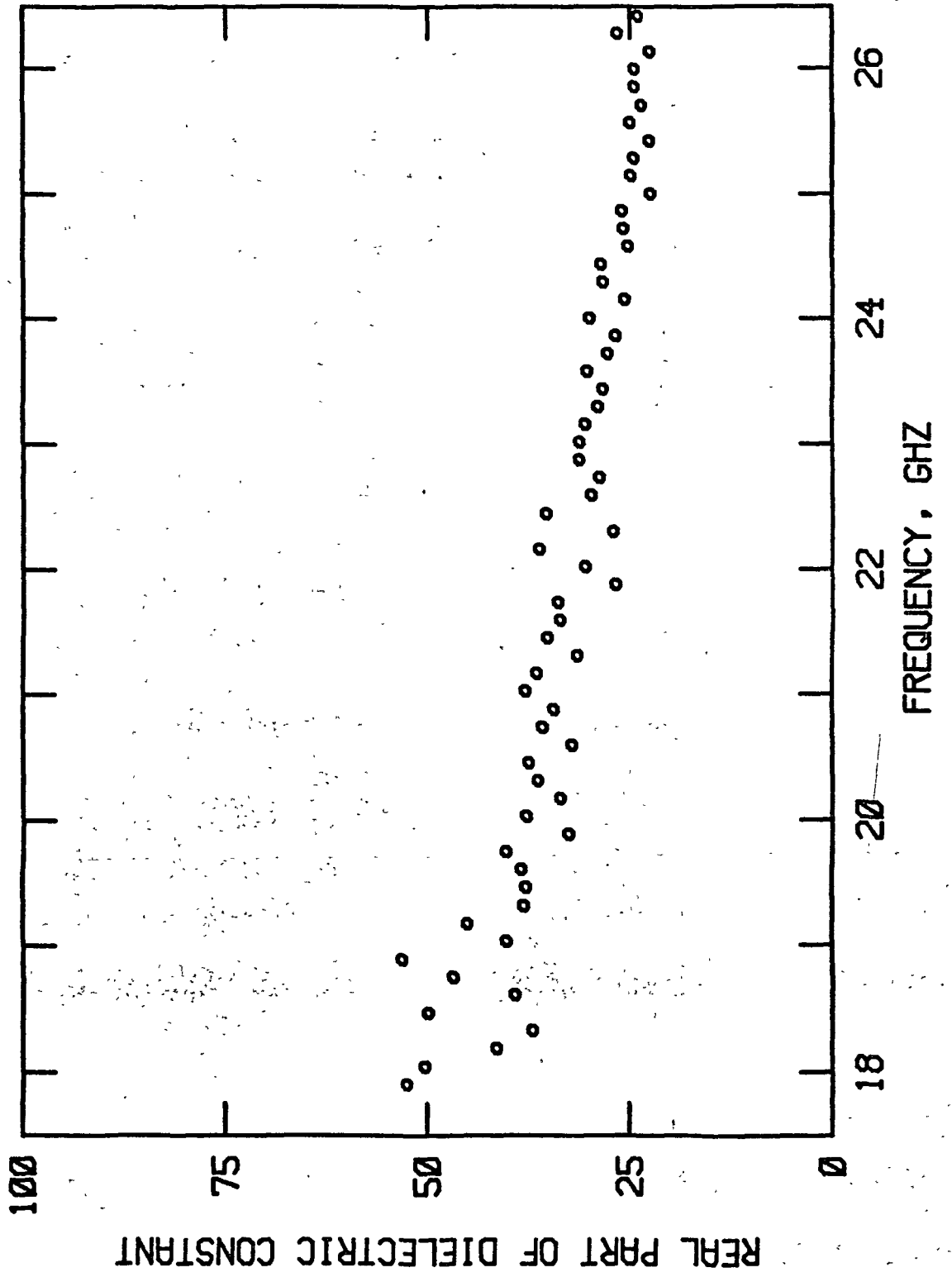


Figure 62.--10 percent KOH.



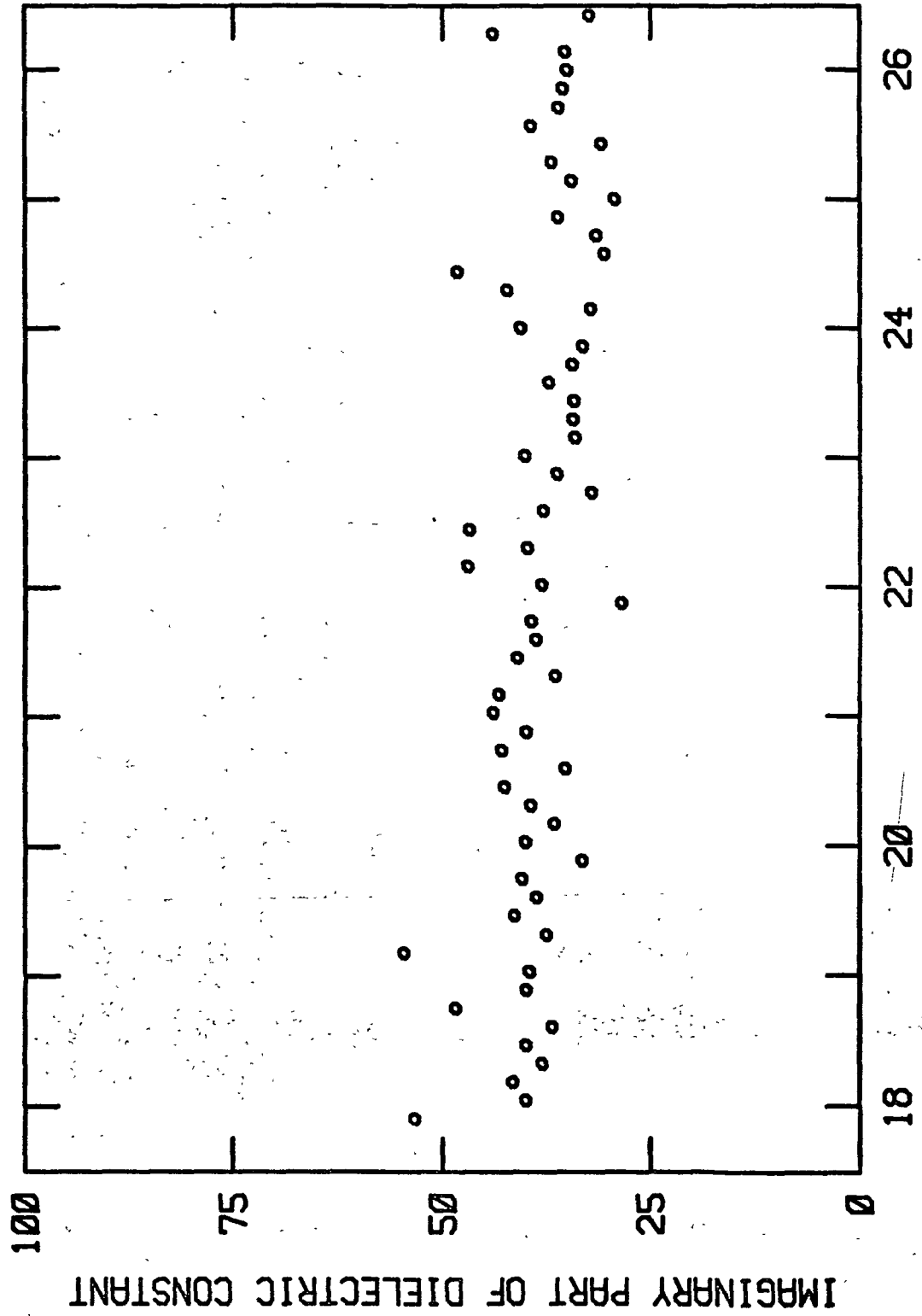


Figure 63.--10 percent KOH.

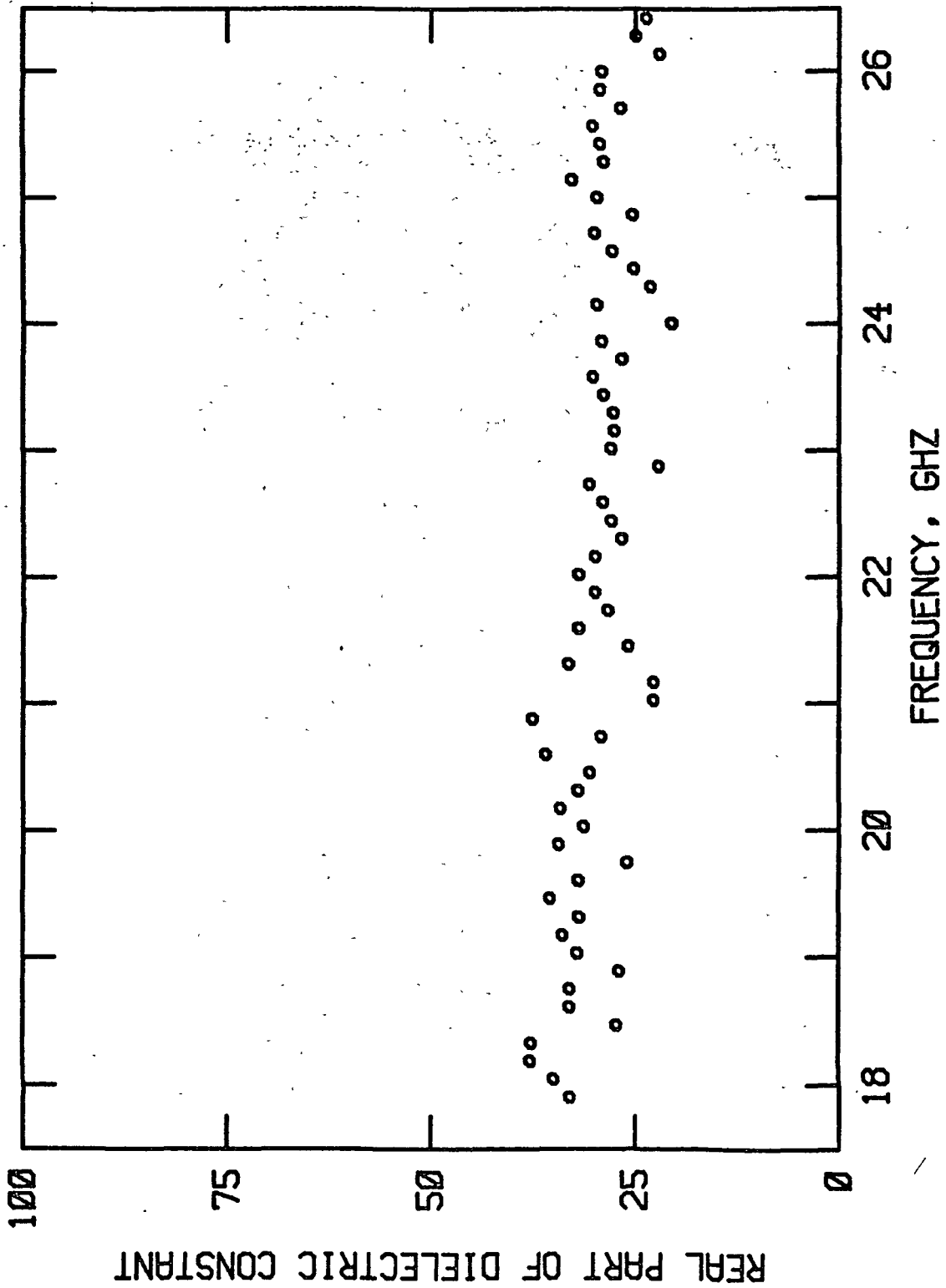


Figure 64.--20 percent KOH.

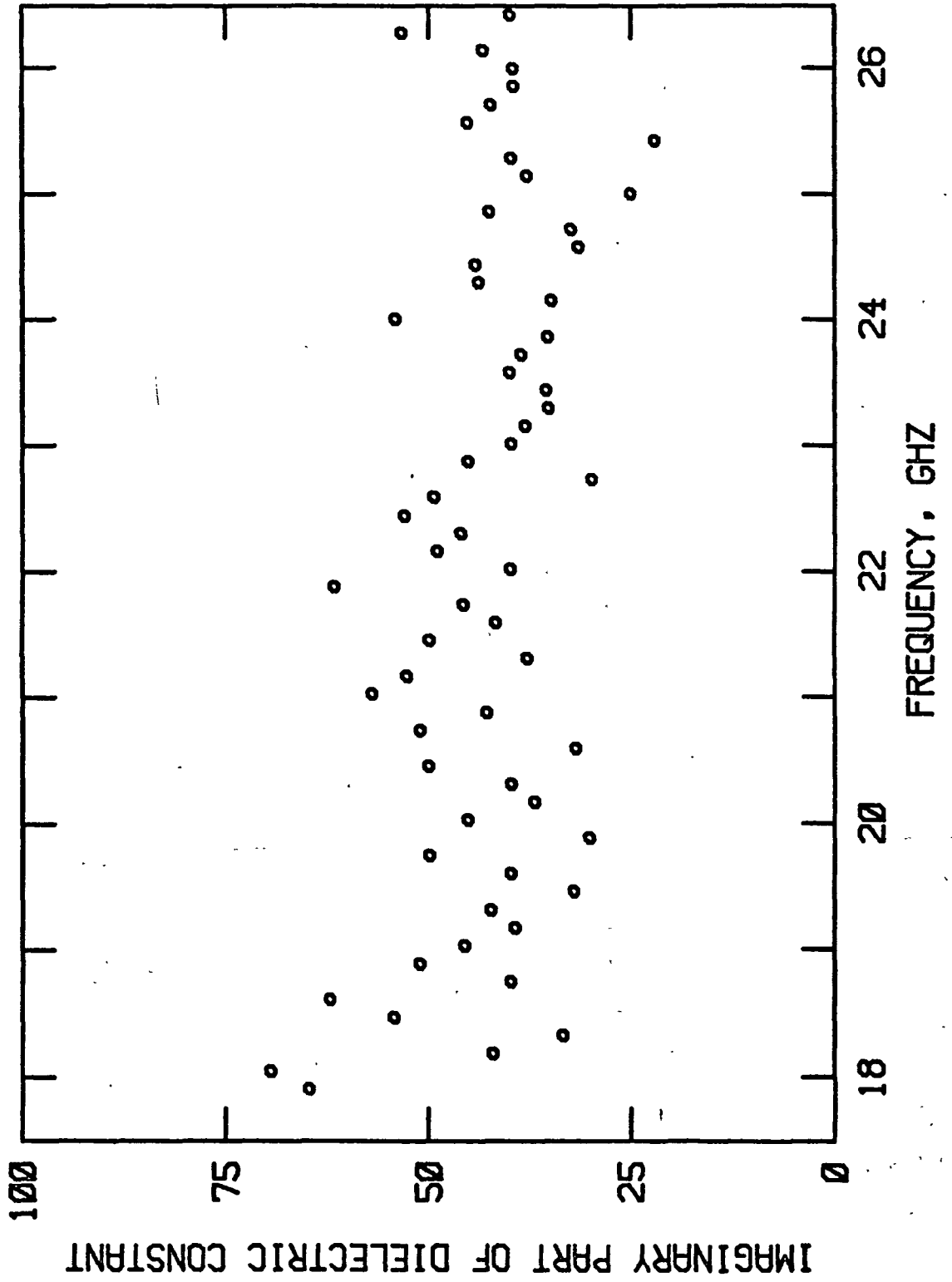


Figure 65.--20 percent KOH.

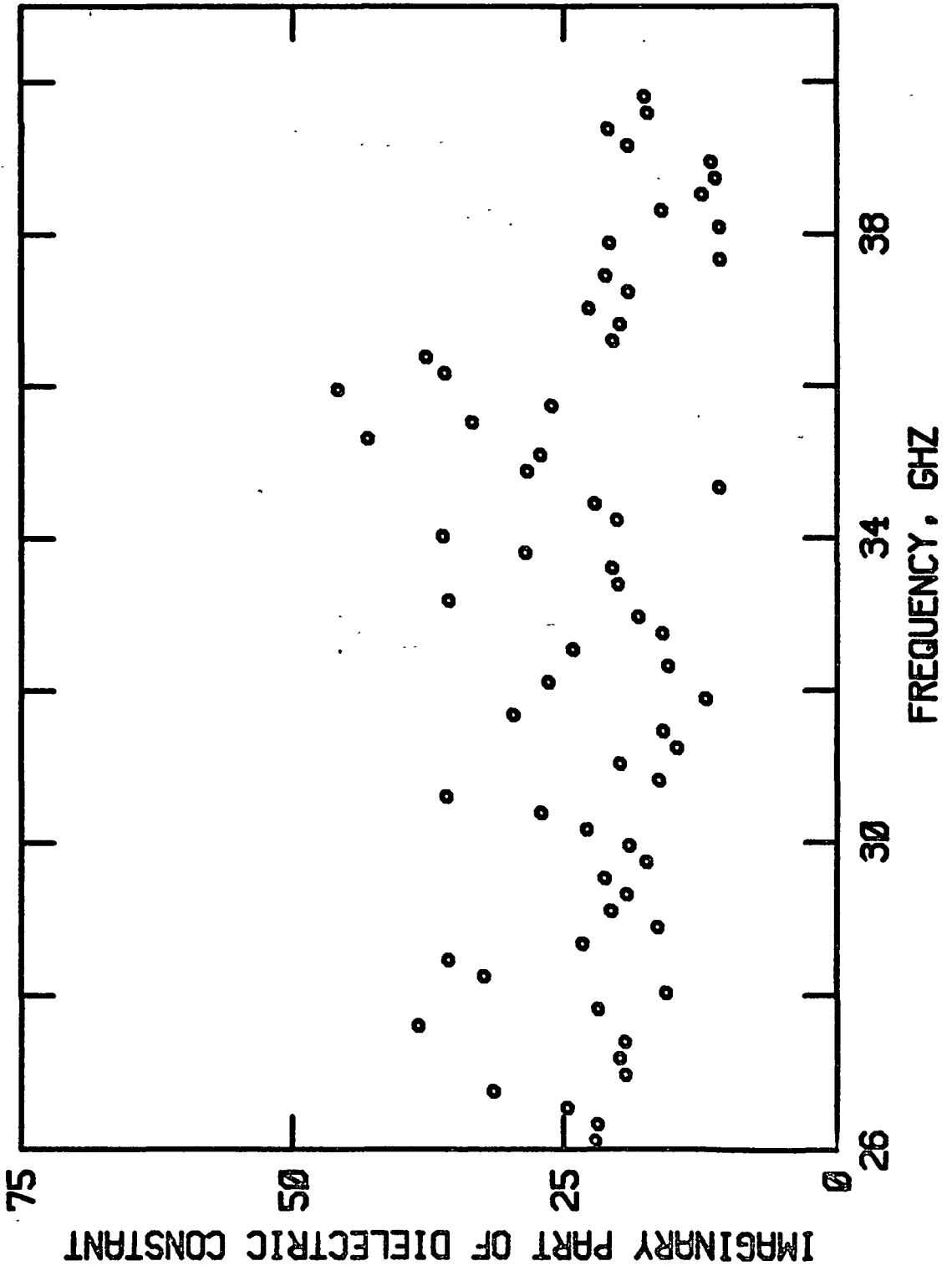


Figure 66.--Water.

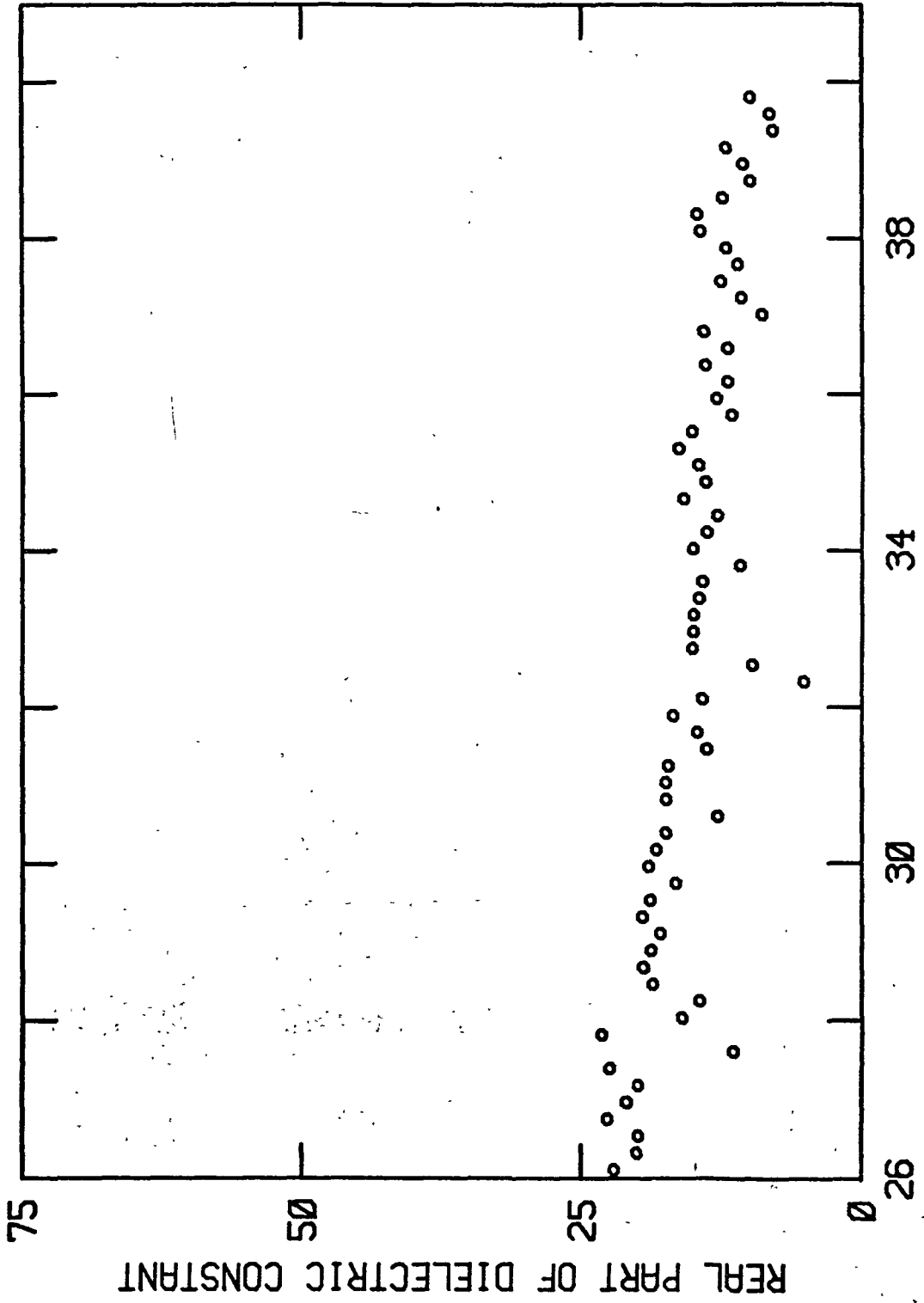


Figure 67.--20 percent KOH.

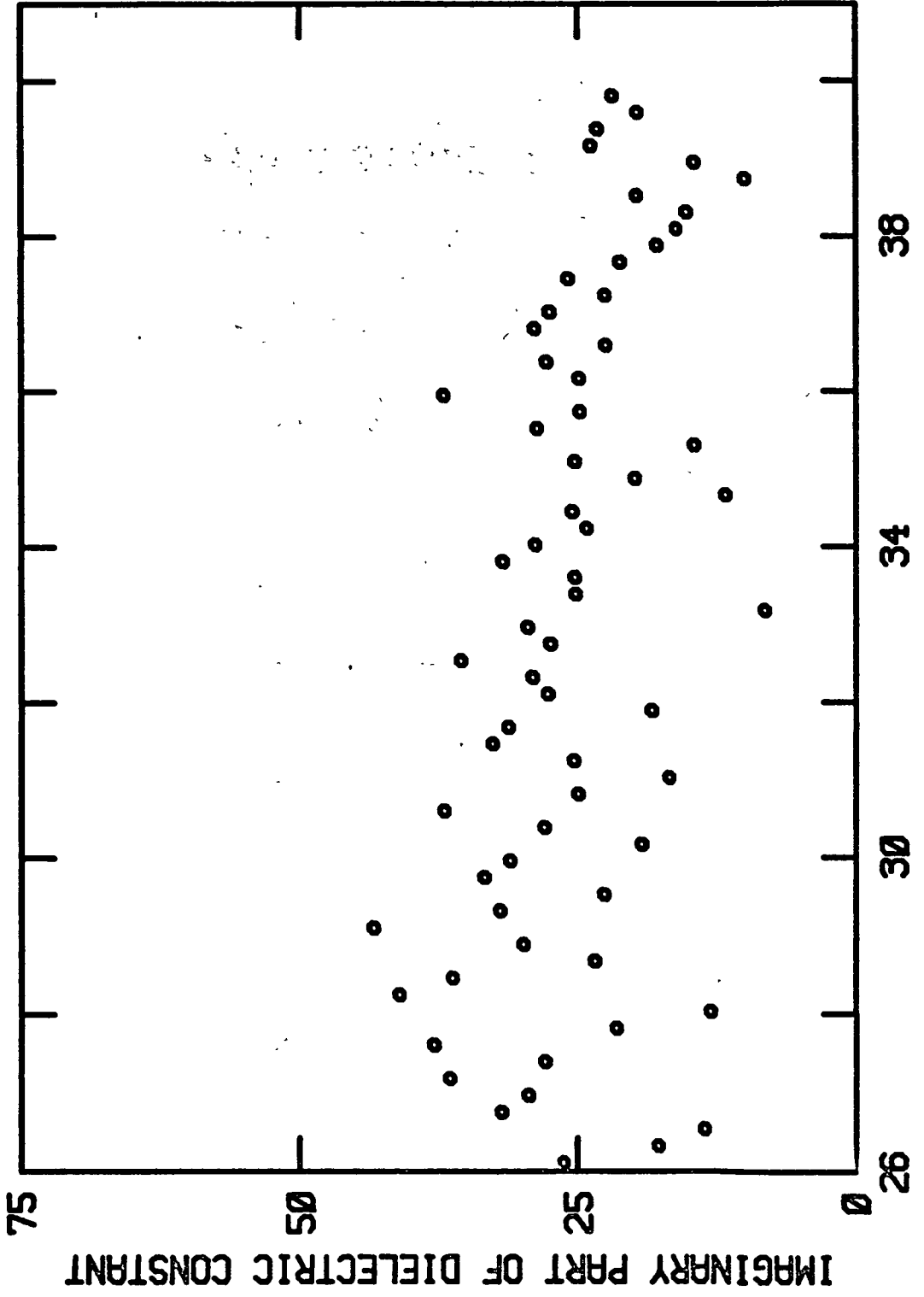


Figure 68.--20 percent KOH.

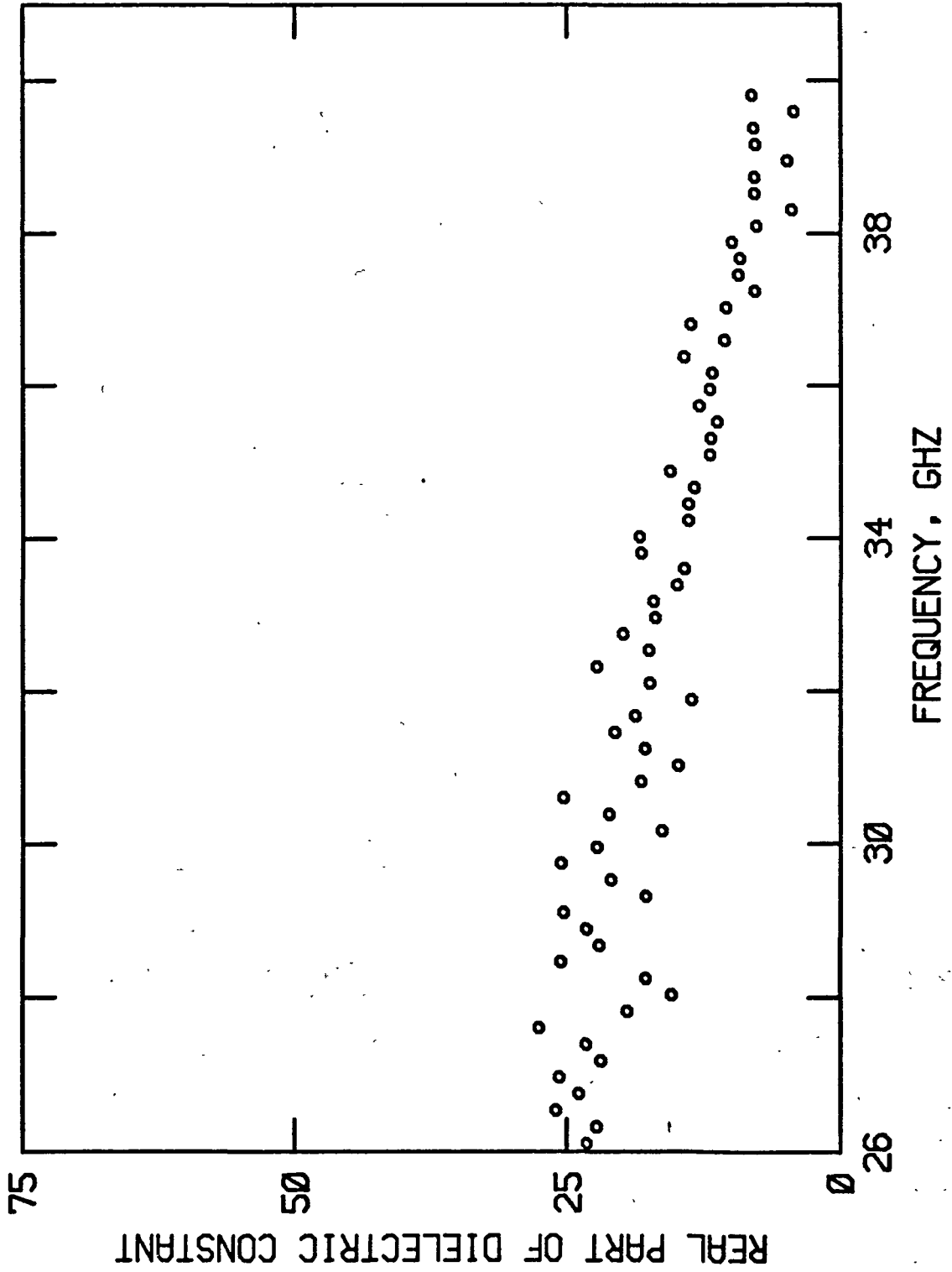


Figure 69.--25 percent KOH.

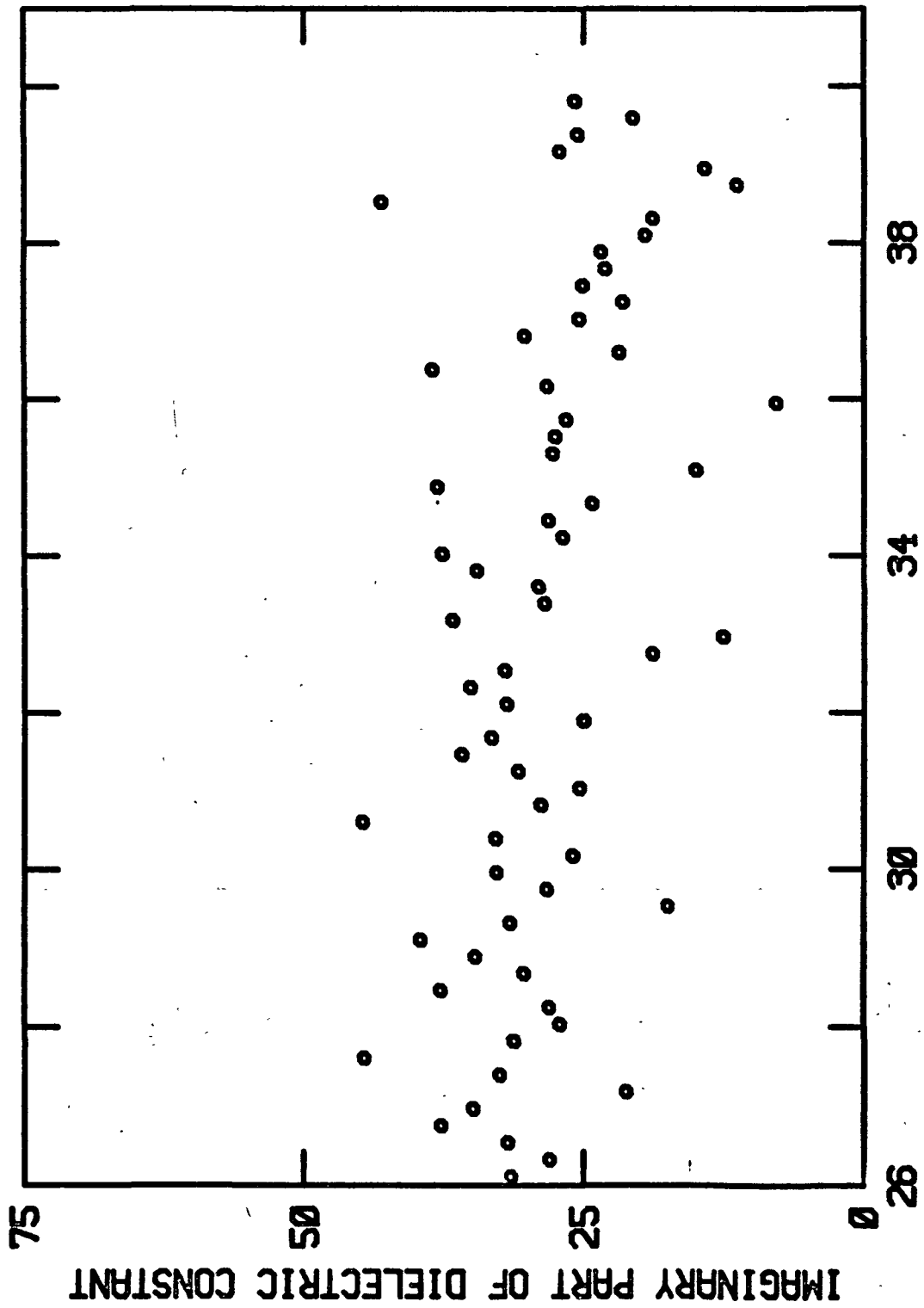


Figure 70.--25 percent KOH.



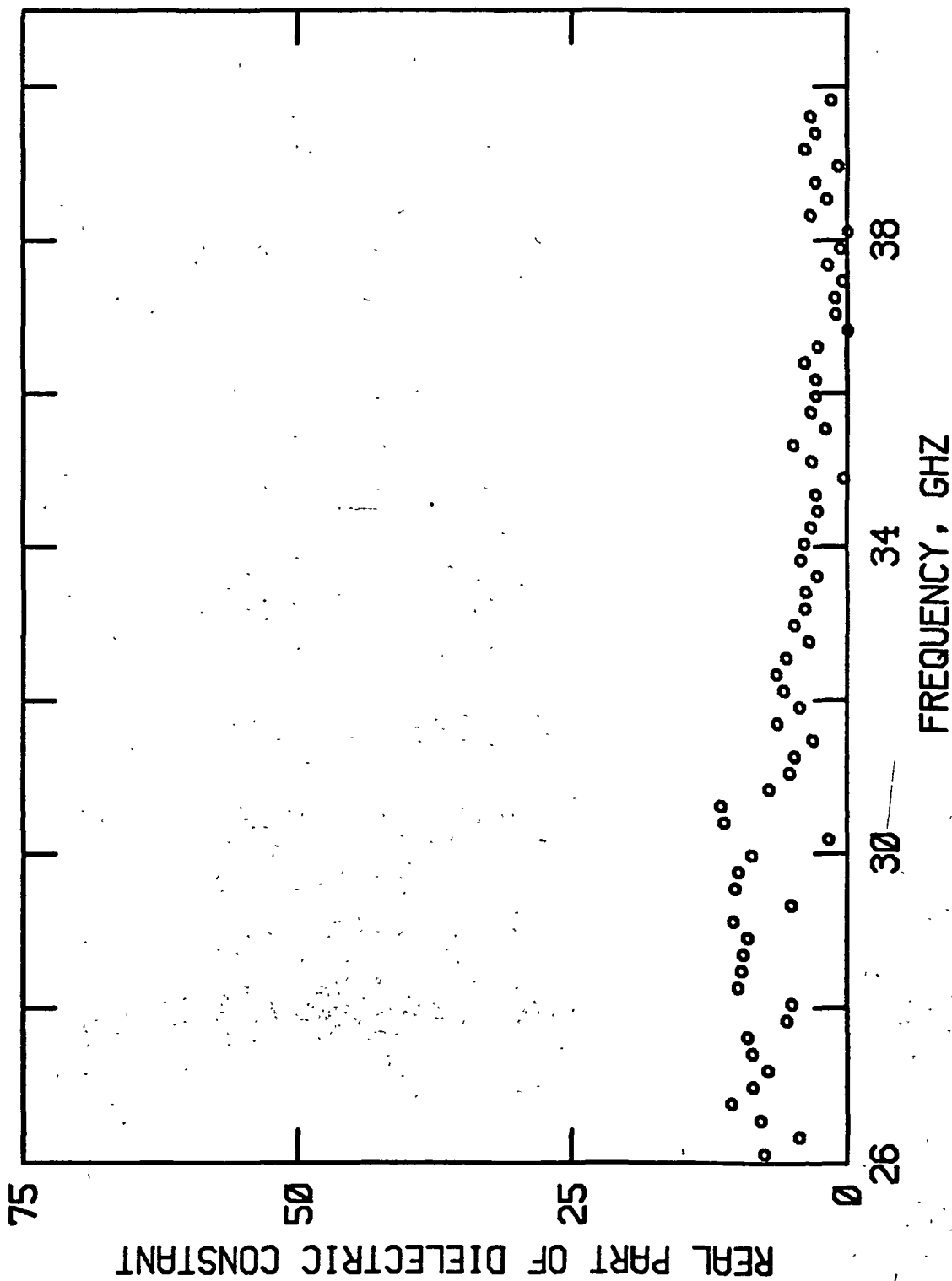


Figure 71.--30 percent. KOH.

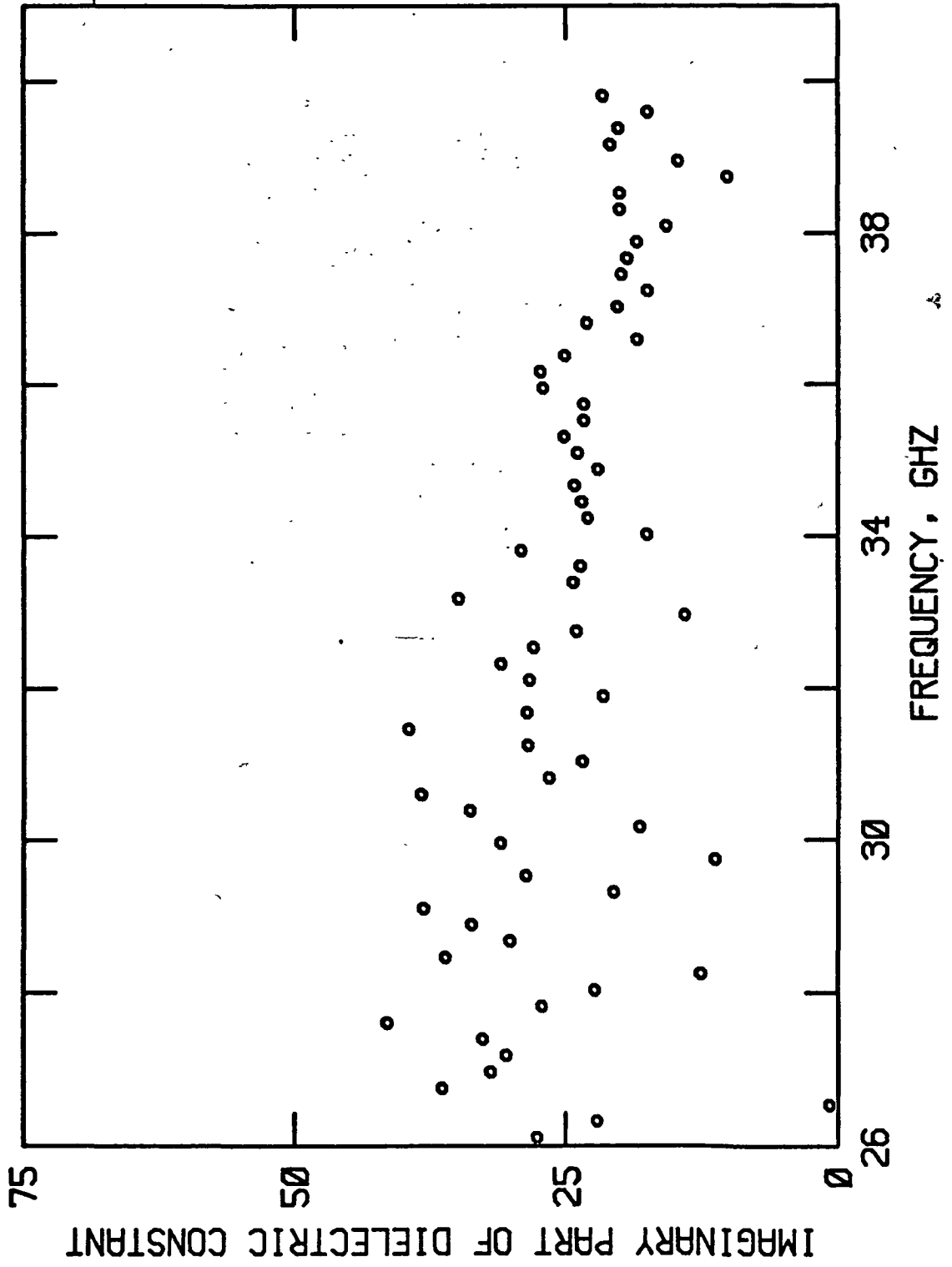


Figure 72.--30 percent KOH.